

**Questions and Clarity: Insights from Applying Computational
Methods to Paleoclimate Archives**

by

Michaela Fendrock

B.A., Wellesley College (2015)

Submitted to the Department of Earth, Atmospheric and Planetary Sciences
in partial fulfillment of the requirements for the degree of

Doctor of Philosophy

at the

MASSACHUSETTS INSTITUTE OF TECHNOLOGY

and the

WOODS HOLE OCEANOGRAPHIC INSTITUTION

May 2022

©2022 Michaela Fendrock.

All rights reserved.

The author hereby grants to MIT and WHOI permission to reproduce and to
distribute publicly paper and electronic copies of this thesis document in whole or in
part in any medium now known or hereafter created.

Author
Joint Program in Marine Geology & Geophysics
Massachusetts Institute of Technology
& Woods Hole Oceanographic Institution
May 9, 2022

Certified by
David McGee
Associate Professor
Massachusetts Institute of Technology
Thesis Supervisor

Certified by
Alan Condron
Associate Scientist
Woods Hole Oceanographic Institution
Thesis Supervisor

Accepted by
Oliver Jagoutz
Chair, Joint Committee for Marine Geology and Geophysics
Massachusetts Institute of Technology/
Woods Hole Oceanographic Institution

Questions and Clarity: Insights from Applying Computational Methods to Paleoclimate Archives

by

Michaela Fendrock

Submitted to the Joint Program in Marine Geology & Geophysics
Massachusetts Institute of Technology
& Woods Hole Oceanographic Institution
on May 9, 2022, in partial fulfillment of the
requirements for the degree of
Doctor of Philosophy

Abstract

It is a scientifically accepted fact that the Earth's climate is presently undergoing significant changes with the potential for immense negative impacts on human society. As evidence of these impacts become clear and common, it becomes ever more important to constrain the nature, magnitude, and speed of changes to Earth systems. A fundamentally important tool to this understanding is the Earth's past, recorded in the geologic record. There, lie examples of climate change under various forcings: important data for understanding the fundamental dynamics of climate change on our planet. However, when a climate signal is written in the geologic record, it is coded into the language of proxies and distorted by time. This thesis endeavors to decode that record using a variety of computational methods on a number of challenging proxies, to draw more information from the climate past than has previously been possible. First, machine learning and computer vision are used to decipher the primary, centimeter-scale textures of carbonate deposits in Searles Valley and Mono Lake, California. This work is able to connect facies in the tufa at Searles, grown during the Last Glacial Period, and those forming presently at Mono Lake. Next, the tracks of icebergs purged during Heinrich Events are simulated using the MIT General Circulation Model. This work, running multiple experiments exploring different aspects internal and external to the icebergs, reveals wind and sediment partitioning as centrally important to the spatial extent of Heinrich Layers. Each of these works considers a traditional geologic archive – a carbonate facies, a marine sediment layer – and uses computational methods to approach that archive from a different perspective. By applying these new methods, more information can be gleaned from the geologic record, building a richer narrative of the Earth's climate history. The final chapter of this thesis discusses effective teaching and strategies for building communities to support teaching practice in Earth Science departments.

Thesis Supervisor: David McGee
Title: Associate Professor
Massachusetts Institute of Technology

Thesis Supervisor: Alan Condron
Title: Associate Scientist
Woods Hole Oceanographic Institution

Acknowledgments

This thesis work was funded by the MIT EAPS Rasmussen and Whiteman Fellowships, NSF Project Number NSF-EAR-1903544, and the WHOI Academic Programs Office.

When I was a sophomore at Wellesley, I spent the summer working in a lab at MIT. I leached soil samples and diluted cave waters for a study investigating climate change during the Last Glacial Period in a place called Bonneville Basin, using a stalagmite from a cave there. The summer was fine, but I left feeling that I knew paleoclimate wasn't for me. I kept in touch with my advisor from the summer, David McGee, who was kind and encouraging and always willing to talk. And when I finally realized that Paleoclimate actually really is for me, David took me back on. David has given me immense space to grow and learn, and has been a profoundly important thought partner in all aspects of my time in graduate school. David is intimately familiar with my motto that "growth comes in discomfort", and has repeatedly demonstrated his dedication to not just my own growth, but to growing with me. I wouldn't be the scientist or teacher that I am today if not for him, and I thank him for all the years of growing and learning together.

I'd next like to thank Alan Condron, my other advisor. Alan and I stumbled across each other in our respective first years: me of my PhD, him at WHOI. Our advisorship has been one of many, many exciting ideas and exhilarating discoveries. Working with Alan has often felt like the imaginary ideal of grad school: the model doesn't work for many frustrating weeks, but then when it does, it works perfectly. Alan and I didn't plan to work together, but I'm so glad we found each other, and I'd like to thank him for the kindness, the guidance, and the thrills.

While David and Alan have been extremely effective scientific co-parents to me, the saying goes that it takes a village. So I'd next like to thank my wonderful committee: Andrew Ashton, Kristin Bergmann, and Carrie Morrill, as well as my defense chair Taylor Perron. I've never been afraid to have a committee meeting, and I've come out of every one with a sense of clarity and a direction forward, with much to consider. Thank you all for your help and thoughtfulness, and for being on my team.

My fellow McGee Lab graduate students, and especially Research Scientist Adam Jost, who has been such an immense help even though I'm not a mass spectrometer.

The Teaching Development Fellows and the Teaching and Learning Lab for advocating for pedagogy and modeling a community of practice.

The Wellesley Geosciences faculty for winding me up, setting me off, and cheering me on.

My family: My dad for teaching me that anything worth doing, is worth doing well. Steve Prefontaine said "to give anything less than your best is to sacrifice the gift", but my dad could have said that. My mom, who has always believed in me more than anyone. She's always made sure I knew I was smart, even when everyone else, including me, said that I wasn't. My sister for reminding me that I'm actually not that smart. But more to the point, that I can believe in myself without taking myself too seriously. My Aunt Bonnie

for being a sounding board and constant, and my Uncle Alan for reminding me to pull the starter, give a mouse a cookie, and otherwise weather the storm of academia. Cousin Erika for challenging me and talking frogs, and other cousin Vince for taking on the responsibility of being the most obnoxious person at the ballpark. And Coby, for being a good boy.

My friends, whom I won't do the disservice of naming, but who have gotten me through all of it.

The Boston Red Sox, for being bad when it was helpful for them to be bad, and good when it was helpful for them to be good. Special thanks to the 2018 Red Sox for bringing it home when I was home; and the 2021 Red Sox for being the scappiest team, when I need some inspiration to be scrappy. And a blessing and a wish for the 2022 Red Sox: may the water be dirty.

The roads and trails and ponds where I rode and ran and swam, and felt calm when nothing was calm. My legs for being patient with me and getting where I needed to go.

Asha, for being the best and truest friend I've had.

And the Earth, where all of this happened.

Contents

1	Introduction	17
1.1	The Significance of Earth’s Past Climate	17
1.2	Proxies and the Difficulty of Reading the Geologic Record	19
1.3	Models, Data, and Modeling Data	20
1.4	Building Pedagogical Practices Commensurate with the Science We Teach . .	22
2	A Computer Vision Algorithm for Interpreting Lacustrine Carbonate Textures at Searles Valley, USA	25
2.1	Abstract	25
2.2	Introduction	26
2.2.1	Areas of Study	29
2.3	Methods	33
2.3.1	Pre-Processing	34
2.3.2	Machine Learning Algorithms	35
2.4	Results	38
2.5	Discussion	41
2.6	Future Work	44
2.7	Conclusions	46
3	Modeling Iceberg Longevity and Distribution During Heinrich Events	49
3.1	Abstract	49
3.2	Introduction	50
3.3	Methods	53
3.3.1	Iceberg Model	53
3.3.2	Experiments	54

3.4	Results	55
3.5	Interpretation and Discussion	61
3.6	Conclusions and Future Work	64
4	A Model for the Effect of Partitioning Sediments in Icebergs on Heinrich	
	Layer Extents	67
4.1	Abstract	67
4.2	Introduction	68
4.3	Methods	71
	4.3.1 Iceberg Model	71
	4.3.2 IRD Module	73
4.4	Results	75
	4.4.1 Lateral Extents of Layers	76
	4.4.2 Thickness of Layers	79
4.5	Discussion	82
4.6	Significance	84
4.7	Future Work	85
5	Towards a Sustained Community of Practice Around Pedagogy in EAPS	87
5.1	Abstract	87
5.2	Introduction	87
5.3	Needs Assessment	89
5.4	Fall Semester Discussion Group	91
5.5	12.s597: Seminar in Teaching in EAPS	91
	5.5.1 Topics and Readings	92
	5.5.2 “Bring a Thing”	98
	5.5.3 Strengths and Growth Areas of this Course	101
5.6	Faculty Panel	102
5.7	Reflections and Looking Forward	103
	5.7.1 Future Iterations Of 12.s597	103
	5.7.2 Future Teaching Development Fellows	104
A	Supplementary Figures	105

List of Figures

2-1	Locations of basins considered in this study: Mono Lake (north) and Searles Valley (south). Locations of tufa considered in this study are indicated by a white box at Mono Lake and by labeling of sites at Searles Valley. Contours are at 50m intervals of meters above sea level.	27
2-2	Examples of the endmember facies relevant to this study: (A) Porous tufa, (B) columnar tufa, (C) nodular tufa with well defined, popcorn-like baubles, and (D) a more weathered example of nodular tufa.	30
2-3	Comparable textures at Searles (left) and Mono (right), as well as similar large-scale structures (bottom row). The “towers” found at Searles (such as those shown here) are found most commonly at the Amphitheatre site, which was found to have the highest proportion of columnar tufa.	32
2-4	Steps in preprocessing tufa images: (A) Original image (scale bar left for reference in this paper but would otherwise be removed), (B) image converted to greyscale to avoid color effects (e.g. the orange on the left of the original image), and (C) equalizing of image histogram for uniformity of shading. This step has the added benefit of emphasizing the textures pictured.	34
2-5	Clusters found by k-means, clustering on the output of the t-SNE algorithm for (left) the images taken at Searles Valley and (right) the images taken at both Searles and Mono Lake. The 0-1 scale on each axis is dimensionless, the output of the t-SNE algorithm. Nominally, the Euclidean distance between points corresponds to their visual similarity. Points plotted in black are the Mono Lake data. Note that the plot on the right is approximately equivalent to the left plot rotated by $\sim 45^\circ$ clockwise.	40

2-6	Distributions of each cluster by basin. Mono is skewed towards cluster 2 (columnar), while Searles is skewed towards cluster 1 (weathered nodules).	40
2-7	Distribution of facies within sites. The Amphitheater has the highest proportion of columnar tufa and is the only Searles site with more than 50% columnar. Mono Lake similarly had proportionally more columnar tufa (Figure 2-6).	42
2-8	Comparison of Searles clusters to environmental data. In the top panel, images are binned into hundredths of a degree bins. In the bottom panel, boxes extend from lower to upper quartile of data, whiskers show range. Orange horizontal line is plotted at the median. Blue circles are outliers.	43
3-1	Panel A: Map of IRD thickness in the North Atlantic deposited during Heinrich Event 1, adapted from Hemming (2004). Each triangle represents the location of a marine sediment core containing HE-related IRD and the corresponding numbers the thickness (in centimeters) of the IRD. Stippling indicates inferred HL extent. Panel B: Simulated iceberg density in the North Atlantic releasing medium sized icebergs from Hudson Bay (red arrow) for the full 10-year Heinrich Event. In agreement with the observation (Panel A) the model shows that icebergs drift across the entire North Atlantic to Europe. The “forking” pattern in IRD in the observations ($\sim 45^\circ\text{N}$, $\sim 20^\circ\text{W}$) seen here can be observed in model results from this study, especially in summer months (Figure 3-4). Note that the line running between $\sim 40^\circ\text{N}, 40^\circ\text{W}$ to $45^\circ\text{N}, 10^\circ\text{W}$ is an artifact of the seam on the models cube-sphere grid, and not a function of the iceberg drift patterns. seam between GCM panels can be seen in these figures.	50
3-2	Simulated ice flux (the sum of the volume of ice from icebergs) through each model grid cell in the temperature sensitivity simulations (LGM [blue lines] and LGM - 3.5°C [red lines]). Contours are drawn at mean and 1% of ice flux in the Atlantic, of which the latter roughly shows the maximum eastward drift of icebergs in our simulations. All iceberg are of the “medium” size class (i.e. $465 \times 753\text{m}$ wide, 260m thick).	56

3-3 Panel A: Simulated mean ice flux through each model grid cell for the three size different iceberg size class experiments. Panel B: Maximum extent of icebergs (based on where ice flux at each cell is $\geq 1\%$ of the mean) for the three experiments. Large icebergs begin with $1000 \times 1620\text{m}$ width and depth, medium icebergs begin with $465 \times 753\text{m}$ width and depth, small icebergs begin with $250 \times 405\text{m}$ width and depth. All icebergs are 260m thick when calved. Means are calculated using only Atlantic cells (Atlantic defined as Longitude between 0° and 55°W). 57

3-4 Locations of simulated icebergs in the North Atlantic in winter (December-January-February; DJF), and summer (June-July-August; JJA) for the three different iceberg size classes based on the cumulative number of icebergs in each model grid cell. Regardless of iceberg size, there is a marked difference in iceberg drift trajectories in the winter and summer months: iceberg drift is much more zonal across much of the North Atlantic during the winter, while the summer iceberg trajectories show a split at around $\sim 45^\circ\text{N}$, 20°W where some portion of the icebergs drifting in a more northeasterly direction. As shown in Figure 3-1a, this split in trajectories is observed in IRD deposited during Heinrich Event 1. 58

3-5 Average locations of icebergs during all four seasons: winter (DJF), spring (MAM), summer (JJA), and fall (SON). As described above, iceberg tracks are observed to fork into two tracks in the summer: one traveling approximately due-east and one branching northeast. Remnants of this forking pattern can be observed in fall months, but absent in the spring. 59

3-6 Simulated change in North Atlantic sea surface salinity (salinity anomaly) during a Heinrich event simulation of medium-sized icebergs from Hudson Bay after 2, 5, 7, and 10 years. Freshening can be seen in the North Atlantic basin between $40^\circ - 50^\circ\text{N}$ where icebergs are most heavily concentrated, as well as farther afield in the Norwegian Sea. Sea surface salinities anomalies are calculated using the difference between numerical simulations performed with and without icebergs. 61

3-7 Prescribed wind forcing in glacial model (CCSM3) simulations for winter (DJF), spring (MAM), summer (JJA), and fall (SON). The seasonal shifts in the wind match the seasonal shifts in iceberg tracks (Figure 3-4). In particular, the summer forking in iceberg drift aligns with winds shifting to a more meridional patterns and blowing in a northeasterly direction. 62

4-1 Schematic for different sediment partitionings in icebergs: A) the “constant” partitioning, B) the “gradient” partitioning, C) the “basal” partitioning, and D) the “striped” partitioning. Sediment concentrations are distributed that each iceberg is calved with an overall 4% IRD concentration. 73

4-2 Heinrich Layer resulting from constant IRD concentration simulation (4% uniformly throughout). Both the spatial extent and approximate thicknesses compare favorably to observed Heinrich Layer extents, with a thin deposit formed near the coast of Portugal. Icebergs are calved at the red stars in the Labrador Sea. 75

4-3 Heinrich Layer produced in the IRD gradient partitioning simulation. The extent of this layer is extremely similar to that in the constant concentration simulation (Figure 4-2), as both simulations contained sediment throughout the full volume of the iceberg. This simulation thus also compares favorably to observed Heinrich Layers. 76

4-4 The Heinrich Layer produced by partitioning sediment in a banded pattern in the iceberg. Despite dropping relatively more sediment in the Labrador Sea, the simulation using icebergs with the striped partitioning of sediment was able to produce a fairly thick (~50cm) deposit at a longitude of about 30°W, farther East than other simulations. 78

4-5 The Heinrich Event simulation using the basal partitioning could not produce a deposit that was either similar to a Heinrich Layer or geologically realistic. Thus, this partitioning is not considered to have significantly contributed to the production of Heinrich Layers. 79

4-6 Comparisons of modeled Heinrich Layers to core data reported in Hemming (2004). Layer thicknesses in core data are compared to (A): simulated layer thickness in the model cell where the core is located; (B): Maximum modeled layer thickness (blue shading) by longitude for the constant concentration simulation; (C): Maximum modeled layer thickness (orange shading) by longitude for the gradient concentration simulation; and (D): Maximum modeled layer thickness (purple shading) by longitude for the striped simulation. Curves of maxima for simulated core thicknesses are smoothed using a 5 point moving mean. 80

A-1 Time series of icebergs in the model system from the beginning to end of a 10-year Heinrich Event. The number of icebergs varies by calving season but is stable on the time scale of the experiment. 106

A-2 Average seasonal magnitude of surface currents during Heinrich Events. These currents do not change with the magnitude or direction necessary to explain the change in iceberg trajectories. 107

List of Tables

2.1	Parameterizations that were run on the full data set, after testing on a representative subset. Bottom row (bolded) was ultimately used for the analysis below.	38
2.2	General distribution of facies between clusters. The right column (“20 end-members”) shows the division of the 20 images from each cluster that plotted farthest from the mean image of the whole data set. The process for this selection is described in-text. Examples of the textures described here can be found in Figure 2-2.	39

Chapter 1

Introduction

1.1 The Significance of Earth's Past Climate

In recent years, it has become an increasing concern that anthropogenic climate change will significantly impact the ability of current and future generations to live comfortably on the planet. With a greater number of observed and predicted high-intensity storms, instances of coastal flooding, droughts, ice loss, and sea level rise, the need to predict the timing and magnitude of these changes has become more urgent (e.g. DeConto et al. 2021, Cook et al. 2018, Knutson et al. 2020, Hsiao et al. 2021). Predicting climate change, however, is made complicated by limitations of data. By nature, records of modern climate change go back at most only a few hundred years, to the beginning of anthropogenic forcings on climate (i.e. the burning of fossil fuels). These data are likewise biased towards the first stages of a long term process: our climate is still changing, and thus data of modern climate change cannot span the full arc of cause and effect. It is therefore helpful to seek more data about how Earth's climate changes under different conditions, information that can be found in the Earth's past and used to predict its future.

In its long history, our planet has undergone massive changes in climate with varying causes, and understanding the details of these events could provide a more robust framework for predicting future climate change. Though no past climate event is a perfect analogue to modern, many have qualities that may provide insight into future climate change. Even if the analogy is imperfect, data of past climate events may span the full narrative of perturbation to climate impact. Given adequate coverage in the geologic record, the timing, magnitude, and rate of change for past climate change can be examined, as can the differences of these

factors between regions. For example, concurrent with climate changes during the Last Glacial Period, some regions experienced increases in rainfall whereas others experienced drought (Wang et al. 2001). Though many of these changes occurred on millennial timescales, longer than modern climate change, examining the dynamics of increases and decreases of precipitation during the Last Glacial Period can contribute to understanding of how precipitation changes in response to global-scale warming or cooling. In studies such as this, the Earth’s past can be used to build understanding about the fundamentals of its climate.

In particular, Heinrich Events are times of abrupt climate change that may be particularly helpful in understanding future climate change. These events occurred during the Last Glacial Period, when extensive ice sheets covered much of North America. Periodically, the Laurentide ice sheet purged “armadas” of sediment-laden icebergs from the Hudson Strait into the North Atlantic where they melted, releasing sediment to the seafloor and fresh water to an ocean current of fundamental climate importance, the Atlantic Meridional Overturning Circulation (AMOC) (Barker et al. 2009). Thus, although these events were local to the North Atlantic, their climate impact was propagated globally: Heinrich Events are coincident with significant changes in the hydrology of the Southwestern United States, the Asian monsoon, and other distant climate systems (McGee et al. 2018, Wang et al. 2001, Li et al. 1996).

On the modern Earth, the AMOC continues to be a main driver of heat transport on the planet, and as ice sheets undergo significant losses during modern climate change, the need to understand the sensitivity of these systems has become all the more clear. Heinrich Events offer the opportunity to examine how the interactions of the AMOC and ice sheets can impact global climate. This task is made complicated, however, by the reality that the Laurentide ice sheet and the icebergs involved in Heinrich Events have long since melted, leaving only traces in the geologic record. An often-used record of Heinrich Events are layers of sediment grains larger than would typically be expected on the seafloor, which extend across the North Atlantic from the Hudson Strait to Portugal. The vast majority of these grains are known to be sourced from North America; stones found on the seafloor off the coast of Portugal were transported there, by icebergs, fully across the Atlantic Ocean from Canada. These sediments, often as diminutive as grains of sand, may hold the key to understanding catastrophic climate change that occurred thousands of years ago.

The first chapter of this thesis explores one of the impacts of Heinrich Events, the

filling of closed-basin paleolakes in the Southwestern United States. Particularly, it explores methods for interrogating the filling and draining of those lakes: shoreline carbonate deposits and their primary textures. The next two chapters investigate Heinrich Events themselves, aiming to decipher sedimentary records and in particular what icebergs would have looked like during Heinrich Events.

1.2 Proxies and the Difficulty of Reading the Geologic Record

While the Earth's past holds information that is central to predicting its climate future, efforts to uncover that past are limited by the geologic record. Only what has been recorded in geologic proxies can be known, and so the geologic record is incomplete: it is not possible to make a fully continuous record of past climate change, as proxies offer only a infrequent windows into complex processes that may vary regionally. Additionally, these proxies record in their own language: they may document a climate signal at an instant moment, or average over some amount of time. The recorded signal may be biased, and the bias may not be linearly predictable, or knowable without an independent proxy. Those who wish to interpret the geologic record thus face multiple challenges: archives are incomplete, and coded into proxy records. These records of paleoclimate, then, must be interpreted with caveats and in the context of the sum of other records. There is additionally the possibility of discovering new proxies, to broaden the possibility of uncovering the dynamics of past climate change.

Tufa, the first paleoclimate archive explored in this thesis, are in the best case proxies for minimum lake depth. Tufa exist in lakes and waterways around the planet, but this thesis will focus on two basins: Mono Lake and Searles Valley, both in California. In the case of these basins, tufa are relevant to an enormous pluvial lake system that existed in the Southwestern United States at the end of the Last Glacial Period on the scale of the Great Lakes (Smith 2009). Except at time of overflow, these lakes were hydrologically closed, meaning that their level was a function of evaporation and precipitation. Thus, these lakes can be used as archives of past wetness, if their level is known (Reheis et al. 2014). One tool for deciphering lake level is the aforementioned tufa (Stine 1990, Guo & Chafetz 2012, Fendrock, Chen, Olson, Lowenstein & McGee 2022). These lake carbonates are known to grow subaqueously, thus where tufa are found, a lake must have been. The precise depth at which tufa may grow, is not well known, however, and thus tufa are limited in that

they can only confidently define a minimum lake level: the lake’s surface elevation may have been much greater than the tufa’s elevation. The first chapter of this thesis, explores the possibility that the centimeter scale texture of tufa may contain untapped paleoclimate information, hinting at a greater potential for the future use of these archives.

Later chapters in this thesis discuss the layers of sediment produced by ice rafting during Heinrich Events, or so-called Heinrich Layers. These deposits vary between Heinrich Events, and it would be a boon to tie the variations of sediment amount and extent to a volume of ice discharge or some other climate forcing. This is an extremely complicated charge, however, since there is very little information about how much sediment an individual iceberg can carry or how that sediment was partitioned in the icebergs that participated in Heinrich Events. Icebergs could have been fully laden with sediment, or there could be an unknown volume of clean ice, with no sediment at all. It is known that Heinrich Events involved a discharge of ice that was involved in a significant perturbation to climate, but the work below attempts to limit the parameter space of that narrative.

In both of these cases, this thesis endeavors to apply new methods to well-studied paleoclimate archives. Using computational tools, work attempts to draw more information from the geologic record, either by exploring a lesser understood facet of the archive, as in the case of tufa, or by limiting the range of possibilities, as in the case of Heinrich Layers. These chapters also work to explore the possible biases of these archives, by approaching them from new, computational angles.

1.3 Models, Data, and Modeling Data

Given the limitations of proxies for past climate, it may be tempting to turn instead to computational models of climate. Global climate models (GCMs) can be effective tools for experimenting on the climate state: simulations of multiple scenarios may be run to interrogate scenarios for past or future climate change (e.g. Meinshausen et al. 2011, Roche et al. 2014). Compared to proxies, GCMs provide high resolution, relatively gapless information about numerous climate diagnostics, for essentially any given region. Thus, GCMs are invaluable tools for understanding the causes, effects, dynamics, and diagnostics of climate change through time, on multiple timescales.

Despite the promise of computational modeling of climate, there are a number of caveats

to their use. Though they tend to agree on general trends of climate change, various GCMs are known to give different regional results of magnitude and even direction of change for a given climate diagnostic for the same experiments (e.g. Screen et al. 2018, Otto-Bliesner et al. 2021). This is likely due to differences of model resolution and physics, which are considered differently in different models. For this reason, model ensembles are often considered in favor of individual models when predicting future climate or interrogating past climate (e.g. Collins et al. 2011, Hargreaves et al. 2013). Even in these cases, however, there exist significant discrepancies between model ensembles and data (e.g. Liu et al. 2014, Neukom et al. 2018). In sum: climate proxies derived from the geologic record are in general spatially and temporally infrequent, and may be biased in their representation of climate events. Global climate models have the benefit of coverage in space and time, but are not always in agreement with each other nor with the climate record. Determining the reality of past climate change must therefore involve thoughtful use of proxy records and global climate models, and consideration of the role of the geologic processes that build paleoclimate archives.

Previous works have shown that significant progress can be made towards reconciling modeled and proxy paleoclimate records using forward models of geologic processes (e.g. Dee et al. 2017, Osman et al. 2021). Specifically, an optimal parameterization of GCMs may be found by determining the actual climate signal that is recorded by a proxy. This may be done using a forward model that explicitly describes geologic processes: a proxy system model (PSM, Evans et al. 2013). Given a range of climate forcings, these models may be used to simulate a suite of possible proxy records. By comparing these results to actual proxy records, they may be used to evaluate the performance of GCMs, and generally to determine the most probable climate state that produced the record of interest. Proxy system modeling, and in general the use of computation to decipher the geologic record, is thus an important avenue for understanding past climate dynamics, and improving the ability to predict future climate change.

This thesis will first apply the general concept of using computation to deepen understanding of the paleoclimate record, by applying a new computational tool, machine learning, to tufa, carbonate deposits believed to be records of past lake level. This chapter endeavors to use these paleoclimate archives in a new way: to broaden their utility as proxies for past precipitation changes. This chapter is therefore more about creating and

improving proxy records of climate change, rather than building proxy system models as described above. The following chapters are more aligned with the goal of building forward models of the production of paleoclimate archives; using an iceberg model, coupled to a global climate model, to narrow the possible climate forcings that could have created Heinrich Layers. First, the impact of size of icebergs involved in Heinrich Events is explored, determining what impact this factor could have on the geologic record. Next, possibilities for sediment partitioning within icebergs are considered as a significant factor for the spatial extent of Heinrich Layers. Each of these chapters successfully employs computational tools to deepen understanding of the paleoclimate records, and uses geologic proxies to draw even richer information from Earth's history. Beyond their raw scientific goals, these chapters of this thesis seek to demonstrate the importance of combining computational tools, including climate models, with geologic records to build detailed narratives of paleoclimate.

1.4 Building Pedagogical Practices Commensurate with the Science We Teach

At its core, academia is about learning. As undergraduate students, we learn primarily from others. Eventually, through graduate school, we progress to creating knowledge with others. This is a transition away from being a student in the classical sense and towards becoming a researcher, an independent discoverer of facts. At the same time, however, should come a parallel transition from receiving and synthesizing knowledge to sharing and creating it. This sharing is important within the scientific community, in the form of writing academic papers and attending scientific conferences. But it should likewise involve guiding younger scientists in their journey to becoming independent researchers. As scientists at institutions with graduate and undergraduate students, teaching is central to academia.

In order to be an effective academic, it is thus important to teach well. In MIT EAPS, specifically, many faculty teach well, but there is a dearth of spaces to discuss pedagogy. Additionally, graduate students and others who may seek to improve their teaching do not have obvious avenues for developing Earth Science-specific pedagogy. There is an expansive literature about the theory of good teaching, including data-supported studies of how students best acquire and incorporate new information in class. In addition to these resources, the support and insight of peers can be essential to building a successful teaching practice.

In EAPS, we have built multiple spaces and platforms to share and receive feedback on research, including seminars, reading groups, and individual lab group meetings. Parallel structures to support sharing and discussing teaching could be invaluable to building and maintaining a culture of celebrating pedagogy in the department.

As the Teaching Development Fellow for EAPS in the 2021-2022 academic year, I have made a number of efforts to build spaces for the discussion of pedagogy in the department. The last chapter of this thesis is spent discussing these efforts, including a needs assessment, a Fall term reading and discussion group, an IAP course for credit, and a Spring term faculty panel. In addition to the specifics of these efforts, this chapter also discusses the reasoning behind the selection of these initiatives, as well as a vision for creating continuity in these efforts in future years. The intention of my time as the EAPS Teaching Development Fellow was to build momentum towards creating a community of practice around teaching in the department. Such a community will serve not only those who presently teach, but also those who are taught and those who wish to teach in the future.

Chapter 2

A Computer Vision Algorithm for Interpreting Lacustrine Carbonate Textures at Searles Valley, USA

2.1 Abstract

Investigations of the paleohydrologies of pluvial lake systems have often employed lake carbonate deposits called “tufa” that grow subaqueously and can be preserved long after the drying of the lake. For this reason, tufa have been used as a proxy for minimum lake level. However, they exhibit a variety of textures that hold the potential to reveal richer paleoclimatological information. With the goal of determining if tufa texture can be used as a proxy for lake environment, this study investigates the textures of tufa at Mono Lake, California in comparison to the fossil tufa in Searles Valley, California. While observations in the last century suggest that the tufa in the Mono basin grew in waters similar to the modern, the tufa at Searles formed during the last glacial period, when the Great Basin contained a system of pluvial lakes on the scale of the modern Great Lakes. The tufa at both basins have been observed to have a range of classifiable textures, and new methods of inspecting visual data could be informative about what factors control these textures. To this end, a t-Distributed Stochastic Neighbor Embedding (t-SNE) algorithm is used to project images of the tufa at Searles and Mono into a coordinate space, allowing for simple, quantitative comparisons of the visual similarity of textures. The textures of tufa at Searles are compared

to each other, as well as to the tufa at Mono. This study performs a robust assessment of the feasibility of Mono Lake as a modern analogue for Searles Valley. It finds that there is a justifiable basis for the comparison of certain fossil facies at Searles to the tufa at Mono, significant progress towards the goal of using texture as a metric for the environment in which tufa formed.

2.2 Introduction

As remnants of a wetter time, enigmatic deposits called tufa have been used as proxies for lake level in closed basin lakes. To first order, these deposits are known to have grown subaqueously. If they are found in a known or suspected lake system, they can be used to assign a minimum lake depth. That is, where tufa are found, there must once have been water. Along these lines, they have been dated using U/Th and radiocarbon dating, constraining the time when the observed lake level was reached (e.g. Broecker & Orr 1958, Kaufman & Broecker 1965, Candy & Schreve 2007). As carbonate deposits, tufa also hold significant potential for gleaning information about lake chemistry (e.g. $\delta^{18}\text{O}$, biological activity, Guo & Chafetz 2014, Petryshyn et al. 2016)). But with greater exploration, there is reason to believe that tufa hold more paleoclimatological information than simply lake chemistry. Depending on the mechanism of their formation, the presence of tufa could also be revealing of specific environmental factors. For example, if the precipitation of tufa was dependent on the presence of phototrophic organisms, tufa would only form shallow enough in the lake that light could penetrate (i.e. the photic zone), limiting the possible range of depths where tufa could grow (DeMott et al. 2020). Alternatively, inorganic precipitation of the tufa may require that the lake have a high alkalinity and an input of Ca ions (e.g. from springs). Gleaning the signature of these mechanisms in the geologic record would thus broaden the potential use of tufa as paleolake proxies. Tufa are found in a number of modern lakes in the United States and elsewhere (e.g. Green Lake, Pyramid Lake, Mono Lake), as well as in paleolakes that are now at significantly lower levels or fully dry (e.g. Lake Bonneville, Lake Manly, Searles Lake) (Ford & Pedley 1996, Ku et al. 1998, Guo & Chafetz 2012, DeMott et al. 2020).

Both preserved and relatively modern tufa exhibit a range of primary, centimeter-scale textures (e.g. Dunn 1953, Guo & Chafetz 2012). Even within a basin, it is likely that tufa

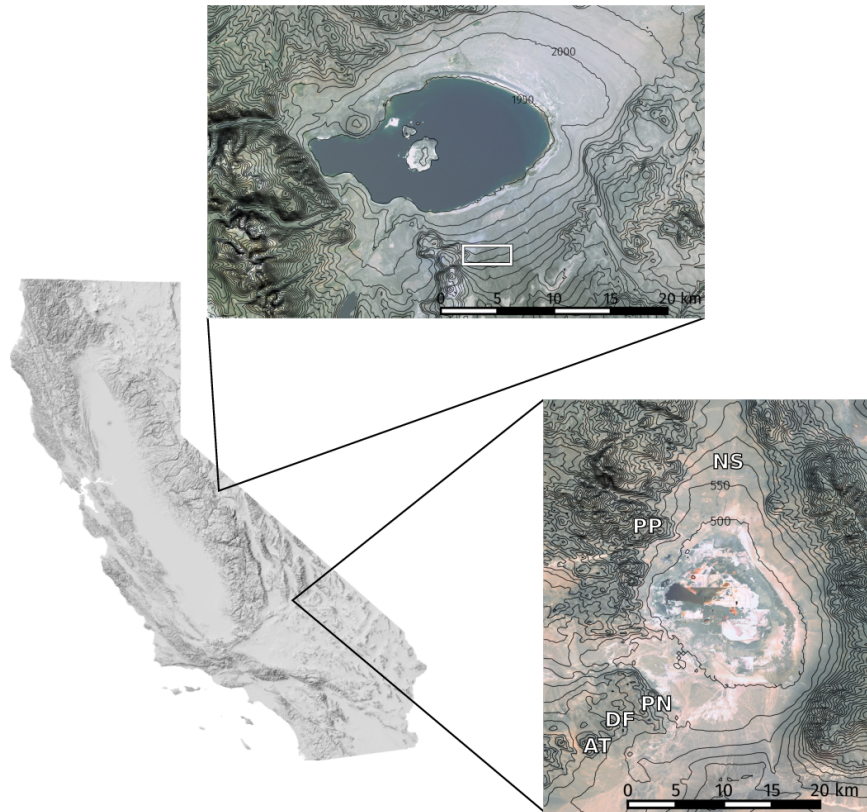


Figure 2-1: Locations of basins considered in this study: Mono Lake (north) and Searles Valley (south). Locations of tufa considered in this study are indicated by a white box at Mono Lake and by labeling of sites at Searles Valley. Contours are at 50m intervals of meters above sea level.

formed in different environments in terms of chemistry, depth, biology, temperature, or some combination of these factors: changes that may be reflected in the primary texture of the tufa (Shearman et al. 1989, Benson 1994). An avenue for exploring this connection could be to make comparisons of fossil tufa to modern tufa, whose growth environment is better understood. Traditional methods such as field comparisons and petrographic observations may be fruitful in these efforts. At Searles Valley, microscopic examinations of the micrometer scale structure of tufa suggested the possibility of microbial or bacterial involvement in the construction of tufa, but could not determine the degree to which such biology was necessary for tufa growth (Guo & Chafetz 2012). Similarly, microscopic inspection of the tufa at Mono find evidence for microbes living on the the tufa, but suggest also that the majority of tufa is precipitated inorganically (Brasier et al. 2018). Indeed, earlier studies of the tufa at Mono found evidence for a purely abiotic precipitation mechanism for the tufa at Mono, driven by mixing of spring and lake waters (Bischoff et al. 1993). Thus, while it is likely that the tufa at Mono was precipitated abiotically, ambiguity remains about the tufa at both of these basins, and new tools may provide valuable perspectives.

To this end, it has been demonstrated that machine learning has the ability to uncover nuances in data sets that are too subtle or complicated for human researchers (e.g. Pérez-Ortiz et al. n.d., Fang & Li 2019, Huntingford et al. 2019). With relative ease, machine learning can thoroughly evaluate a data set, while at the same time rigorous computational iteration allows for confidence that the best solution has been found. A form of this, the field of computer vision is concerned with using computers to better understand visual data such as digital images.

Here, a computer vision algorithm is used to objectively classify tufa textures in two closed basin lakes: Searles Valley, CA and Mono Lake, CA (Figure 2-1). Closed basin lakes are basins with no outflows. As a result, the level of these lakes depends on the difference between precipitation into the lake or its inflows, and evaporation out of the lake ($P - E$). Studies have attempted to solidify the relationship between past climate and paleolake level using hydrological balance models (e.g. Hostetler & Bartlein 1990), however these efforts are limited by knowledge of past lake level. If evidence of the depth of a closed basin lake can be gleaned from the geologic record, it can be used to constrain modeling efforts. This work assesses the utility of computer vision as a complement to more traditional, field-based geologic investigations. It also investigates the relationship between computer vision-based

classifications of tufa texture and environment, including an assessment of the comparability of the better understood Mono Lake tufa to the fossil tufa in Searles Valley. Specifically, a machine learning algorithm is used to compare tufa textures found within Searles and Mono to ask the following questions: **1)** Is a particular facies of tufa at Searles objectively visually similar to those at Mono? And **2)** Can the variance of tufa textures at Searles Valley, CA be tied to their elevation – perhaps corresponding to instances of comparable lake conditions or background climate?

2.2.1 Areas of Study

Searles Valley

During the late Pleistocene, the drainage from the Sierra Nevada flowed through the Owens River into Owens Lake (Peng et al. 1978, Figure 2-1). When P - E was high enough, Owens Lake would overflow into China Lake, which, with sufficient precipitation, would in turn overflow into Searles. The chain would continue with Panamint Lake and then Lake Manly (present-day Death Valley, Jayko et al. 2008). When Searles did not overflow, it was the terminus of the drainage and could be considered a true closed basin lake. This was the case for much of the lake's history, and during these times its level was an indicator of the up-stream hydrology of the lake system described above (Smith 2009). The lake level history of Searles is thus of great interest for deciphering the hydroclimate of the Great Basin in the Late Pleistocene. Past studies gleaned past lake level by inferring relative lake depth from salts in sediment cores, revealing a history of dramatic lake level change (Smith 2009). However, shoreline studies are necessary to accurately determine the magnitude of lake level change and constrain the true depths that the lake reached in its past.

In addition to sediment cores, past researchers have used the extensive tufa deposits at Searles to investigate its hydrological past. The tufa in Searles Valley exhibit a variety of morphologies and textures from the almost 50m tall Pinnacles in the south of the basin to the more localized mounds higher on the shores of the paleolake (locations shown in Figure 2-1). In studies based in the Pinnacles, the Searles tufa offer a distinctive stratigraphy (Scholl 1960, Guo & Chafetz 2012). The four reported facies are: porous, nodular, and columnar tufa; and finely laminated crusts (Figure 2-2). The porous tufa are the most common in north and central parts of the Pinnacles, and exhibit a somewhat open texture with subplanar fabrics,

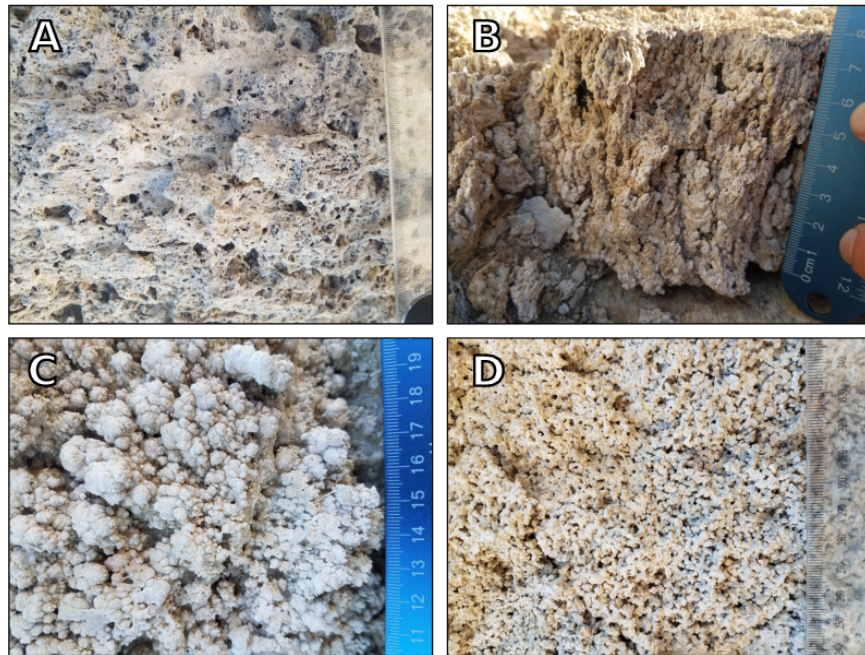


Figure 2-2: Examples of the endmember facies relevant to this study: (A) Porous tufa, (B) columnar tufa, (C) nodular tufa with well defined, popcorn-like baubles, and (D) a more weathered example of nodular tufa.

resembling the exterior of a wasps' nest. From stratigraphic context, Guo & Chafetz (2012) suggest that one interval of porous tufa is believed to be the youngest deposit in the Searles tufa, and another is believed to be the oldest. The nodular tufa overlay the older porous tufa layer and occur most commonly in the northern Pinnacles. They have a popcorn-like texture and are composed of multiple generations. The columnar tufa overlay the older porous tufa and occur most commonly in the middle group. They resemble asparagus bunches and are found in various states of weathering. The finely laminated crusts areas described, and are found draping either the nodular or columnar tufa. The stratigraphy defined by Guo & Chafetz (2012) at the Pinnacles is thus (from inner to outer/oldest to youngest): older porous tufa, columnar or nodular tufa (depending on part of the basin), finely laminated crust, younger porous tufa. The finely laminated crusts are not considered in this study, as the exposure of this facies is too limited to produce an adequate sample size.

Despite this well defined stratigraphy, the mechanism and conditions surrounding the formation of the tufa and its various facies are not well known. While some deposits are reasonably interpreted as "shoreline" (i.e. shallow) tufa, others, such as the Pinnacles, seemingly must have formed at significant depth. The usefulness of these deposits could thus

be improved with a better understanding of how they formed as well as what controls the observed variability of texture. Should the variety of textures seen in tufa prove to correspond to a particular depth or chemical regime in the lake (e.g. saturation state), the carbonate deposits could be used to more precisely constrain lake level and environment at the time of deposition. Comparison of the variability of tufa textures within Searles Valley will address the second question posed above: does the variability of the textures of tufa in Searles correspond to their elevation in the basin?

Mono Lake

Mono Lake is north of Searles in the Eastern Sierra Nevada. Mono is in a structural basin of the Eastern Sierra, a tectonically and volcanically active area (Stine 1990). Also a closed basin lake, the level of Mono reflects the drainage of the Eastern Sierra. During the late Pleistocene, a larger lake known as Lake Russell filled the Mono basin (Benson et al. 1990)). Like most other Great Basin lakes, the most recent highstand in the Mono basin occurred during Heinrich stadial 1 (Munroe & Laabs 2013). Records of higher lake-level can be found in shoreline features at high elevation in the basin, cores from the lake, and other geomorphic evidence including stream cuts through deltas and other lacustrine deposits (Stine 1990).

At Mono Lake, the interaction of Ca^{2+} rich spring water with the carbonate-rich lake water contributes to the growth of tufa (Dunn 1953, Scholl & Taft 1964, Council & Bennett 1993). These tufa are home to algal communities that are believed to promote their growth, though not significantly enough to classify them as “microbialites” (Scholl & Taft 1964, Brasier et al. 2018). Indeed, the saturation state of water is believed to be the primary driver of the deposition of tufa at Mono Lake (Council & Bennett 1993). One mechanism for their formation would be that spring water percolates through the shaft of the tufa and is discharged from the top, and carbonate is precipitated on the outside of the structure (Scholl & Taft 1964). The diversion of Eastern Sierra water by the Los Angeles Aquaduct lowered Mono Lake’s level by almost 15m, exposing tufa along much of the lake’s shoreline (Vorster 1985). The Mono Lake tufa can thus be explored in detail from land, though the lake is believed to still be actively forming the deposits, a process that has been observed visually within the last century (Dunn 1953, Bischoff et al. 1993). Previous researchers (e.g. Dunn 1953) have noted the presence of 3-4 facies of tufa, with more porous tufa deeper in the lake or at its shore, and more dense, nodular-type tufa above shore (i.e. from a time when

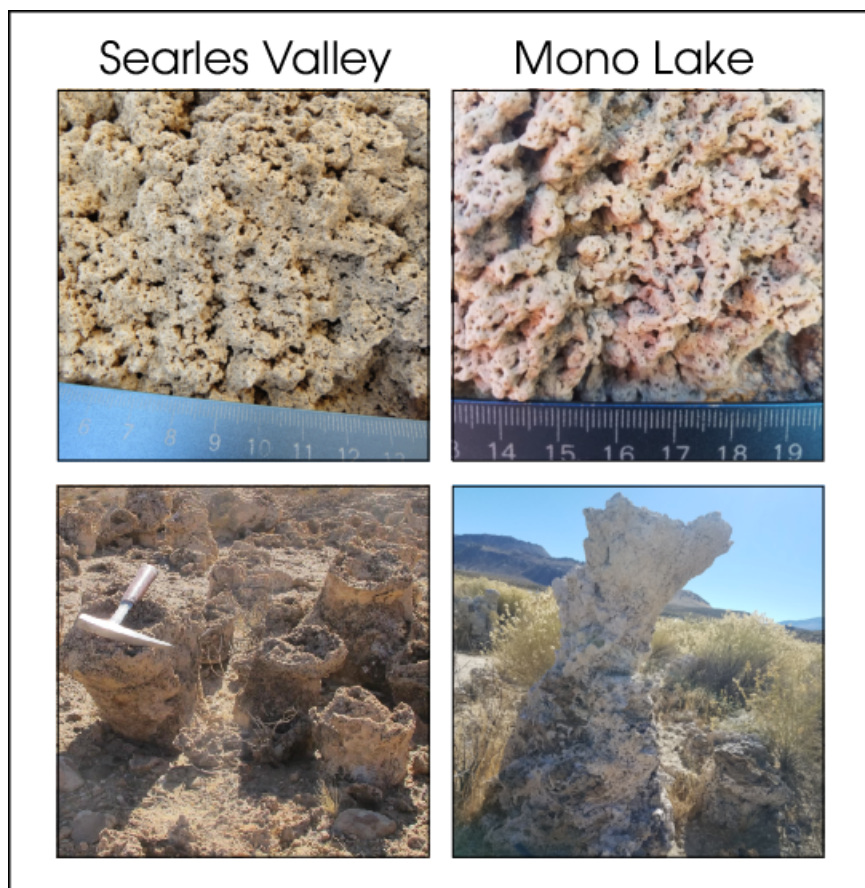


Figure 2-3: Comparable textures at Searles (left) and Mono (right), as well as similar large-scale structures (bottom row). The “towers” found at Searles (such as those shown here) are found most commonly at the Amphitheatre site, which was found to have the highest proportion of columnar tufa.

lake level was higher). These facies were not necessarily observed or captured in this study. However, given that past workers had access to the North Shore of Mono Lake (which was not accessible for this study), it is reasonable to expect that the range of tufa seen at Mono Lake in this study is smaller than that of previous studies. Likewise, the tufa available for inspection to this study were all at approximately the same elevation (modern lake level), thus a within-basin comparison of tufa texture to elevation was not possible.

Comparison of the tufa observed at Mono Lake will address the first question posed above: how do the tufa at Searles compare visually to the tufa at Mono? How does this comparison inform the interpretation of the environment in which the Searles tufa formed?

2.3 Methods

Data for this project were collected during field seasons in October of 2018 at Searles and Mono Lakes, and January 2020 at Searles. The data set consists of $\sim 1,500$ images collected of the textures of the tufa at the two lakes. Photo sites were chosen by exposure: all outcrops available and accessible in Searles and Mono were photographed. Photos were taken where textures were best exposed: this means that nodular and porous tufa were imaged in planform, whereas columnar tufa were imaged in cross section. It is possible that this difference could introduce unexpected biases to the results of this study. However, the orientation of images in cross-section or planform was an unavoidable limitation of how the textures were exposed.

The field of view captured in these images varied somewhat in size, but were ~ 10 cm across (scale bar later removed for processing). In collecting images, effort was taken to maintain uniform lighting (e.g. by shadowing on particularly bright days) and to avoid major, non-primary textural features such as cracks or plant overgrowth. The data processing of this project was performed in four parts, discussed in greater detail below: (1) the data were preprocessed to normalize for visual and structural similarity, (2) A t-SNE algorithm was applied to the images to reduce the dimensionality of the data, (3) a k-means clustering algorithm was used on the results of (2), and (4) clusters from part (3) were compared to environmental data (e.g. elevation, locality). These steps reduced the data from raw field images into data points that could be more easily numerically manipulated in later steps, and compared to each other in a quantitative manner.

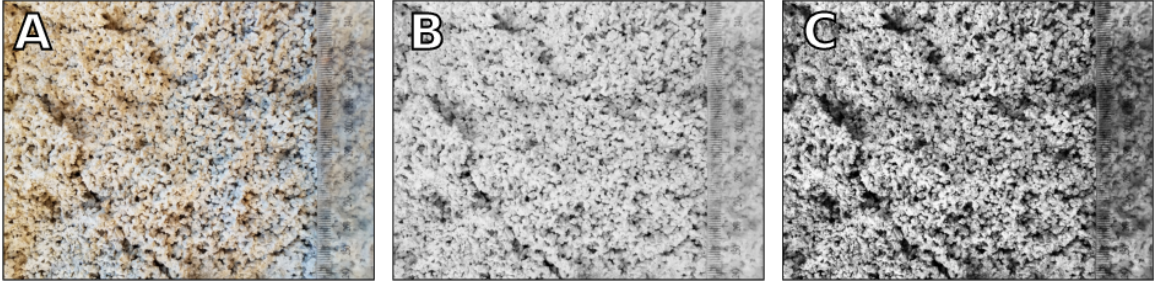


Figure 2-4: Steps in preprocessing tufa images: (A) Original image (scale bar left for reference in this paper but would otherwise be removed), (B) image converted to greyscale to avoid color effects (e.g. the orange on the left of the original image), and (C) equalizing of image histogram for uniformity of shading. This step has the added benefit of emphasizing the textures pictured.

2.3.1 Pre-Processing

Images were pre-processed with the goal of eliminating all features irrelevant to the textures pictured. The information of color and lighting were not relevant to the goal of the algorithm: to classify the variability of the textures in the tufa. Thus, all pre-processing was in effort to normalize images across these parameters (Figure 2-4). Images were considered to be on a reasonably comparable scale as collected, so scale bars were cropped out and no further steps were taken to normalize scale. Then, all images were converted to greyscale to remove color effects. Though the tufa are broadly similar in color, there is a possibility of differences between images due to lighting effects and camera white balance. The image histogram was then equalized to remove remaining lighting effects. Though effort was made in the field to have uniform lighting in images, this was not always possible. To minimize the possibility of the algorithm clustering on lighting effects (rather than actual geologic information), histogram normalization brightens darker areas in the image and darkens lighter ones creating the effect of uniform lighting. Finally, the t-SNE algorithm used here requires image inputs of uniform size. Thus, images were trimmed to the size of the smallest image in the data set after the scale was removed. Trimming was done from the edges to retain the center of the image, where the image taker would have directed their focus.

2.3.2 Machine Learning Algorithms

t-Distributed Stochastic Neighbor Embedding

t-Distributed Stochastic Neighbor Embedding (t-SNE) is an algorithm used to transform complex, high-dimensional data sets into a more manageable space of 2 or 3 dimensions (Van der Maaten & Hinton 2008). In addition to Uniform Manifold Approximation and Projection (UMAP), t-SNE has become one of the standard algorithms for managing high dimensional data by projecting it into lower dimensions, both are used commonly in health care applications (e.g. Abdelmoula et al. 2016, Li et al. 2017, Kobak & Berens 2019), and increasingly in the Earth sciences (e.g. Klimczak et al. 2020, Njock et al. 2020). In direct comparisons, UMAP and t-SNE have been found to have similar results (Becht et al. n.d., Kobak & Linderman 2019). This study uses t-SNE, but it is expected similar results would be found using UMAP. Other algorithms exist for comparing the similarity of images (e.g. Convolutional Neural Nets, Artificial Neural Nets), but this study focuses solely on the effectiveness of t-SNE.

As mentioned above, the specific function of these algorithms is to project complicated, high-dimensional data into a more manageable space. Though images are often (and not incorrectly) thought of as two-dimensional, in the case of digital images, their dimensionality can also be considered equal to the number of pixels. In this case, each pixel is a vector with magnitude equivalent to the pixel's color value. When plotting digital image data in this space, the relative location of the images will correspond to where the variability within the images lies: their visual similarity (Alfeld et al. 2018, Pouyet et al. 2018, Linderman & Steinerberger 2019). However, as this space has a number of dimensions equal to the number of pixels in each image, working with data in this way is extremely difficult. t-SNE allows for the projection of data from higher dimensions into two dimensions, where they can be more easily manipulated. The projection step maintains the relative distance of data points to each other and thus also maintains the overall structure of the data set (Linderman & Steinerberger 2019).

In the implementation of t-SNE in this study, each image is considered an object and each pixel in the image is considered a dimension of that object. A probability ($p_{i|j}$) of similarity between objects (e.g. x_i and x_j):

$$p_{i|j} = \frac{\exp(-\|x_i - x_j\|^2/2\sigma_i^2)}{\sum_{k \neq i} \exp(-\|x_i - x_k\|^2/2\sigma_i^2)} \quad (2.1)$$

where σ is the variance of a Gaussian surrounding object x_i . This Gaussian is computed depending on the parameterization of t-SNE, and has a larger bandwidth where the spread of the data is greater. Considering N objects, the probability p_{ij} is computed from the above values as:

$$p_{ij} = \frac{p_{j|i} + p_{i|j}}{N} \quad (2.2)$$

p_{ij} is thus the probability that x_i and x_j would be neighbors if all objects in the set were lined up by similarity (p_{ii} is set to zero). The algorithm then learns a map with corresponding points (i.e. y_i, y_j) that represent the similarities in p_{ij} . From this space, the probability of similarity between y -space points (q_{ij}) is computed:

$$q_{ij} = \frac{(1 + \|y_i - y_j\|^2)^{-1}}{\sum_{k \neq i} (1 + \|y_i - y_k\|^2)^{-1}} \quad (2.3)$$

q_{ii} is also set to zero. Finally, the locations on the final map are found by reducing the Kullback-Leibler divergence of the distribution of Q from that of P using gradient descent:

$$KL(P||Q) = \sum_{i \neq j} p_{ij} \log \frac{p_{ij}}{q_{ij}} \quad (2.4)$$

In the resulting data, objects are projected from their higher dimensional space into two dimensions. In simplest terms, the t-SNE algorithm calculates distances between objects in a high dimensional space. It then iteratively organizes objects in lower dimensional space, so that their relative distances are the same as (or as close as possible to) in their original higher dimensionality.

In this implementation, the “distances” are calculated based on the greyscale pixel values of the data, so the distances between objects should correlate to their visual similarity. Each object began with a dimensionality equal to the number of pixels, and ended as a 2-D object, each dimension a value between zero and one. When plotted by these dimensions, with the Euclidean distances between points proportionate to the visual similarity between corresponding images, we are able to observe the similarity of images as numerical data and view once qualitative relationships, quantitatively.

k-means

An unsupervised k-means clustering algorithm was then applied to each set of images corresponding to the basins (Mono and Searles). k-means clustering seeks to sort a data set into k clusters by similarity, with the Euclidean distances between clusters relating to the similarity between them (Pedregosa et al. 2011). In this study the k-means clustering was applied to the two dimensions resulting from the t-SNE algorithm, with the dimensions corresponding to visual similarity (Celik 2009). The parameter k (the prescribed number of clusters) was set to three to correspond to the hypothesized number of facies (nodular, columnar, porous).

Following the clustering of images from Searles alone, the algorithm was then run on the full combined set of images, determining the best clustering for the full data set including the images from Mono. A machine learning technique such as this is favored for its objectivity in image comparison, as well as the relative facility with which it can process 1,500+ images Kanungo et al. (2002).

Choice of Parameters

Two parameters are adjustable when using t-SNE: the number of iterations the algorithm goes through, and the perplexity. The algorithm “learns” each time it iterates through the steps defined above. One must then allow it enough “tries” to learn how to best project the data into a smaller dimensional space. However, too many iterations will make the algorithm unnecessarily slow. Perplexity is a measure of how the algorithm should weigh the similarity of neighboring data points as compared to the data set on a whole (Wattenberg et al. 2016). Since the nature of the clustering of the data was not well understood a priori, multiple parameterizations were tried to determine which would be best suited to the data. First, the algorithm was run on a representative subset of 20 images with each combination of perplexity 1 - 20 and for iterations of 250, 500, 1000, 2000, 3000, 5000, 7000, 10000, and 20000, with the intention of narrowing down the best possible parameterization while optimizing computing time. From these results, the algorithm was then run on the full data set using the parameterizations defined in Table 2.1.

For each of these t-SNE parameterizations, k-means clustering was performed and a number of clustering metrics were computed (Silo score, Calinski score, Davies Bouldin

Table 2.1: Parameterizations that were run on the full data set, after testing on a representative subset. Bottom row (bolded) was ultimately used for the analysis below.

Perplexity	Number of Iterations
17	250
19	250
9	250
19	3000
20	250
18	20,000

index; Palacio-Niño & Berzal (2019)). Unfortunately, the t-SNE parameterizations that were able to produce the k-means clusterings with the best metrics, also were interpreted as demonstrating artifacts of overfitting, including elongated mapping into lower dimensional space, as if points were plotted along a line (Wattenberg et al. 2016). Thus, the t-SNE parameterization with the least appearance of overfitting was chosen, a perplexity of 18 with 20,000 iterations, though its clustering metrics were relatively unfavorable. The realization that while the resulting clusters were less tight or separated, they generally contained the same set of points instilled confidence in this choice of parameters.

2.4 Results

The products of the t-SNE and k-means algorithms on the Searles data alone as well as with Mono data are shown in Figure 2-5. The clusters found by k-means abut each other and are not separated by space. If the clusters found by k-means are defined by visual similarity, they ought to each correspond to the three facies defined by (Guo & Chafetz 2012, nodular, columnar, porous), which were also defined by visual similarity. Images in each cluster were manually inspected to determine which facies were most common in each cluster – the result of this inspection can be found in Table 2.2. Porous tufa were distributed approximately evenly between clusters, seemingly not recognized as a separate facies. Rather, the more weathered facies, particularly the weathered nodules shown in Figure 2-2, were mostly in cluster 1 with some porous images. Cluster 2 was primarily the columnar tufa, with porous tufa that had a more elongate texture. Similarly, cluster 3 was nodular tufa with porous tufa with a somewhat nodular-like texture. None of the clusters excluded any of the facies, but roughly maintained the groupings described here with proportionally more of the relevant

Table 2.2: General distribution of facies between clusters. The right column (“20 endmembers”) shows the division of the 20 images from each cluster that plotted farthest from the mean image of the whole data set. The process for this selection is described in-text. Examples of the textures described here can be found in Figure 2-2.

Cluster Number	Facies	<i>20 endmembers</i>
1	Weathered nodular	<i>11 weathered nodular, 9 porous</i>
2	Columnar	<i>7 columnar, 13 porous</i>
3	Nodular	<i>2 weathered nodular, 9 nodular, 9 porous</i>

facies. Images of porous tufa were evenly distributed between clusters, likely because the texture of the porous tufa can at times appear like that of the other facies. Thus, in the following discussion the porous tufa will be ignored and the clusters will be referred to by the other facies they contained (per 2.2).

To confirm the facies assignments, the 20 images that plotted the furthest from the center of all the clusters were found for each cluster. That is, all three clusters are plotted on axes that range from 0-1 in x and y: the 20 points for each cluster were the farthest from the coordinate (0.5, 0.5). These points should be farthest from the “average image” for the whole data set, which would plot at (0.5, 0.5), and should thus be “endmember examples” of each cluster. A facies was then assigned to the set of 20 from each cluster. About half of each set of 20 were images of porous tufa, but the rest were as described above (cluster 1: weathered nodular, cluster 2: columnar, cluster 3:nodular). The results of this analysis are described in Table 2.2.

Black points in Figure 2-5 are the images collected at Mono Lake. Their distribution demonstrates that the textures of Mono overlap well with those at Searles, indicating that it is not necessary to consider them to be a separate facies from Searles. Likewise, the distribution of Searles data between clusters did not change with the inclusion of the Mono Lake data. That is, the addition of the Mono data did not significantly skew the distribution of clusters. This confirms a general observation in the field that the Mono Lake tufa are visually comparable to some tufa found at Searles.

The distribution of clusters between basins shows a marked preference for columnar tufa at Mono Lake and for weathered nodular tufa at Searles (Figure 2-6). The remaining images are approximately evenly distributed between the other two clusters at each basin, but with slightly more nodular tufa at Mono and slightly more columnar tufa at Searles. Almost half of the images from each basin are in the dominant cluster.

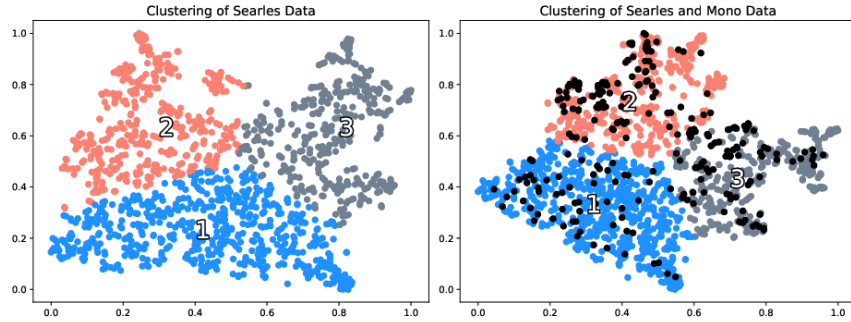


Figure 2-5: Clusters found by k-means, clustering on the output of the t-SNE algorithm for (left) the images taken at Searles Valley and (right) the images taken at both Searles and Mono Lake. The 0-1 scale on each axis is dimensionless, the output of the t-SNE algorithm. Nominally, the Euclidean distance between points corresponds to their visual similarity. Points plotted in black are the Mono Lake data. Note that the plot on the right is approximately equivalent to the left plot rotated by $\sim 45^\circ$ clockwise.

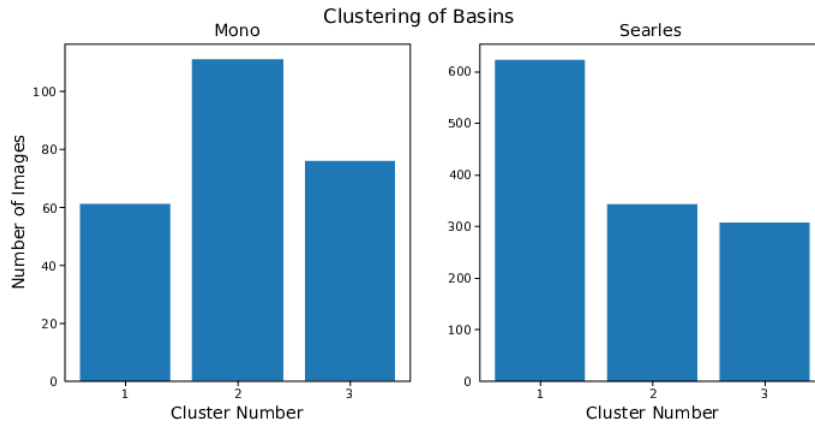


Figure 2-6: Distributions of each cluster by basin. Mono is skewed towards cluster 2 (columnar), while Searles is skewed towards cluster 1 (weathered nodules).

The clustering of images collected at Searles was compared to the spatial and elevational distribution of those images (Figure 2-8). Despite the $>200\text{m}$ spread in the elevation of data collected at Searles, no real elevation dependence can be observed between tufa facies. The latitudinal and spatial distribution of clusters were also considered (Figure 2-8). Latitude and field site were treated as separate variables to allow for inspection of local effects such as the exposure of a site (i.e. sheltered from the wind versus exposed to wave action). There is not a strong relationship between the clusters found in this study and latitude/field site. Roughly, though, columnar tufa tend to be more common south in the basin, whereas nodular is proportionally more northern. The northern sites (North Shore and Pioneer Point) have on average 46% nodular and 19% columnar, whereas the southern sites (Amphitheatre, Desperate Forest, and Pinnacles) have on average 22% nodular and 40% columnar.

Nodular tufa is generally found more commonly at the site referred to as “Pioneer Point”. Weathered nodular and columnar tufa are found at the site referred to as “the Amphitheater” (Figure 2-7). Indeed, the Amphitheatre is the only site at Searles with more than 50% of images falling in the “columnar” classification. This is notable, as the Amphitheater is the site in Searles with the most prominent and well-preserved “towers”, structures similar to those found at Mono where columnar tufa was also the dominant facies (Figure 2-3).

2.5 Discussion

The poor clustering of the results of the t-SNE projection could be attributed to a number of factors. First, the processes (e.g. biotic or abiotic precipitation of carbonate) producing end-member tufa textures could be acting at the same time most cases, producing intermediate textures. For example, it is possible that subsequent generations of tufa do not fully erase past textures, and instead work over them. It was observed in the field that columnar tufa may appear to grade into nodular as a primary texture (i.e. not as an effect of weathering). This is not mutually exclusive with the observation of Guo & Chafetz (2012) that these textures are distinct in different regions of the Pinnacles. Rather, it suggests that these facies could be coeval, but variations of lake conditions lead to different morphological expressions. It is also possible that the poor clustering of the data could be a result of a failure or poor parameterization of the t-SNE algorithm. However, this seems unlikely given the number of parameterizations that were tested.

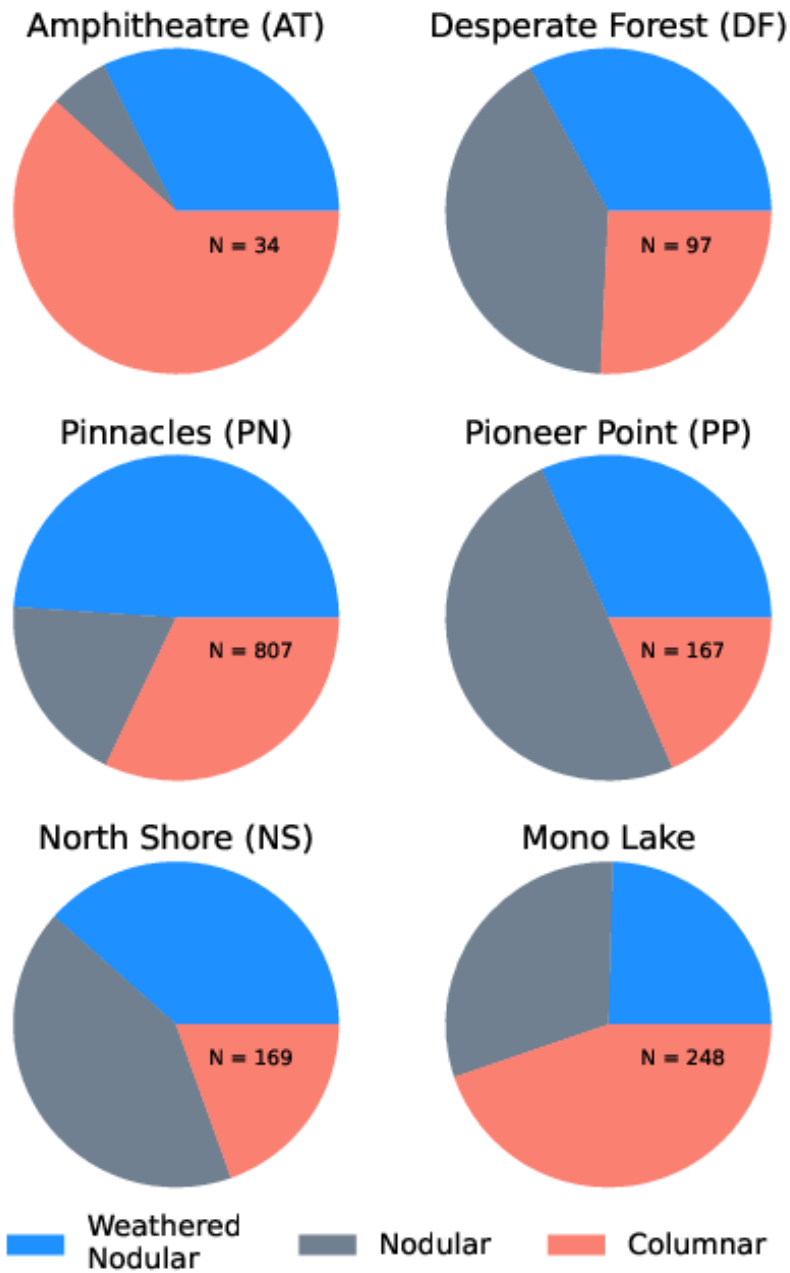


Figure 2-7: Distribution of facies within sites. The Amphitheater has the highest proportion of columnar tufa and is the only Searles site with more than 50% columnar. Mono Lake similarly had proportionally more columnar tufa (Figure 2-6).

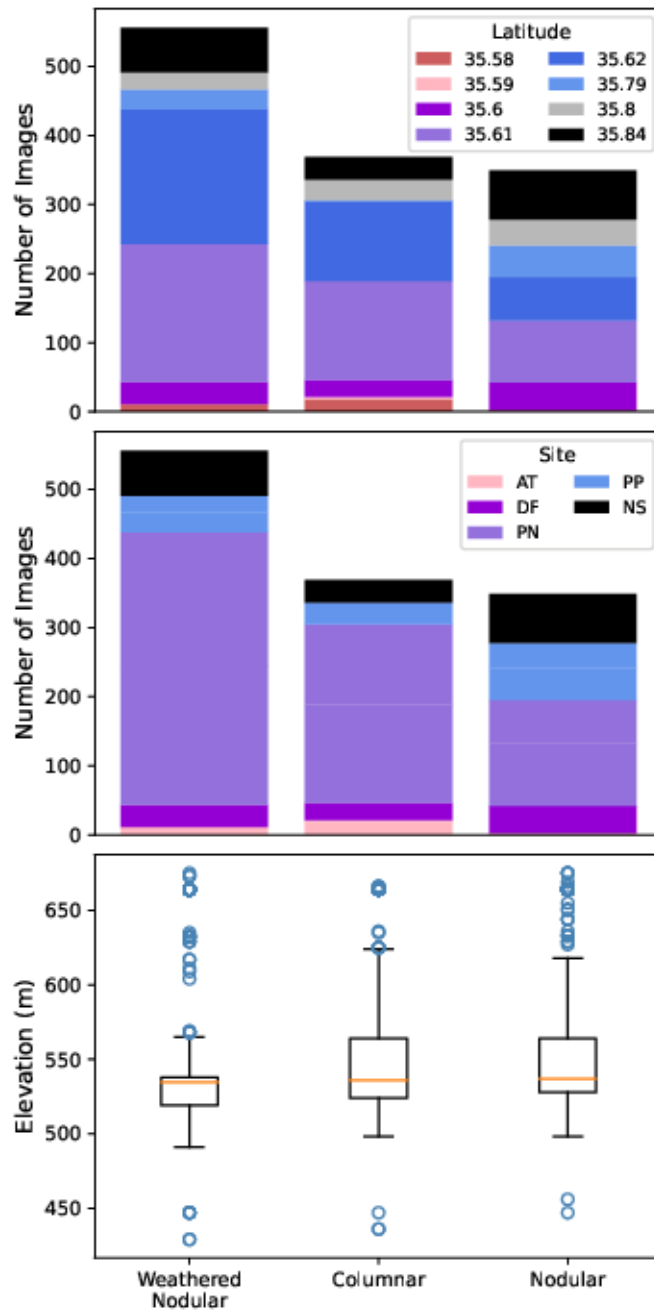


Figure 2-8: Comparison of Searles clusters to environmental data. In the top panel, images are binned into hundredths of a degree bins. In the bottom panel, boxes extend from lower to upper quartile of data, whiskers show range. Orange horizontal line is plotted at the median. Blue circles are outliers.

Since cluster 1 seems to be a primarily weathered facies, the dominance of cluster 1 at Searles could simply be because the tufa there are older, and thus more likely to be weathered. However, a statistical basis for correlating tufa texture to elevation could not be found. Thus, this study finds the answer to question 2) above “Can the variance of tufa textures at Searles Valley, CA be tied to their elevation – perhaps corresponding to instances of comparable lake conditions or background climate?”) is that the variance of tufa textures at Searles Valley, CA cannot be tied to their elevation in the basin.

The preponderance of columnar tufa at Mono Lake could indicate that the process responsible for producing this facies dominates tufa production at Mono Lake. Precipitation of tufa at Mono Lake is believed to be a primarily abiotic process, the result of spring discharge into the lake (Council & Bennett 1993). Also relevant to this comparison is the result that columnar tufa is the most common facies at Mono, as well as at the Amphitheater in Searles. As mentioned above, the Amphitheater at Searles is notable for the tufa “towers” that are prevalent there. These towers are found elsewhere in Searles, but are most common at the Amphitheater. Interestingly, Mono’s second most prevalent facies, the nodular tufa, is the dominant facies at Pioneer Point, a site where towers can also be found. The co-occurrence of these facies, especially the columnar tufa, with towers could indicate that the towers at Searles (of unclear origin) are the product of processes similar to those working at Mono (i.e. spring discharge).

2.6 Future Work

In this study, t-SNE is used largely as an unsupervised algorithm. That is, all the data are used together to allow the algorithm to find a “best” (most statistically defensible) solution; there does not exist a “training set” of data from which the algorithm learns. Since one of the aims of this work was to determine if t-SNE was able to find the same set of facies as human researchers, it was not considered necessary or even favorable to use a supervised algorithm. However, in light of this study, it would be worthwhile to compare the results found here to the facies defined by humans on the same data set. Such an effort would direct future work to refine the t-SNE and k-means algorithms for use on tufa data sets. It would likewise be of interest to compare the results of this study to the same analyses performed using different algorithms (e.g. UMAP, Convolutional Neural Nets, Artificial Neural Nets,

etc). This work demonstrates the utility of just one algorithm, and expanding to others would allow for more robust interpretations of tufa textures and their contexts.

While this study uses a "large" data set of 1,500+ images, machine learning algorithms almost always benefit from more data. A conclusion of the January 2020 field campaign was that (short of the discovery of new outcrops) further imagery is not necessary from Searles, as images have been collected of virtually all outcrops. However, future works could improve this effort by collecting more images from Mono Lake. An even richer study could include data from other basins with tufa grown in waters with a distinct chemistry such as Bonneville Basin, Pyramid Lake, and Death Valley (Lake Manly), or in the Altiplano-Puna plateau of the central Andes. The Eocene Green River Formation in Colorado could be another target for future work, particularly since they are rarely exposed in three dimensions (Awramik & Buchheim 2015, Jagniecki et al. 2021). That is, for more ancient tufa, texture may be one of the only properties available for investigating these deposits.

Applying this method to other basins would require comparable numbers of images from all basins considered (i.e. hundreds of images). Given a basin with enough tufa outcrop to produce such a data set, a similar procedure to that presented in this paper would be performed. Whether or not images from different basins clustered together or apart would inform the viability of tufa texture as a proxy across basins. The parameterization of the algorithm or algorithms used would need to be adjusted to suit the expanded data set, including allowing for the possibility of different k values in k-means. However, diversifying the data set with a set of images from a totally distinct watershed, one whose chemistry is known to be distinct from others in the data set (i.e. Mono), would allow for a more thorough testing of the hypothesis that a different lake chemistry produces different textures of tufa. If comparable tufa textures are found across multiple lake systems, that texture could be indicative of a comparable growth environment between basins, at the time of deposition of the tufa. This information would allow for the tufa texture to be used as a direct proxy of lake chemistry and, in turn, depth.

Similarly, analyses like the one above would be made more rich with the inclusion of other environmental data. With the addition of data from more modern lakes, it would be possible to compare tufa texture to direct measurements of lake chemistry (e.g. alkalinity). Though beyond the scope of this study, future works could perform these kinds of analyses at Mono Lake. In older tufa, it could be revealing to compare tufa texture to the other

proxies (e.g. Sr isotopes for groundwater). This work was limited to physical measurements in the field, but future works could improve upon it by including other basins or types of data, with the ultimate goal of using tufa texture as a proxy for depth in paleolakes.

2.7 Conclusions

The finding that the tufa at Mono are most visually similar to the columnar facies at Searles, and that the columnar facies is found most commonly at sites in Searles where tufa towers are also found, suggests that the response to question 1) posed above (“Is a particular facies of tufa at Searles objectively visually similar to those at Mono?”) is that there is reasonable basis for the columnar facies being analogous to the tufa found at Mono Lake. In the context of past work, this study suggests a more abiotic, Mono-like origin for the Searles tufa, particularly in sites where columnar tufa can be found. That is, if the tufa at Mono are representative of the endmember spring-contribution facies, then these results would imply that a higher prevalence of columnar tufa is indicative of a greater spring contribution. This is a step towards the goal of tying tufa texture to formation environment.

The findings above do not exclude the possibility of a biological mechanism contributing to the formation of the tufa at Searles, but they also do not validate it. Thus, this study cannot recommend any biologically-based assumptions about the depth at which the tufa at Searles Valley formed. Future work is certainly needed to solidify these results. However, this work demonstrates that, with some tuning, machine learning studies of this kind have the potential to be useful in gleaning rich information from the geologic past. Considering images as 2-dimensional data that can be plotted and utilizing clustering methods allows for more rich comparisons of geologic images and their environment.

Machine learning and computer vision methods such as the ones used in this paper have the potential to draw further information from the geologic record than has previously been possible. As demonstrated here, these methods have the ability to represent data differently: images can be plotted by similarity, visual trends in facies can be quantified. By pursuing these new avenues of interrogating the geologic record, the geologic community has the potential to uncover new information from data sets and formations that have already been investigated with other techniques. Machine learning, in combination with more traditional methods and in the context of past research, can thus be a tool for deepening understanding

of the Earth's past.

Chapter 3

Modeling Iceberg Longevity and Distribution During Heinrich Events

3.1 Abstract

During the last glacial period (120-12ka), the Laurentide ice sheet discharged large numbers of icebergs into the North Atlantic. These icebergs carried sediments that were dropped as the icebergs melted, leaving a record of past iceberg activity on the floor of the subpolar North Atlantic. Periods of significant iceberg discharge and increased ice-rafted debris (IRD) deposition, are known as Heinrich Events. These events coincide with global climate change, and the melt from the icebergs involved is frequently hypothesized to have contributed to these changes in climate by adding a significant volume of cold, fresh water to the North Atlantic. Using an iceberg model coupled with the MITgcm numerical circulation model, we explore the various factors controlling iceberg drift and rates of melt that influence the spatial patterns of IRD deposition during Heinrich Events. In addition to clarifying the influence of sea surface temperature and wind on the path of an armada of icebergs, we demonstrate that the same volume of ice can produce very different patterns of iceberg drift simply by altering the size of icebergs involved. We note also a significant difference in the seasonal locations of icebergs, influenced primarily by the changing winds, and show that the spatial patterns of IRD for Heinrich Event 1 most closely corresponds to where icebergs are located during the summer months. Consistent with proxy evidence, the ocean must be several degrees colder than temperatures estimated for the Last Glacial Maximum in order

for icebergs to travel the distance implied by Heinrich Layers.

3.2 Introduction

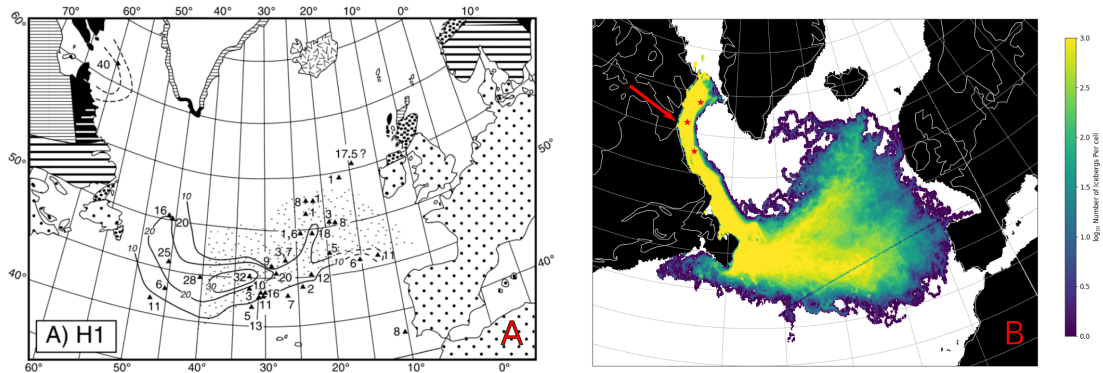


Figure 3-1: Panel A: Map of IRD thickness in the North Atlantic deposited during Heinrich Event 1, adapted from Hemming (2004). Each triangle represents the location of a marine sediment core containing HE-related IRD and the corresponding numbers the thickness (in centimeters) of the IRD. Stippling indicates inferred HL extent. Panel B: Simulated iceberg density in the North Atlantic releasing medium sized icebergs from Hudson Bay (red arrow) for the full 10-year Heinrich Event. In agreement with the observation (Panel A) the model shows that icebergs drift across the entire North Atlantic to Europe. The “forking” pattern in IRD in the observations ($\sim 45^\circ\text{N}$, $\sim 20^\circ\text{W}$) seen here can be observed in model results from this study, especially in summer months (Figure 3-4). Note that the line running between $\sim 40^\circ\text{N}$, 40°W to 45°N , 10°W is an artifact of the seam on the models cube-sphere grid, and not a function of the iceberg drift patterns. seam between GCM panels can be seen in these figures.

The former Laurentide Ice Sheet (LIS) was an extensive ice sheet that covered the North American continent for a significant portion of the Quaternary period (2.58Ma – present). During its history, the LIS had many intervals of advance and retreat, corresponding to glacial maxima. During maxima, the LIS was more than 4km thick at its center in Northeast Canada, and had several large ice streams discharging icebergs into the western subpolar North Atlantic, especially through Hudson Bay (Dyke & Prest 1987, Margold et al. 2018). Sediment cores from the North Atlantic present evidence of episodic discharge from the LIS in the form of ice rafted debris (IRD), which can be found from the Labrador Sea across the basin to Portugal (Hemming 2004, Figure 3-1). The spatial extent and thickness of Heinrich Layers varies between events, variability that has been attributed to changes in the volume of ice involved as well as to shifting climate (Dowdeswell et al. 1995, Ruddiman 1977).

While it is clear that these sediments were transported by icebergs, the exact mechanism of these events is not clear. It has been suggested that the observed periodicity of Heinrich Events is due to instabilities inherent to a growing Laurentide Ice Sheet (MacAyeal 1993 *a, b*, Alley & MacAyeal 1994). In this scenario as the LIS grows it periodically reaches a size that is unstable and requires the purging of mass in the form of armadas of icebergs. An alternative suggestion involves an ice shelf on the Labrador Sea possibly transporting icebergs, particularly sediment-laden icebergs, farther than could persist in open water (Hulbe 1997). It has additionally been noted that subsurface warming in advance of a Heinrich Event could promote the collapse of such an ice shelf, releasing the fresh water necessary to produce the climate signal found in association with a Heinrich Event (Marcott et al. 2011). It has therefore been proposed that the removal of the ‘buttressing effect’ of a large ice shelf led to the acceleration of the Hudson Strait Ice Stream and the production of large numbers of sediment-laden icebergs (Alvarez-Solas et al. 2013, e.g.). Each of these scenarios would result in a different estimate of the volume of fresh water involved and thus a different climate forcing. Disentangling this mechanism will require a fine scale understanding of the mechanics of a Heinrich Event.

While Heinrich Events were localized to the North Atlantic, they coincide with global climate change (Broecker 1994). For example, stalagmite records from China indicate minima in the strength of the Asian monsoon during Heinrich events (Wang et al. 2001), while sediment cores from the Okinawa Trough in the East China Sea show cooling for Heinrich Events 1-5 (Li et al. 2001). Additionally, lake records from the southwestern United States show maximum lake size coincident with Heinrich Events (McGee et al. 2018). These examples along with numerous others signify the abrupt and global significance of the climate change associated with Heinrich events. This significance suggests the existence of a mechanism for propagating the impacts of Heinrich Events from the North Atlantic to the rest of the globe. It has been often suggested that the disruption of the AMOC is central to the global impact observed to coincide with Heinrich Events (Broecker 1994, McManus et al. 2004, Boyle & Keigwin 1987).

In this scenario, the large input of cool, fresh water disrupts the formation of deep water in the North Atlantic and slows the overturning circulation (Broecker 1994, Oppo et al. 2015, Keigwin & Lehman 1994); the resulting changes in heat input into the mid-latitude atmosphere of the Northern Hemisphere and in cross-equatorial ocean heat transport then

lead to global climate impacts. It has been observed that Heinrich Events coincide with periods of Northern Hemisphere cooling and Southern Hemisphere warming (Blunier & Brook 2001, Ahn & Brook 2008). Reconstructions of Heinrich Event 4 (~60,000 year ago) based on foraminifera assemblages have suggested that a 2 - 3°C summer cooling and a 1.5-3.5‰ decrease in salinity could reasonably be expected at the sea surface in the North Atlantic during a Heinrich Event, with more cooling in different parts of the basin and during other seasons (Cortijo et al. 1997, Maslin et al. 1995, Hemming 2004). Modeling efforts have attempted to constrain the impact of fresh water on $\delta^{18}\text{O}$ and other proxies (Roche et al. 2014), as well as northern North Atlantic subsurface warming (He et al. 2020). Questions still remain about the volume, origin, and distribution of the fresh water involved, however.

Iceberg models have been used in attempts to constrain the locations and trajectories of icebergs and their melt during Heinrich Events. Some such studies have found that directly modeling the melt of icebergs (rather than simply freshening the North Atlantic by adding liquid fresh water) hastens the impact of fresh water on climate (Jongma et al. 2013, Levine & Bigg 2008). A separate study directly modeled the extent of Heinrich Layers and accompanying ice volume, based upon an assumed concentration and distribution of sediments in icebergs (Roberts et al. 2014). Both of these studies used models with relatively coarse spatial resolution oceans ($\sim 3^\circ$). Finer scale modeling is however necessary to more accurately resolve individual iceberg tracks and precisely where IRD was deposited during Heinrich Events. To-date, previous modeling efforts using finer scale grids have tended to focus on the transport of icebergs and fresh water along the Eastern seaboard of the United States (Hill & Condrón 2014, Condrón & Hill 2021), rather than the more extensive region of IRD found across the IRD belt. Using a model with a fine scale ($1/6^\circ$; 18-km) ocean, this work investigates the sensitivity of patterns of iceberg tracks to both iceberg size and to changes in climatic (environmental) factors. Below we attempt to constrain the impact of the size of icebergs on their ability to reach the extents suggested by Heinrich Layers. We also investigate climatic controls on these results, including the seasonality of iceberg location and the influence of sea surface temperature.

3.3 Methods

3.3.1 Iceberg Model

The Massachusetts Institute of Technology Global Circulation Model (MITgcm) was developed at MIT for studying the ocean, atmosphere, and climate (Marshall et al. 1997). In this study, we use a version of the model with an eddy-permitting horizontal global ocean grid resolution of $1/6^\circ$ (~ 18 -km) and 50 vertical levels in the vertical with spacing set from ~ 10 m near the surface to ~ 450 m at a depth of ~ 6000 m (Condrón & Hill 2021, e.g.). This resolution is notable and important: whereas all of the models included in phase 4 of the Paleoclimate Modeling Intercomparison Project have 1 - 2° spatial resolution, the resolution of our configuration of MITgcm is ~ 5 - 10 times that. This fine resolution allows for tracing the tracks of individual icebergs, which is necessary for the results discussed below. The experiments performed in this study are completed with the model at equilibrium in regards to icebergs in the system. That is, the number of icebergs in the system of the model changes seasonally, but the number of icebergs calved into the system is equal to the number that melt on the timescale of these experiments (Figure A-1).

In the model, ocean tracer transport equations are solved using a seventh-order monotonicity preserving advection scheme. There is no explicit horizontal diffusion, and vertical mixing follows the K-Profile Parameterization. The ocean model is coupled to an iceberg model (Condrón & Hill 2021) and a dynamic-thermodynamic sea ice model (Losch et al. 2010), the latter of which assumes a viscous-plastic ice rheology and computes ice thickness, ice concentration, and snow cover. The model was configured to simulate glacial (LGM) boundary conditions following that of (Hill & Condrón 2014): sea-level is 120 m lower than modern-day and Northern Hemisphere ice sheets are at their full glacial extent based on multiple reconstructions (Lambeck & Chappell 2001, Dyke et al. 2002). Since the atmosphere is not coupled in these experiments, the model is forced with averaged monthly outputs from fully coupled Community Climate System Model LGM, which is parameterized using PMIP-2 protocols (Otto-Bliesner et al. 2006) This setup is consistent with (Condrón & Hill 2021).

The iceberg module of MITgcm (Condrón & Hill 2021, MITberg) can be used to track the paths and fates of icebergs of multiple sizes. Individual icebergs are simulated as Lagrangian particles, with their horizontal acceleration calculated from the equation of motion for an

iceberg:

$$m \frac{d\vec{v}}{dt} = -mf\hat{z} \times \vec{v} + \vec{F}_a + \vec{F}_w + \vec{F}_s + \vec{F}_p \quad (3.1)$$

where m is the mass of the iceberg, v is iceberg velocity, t is time, and the five terms on the right-hand side represent the various forces exerted on an iceberg: the Coriolis force $-mf\hat{z} \times v$, where f is the Coriolis parameter and \hat{z} is the vertical unit vector; wind drag, F_a ; water drag, F_w ; sea ice drag, F_s ; and the horizontal pressure gradient, F_p . Icebergs have a multi-level keel model where ocean drag on icebergs is the sum of the movement of water at all vertical ocean model levels the iceberg penetrates through.

Additionally, iceberg deterioration (i.e. melt) with time occurs from solar radiation, sensible heating, wave erosion, and buoyant vertically convection. The cold, fresh water produced by iceberg melt is released into the model, and thus the impact of iceberg melt in the ocean can be tracked.

3.3.2 Experiments

Experiments were chosen to constrain factors that are not well understood or have not been extensively explored in previous studies, particularly the influence of iceberg size and sea surface temperature on iceberg paths and longevity. In the default MITgem LGM simulations, experiments were run for 10 years, with 6272 km³ of ice discharged each year (approximately 0.2 Sv, or 0.2×10⁶ m³/s). Regardless of the size of individual icebergs used in our simulations, the same volume of ice was discharged in each experiment. Icebergs were calved at the locations close to Hudson Strait (as marked in Figure 3-1).

With this backdrop, the sensitivity of iceberg drift trajectories and longevity to changing sea surface temperature was tested. Due to the time required to run these experiments, the simulated Heinrich Events lasted 10 years. Simulations were performed in both the default LGM ocean, and with the ocean cooled by 3.5°C (hereafter “LGM – 3.5°C”). As discussed above, past works have suggested a colder ocean during Heinrich Events than the LGM, with a possible range of 3-4°C (Hemming 2004, Cortijo et al. 1997). Given the uncertainties surrounding Heinrich Event sea surface temperatures and concerning the ability of CCSM3 to represent the LGM ocean, 3.5°C was chosen as an intermediate of the range of possible temperatures. This choice is also consistent with previous modeling simulating Heinrich

Events (Condrón & Hill 2021). The results of these experiments are discussed in detail in the next section.

To study the effect of different iceberg sizes on the patterns of iceberg drift and thus where IRD would have been deposited during Heinrich Events, we performed a suite of experiments using three size classes: small, medium, and large. In all cases icebergs begin with a thickness of 260m, with small, medium, and large icebergs having widths of 250, 465, and 1000m respectively. Icebergs always have a fixed width to length ratio of 1.62 (i.e. $\text{Length} = 1.62 \times \text{Width}$) to mimic observed iceberg proportions (Dowdeswell et al. 1992, Mugford & Dowdeswell 2010). While much larger icebergs have been observed in the modern ocean and may have been involved in Heinrich Events, the parameterization of icebergs as Lagrangian particles in MITberg prevents the realistic simulation of larger icebergs. Thus, icebergs larger than 1000m on a side are not considered. While previous works (Jongma et al. 2013, Roberts et al. 2014, e.g.) have used a range of iceberg sizes meant to replicate those observed in modern icebergs, this study seeks to disentangle the role of iceberg size. To clarify this impact, in each experiment all icebergs have the same size when calved. Additionally, to be consistent with previous modeling experiments and given the more realistic results in SST experiments, these size experiments used the LGM – 3.5°C ocean.

3.4 Results

Our first set of iceberg experiments compare the trajectories of icebergs in an ocean cooler than the LGM to the extent of observed Heinrich Layers. We find that releasing medium-sized (465×753m wide, 260m thick) icebergs with LGM ocean temperatures cooled by 3.5°C leads to an iceberg drift pattern that is remarkably similar to patterns of IRD thickness in the North Atlantic (Figure 3-1). In agreement with observations, the model shows that icebergs fully transverse the North Atlantic basin to the western coast of Europe. Significantly, the pattern of iceberg drift in the model is more extensive than the observations. This could suggest that the sediment load of icebergs is entirely lost before the icebergs completely melt. As such, the region that fresh water is added to the ocean could be much more extensive than the patterns of IRD on the seafloor suggest. The pattern of IRD deposited during Heinrich Event 1 shows what appears to be split, or “forking”, pattern in the trajectories

of icebergs around 45°N, 20°W, with some icebergs heading in a more northeast direction and others continuing on an easterly course. Quite remarkably, our high-resolution iceberg model simulations also capture this feature in drift trajectories, suggesting that our modeling captures subtleties of iceberg movements that can be traced in the geologic record.

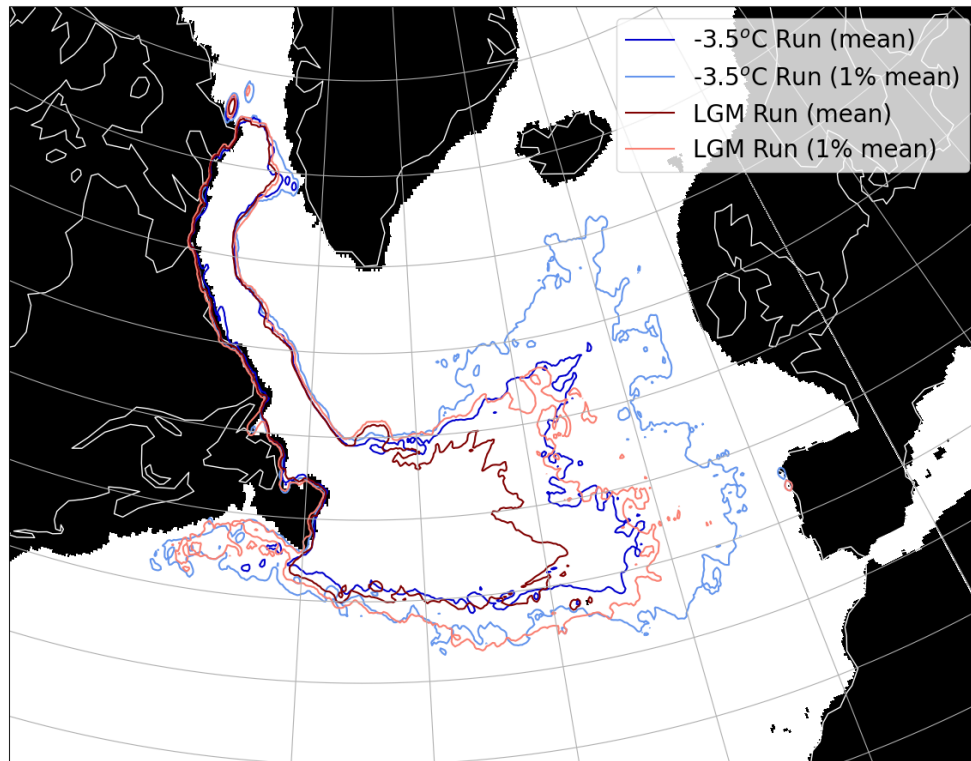


Figure 3-2: Simulated ice flux (the sum of the volume of ice from icebergs) through each model grid cell in the temperature sensitivity simulations (LGM [blue lines] and LGM - 3.5°C [red lines]). Contours are drawn at mean and 1% of ice flux in the Atlantic, of which the latter roughly shows the maximum eastward drift of icebergs in our simulations. All icebergs are of the “medium” size class (i.e. 465×753m wide, 260m thick).

To further explore the parameters influencing iceberg drift, a number of additional sensitivity experiments were then performed. In a second simulation, now with the ocean set to default LGM temperatures, medium-sized icebergs were released. In this simulation, the overwhelming majority of icebergs melted before reaching the distances implied by Heinrich Layers (Figure 3-2). Additionally, the mean extent of ice flux (calculated as the sum of the volumes of individual icebergs that reach a cell) in the North Atlantic only reached 30°W: most of the icebergs did not extend past the midpoint of the ocean basin. In addition, the maximum extent of ice flux through cells (1% of the mean) barely reached 20°W. Meanwhile,

the Atlantic mean location of ice volume in the LGM – 3.5°C simulation was approximately the same as the location of 1% of the mean in the LGM simulation without cooling, with the maximum extent of ice volume beginning to extend around the basin with the subpolar gyre towards Iceland.

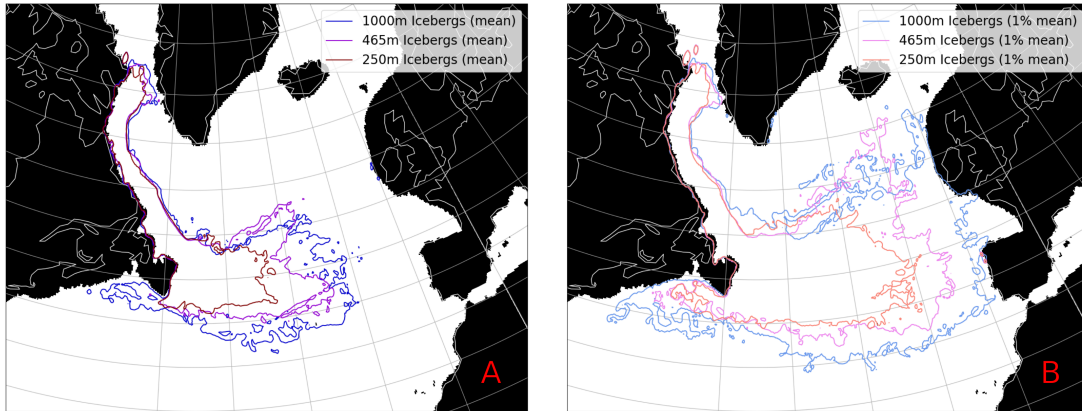


Figure 3-3: Panel A: Simulated mean ice flux through each model grid cell for the three size different iceberg size class experiments. Panel B: Maximum extent of icebergs (based on where ice flux at each cell is $\geq 1\%$ of the mean) for the three experiments. Large icebergs begin with 1000×1620 m width and depth, medium icebergs begin with 465×753 m width and depth, small icebergs begin with 250×405 m width and depth. All icebergs are 260m thick when calved. Means are calculated using only Atlantic cells (Atlantic defined as Longitude between 0° and 55° W).

With the established result of a more realistic iceberg extent in the LGM - 3.5°C ocean, these conditions were used to run an additional set of experiments examining the longevity and tracks of three different sizes of icebergs (small, medium, large). The mean extent of the small class of icebergs (250×405 m wide, 260m thick) was comparable to that found in the LGM simulation without additional cooling, implying that increasing iceberg size and decreasing SST have similar impacts on the longevity of icebergs. Predictably, the mean extent of the largest class (1000×1620 m wide, 260m thick) of icebergs calved from Hudson Bay, Canada, reached farther east than that of the small and medium sized icebergs (Figure 3-3). However, the effect of iceberg size on eastward drift was even more pronounced in the maximum extent of iceberg drift (based on 1% of the mean ice flux at each grid cell) (Figure 3-3). While the maximum eastward extent of the smallest icebergs only reached $\sim 20^\circ$ W and the medium class began to circulate around the gyre, the maximum extent of the largest icebergs reached the coastline of Europe before continuing back west towards Iceland.

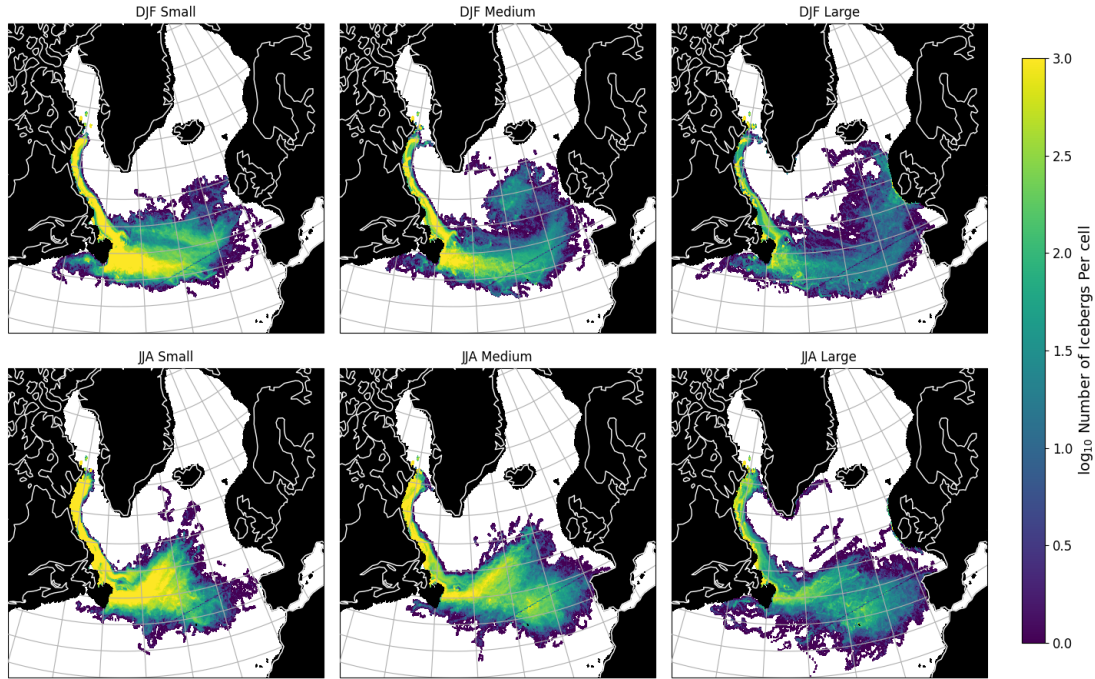


Figure 3-4: Locations of simulated icebergs in the North Atlantic in winter (December-January-February; DJF), and summer (June-July-August; JJA) for the three different iceberg size classes based on the cumulative number of icebergs in each model grid cell. Regardless of iceberg size, there is a marked difference in iceberg drift trajectories in the winter and summer months: iceberg drift is much more zonal across much of the North Atlantic during the winter, while the summer iceberg trajectories show a split at around $\sim 45^\circ\text{N}$, 20°W where some portion of the icebergs drifting in a more northeasterly direction. As shown in Figure 3-1a, this split in trajectories is observed in IRD deposited during Heinrich Event 1.

The results above suggest that increasing the size of the icebergs produces a similar change in eastward drift to decreasing the temperature of water surrounding them. However, these effects are not exactly equivalent. Particularly, in plots of iceberg trajectory, a “forking” pattern can be seen particularly in the ice volume extents of the medium size class and (to a lesser extent) the smaller size class. This behavior becomes more marked when plotting the seasonal location of icebergs (Figure 3-4). Significantly, for all three sizes of icebergs, the split in iceberg trajectories can be seen in the summer (June, July, August) and continuing into the Fall (Sept, Oct, Nov), but not in Winter or Spring (Figure 3-5). For progressively smaller icebergs, the northeast-travelling fork becomes longer relative to that travelling east, contributing to fewer icebergs reaching more eastern parts of the basin. As noted previously, observed thickness of IRD deposited during H1 found in marine sediment cores (Figure 3-1a)

shows a very similar “fork” in iceberg trajectories at around 25°W in the North Atlantic. This agreement between the observations and our numerical model could suggest that during Heinrich Event 1, the release of icebergs in summer months dominated the ultimate extent of Heinrich Layers, either due to increased discharge of ice, increased sediment load in icebergs, or a combination of factors. A more in-depth comparison of model results and core data could reveal further observations of this kind, particularly in the case where the deposition of IRD is more explicitly modeled.

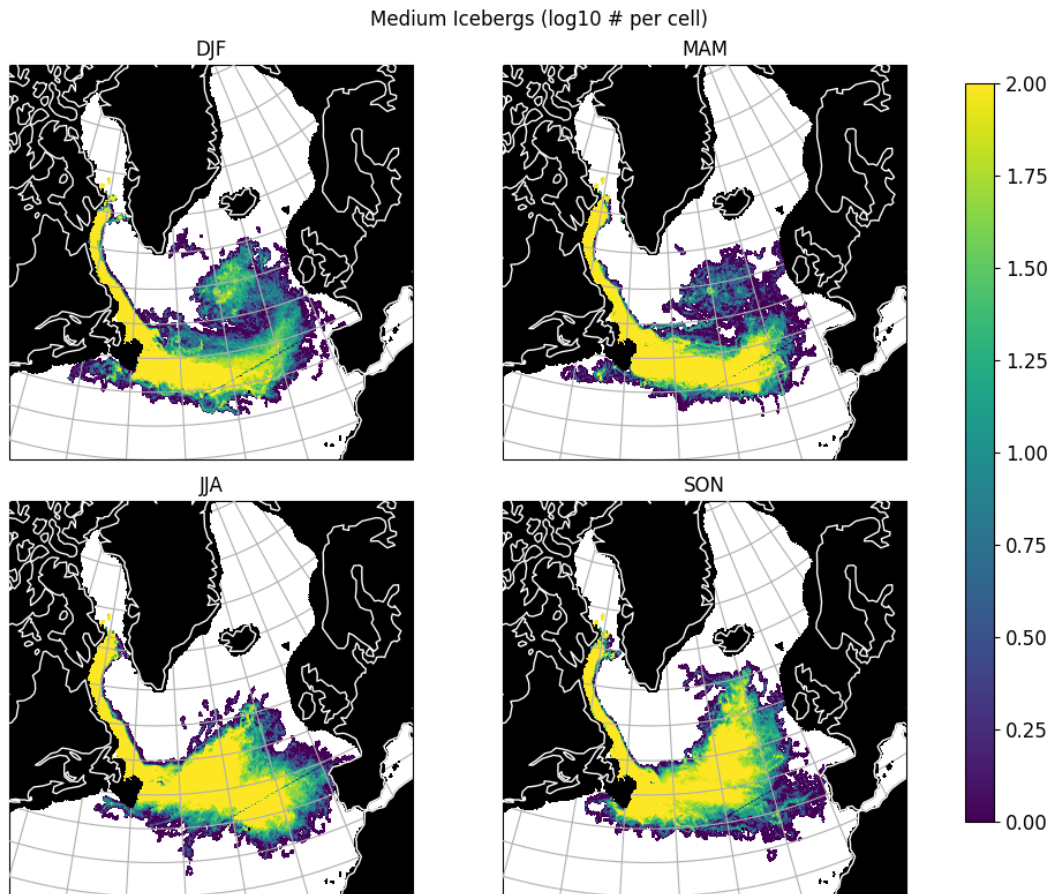


Figure 3-5: Average locations of icebergs during all four seasons: winter (DJF), spring (MAM), summer (JJA), and fall (SON). As described above, iceberg tracks are observed to fork into two tracks in the summer: one traveling approximately due-east and one branching northeast. Remnants of this forking pattern can be observed in fall months, but absent in the spring.

In addition to exploring changes in iceberg trajectories we also examined the impact of melting icebergs on the salinity of the North Atlantic. This was of particular interest given the hypothesized role that melting icebergs played in altering large-scale ocean circulation

and climate (Broecker 1994, McManus et al. 2004, Boyle & Keigwin 1987). In a 10-year run, the salinity had not stabilized and the North Atlantic continued to freshen (Figure 3-6). However, in this time the region that experienced the highest density of icebergs, the “IRD belt” between 40°–50°N, was ~ 1 PSU fresher than an experiment without icebergs. As the simulated Heinrich event progressed, however, the additional freshwater input to the ocean from melting icebergs propagated away from this region and was seen outside of the immediate tracks of the icebergs, particularly into the Norwegian and Greenland Sea where open ocean deep convection is known to occur. After ~ 10 years of simulation, the entire subpolar North Atlantic basin became generally fresher compared to that without the input of fresh water from icebergs released during a Heinrich Event. There are two notable exceptions to this however: a $\sim 0.5^\circ$ square region area east of modern-day Newfoundland (Orphan Knoll) and a larger area in the Norwegian Sea both became saltier. Though the salinity field is unlikely to have stabilized in the 10-year run, the result at Orphan Knoll is consistent with past research that has noted the absence of freshening during Heinrich Events in this location (Keigwin et al. 2005).

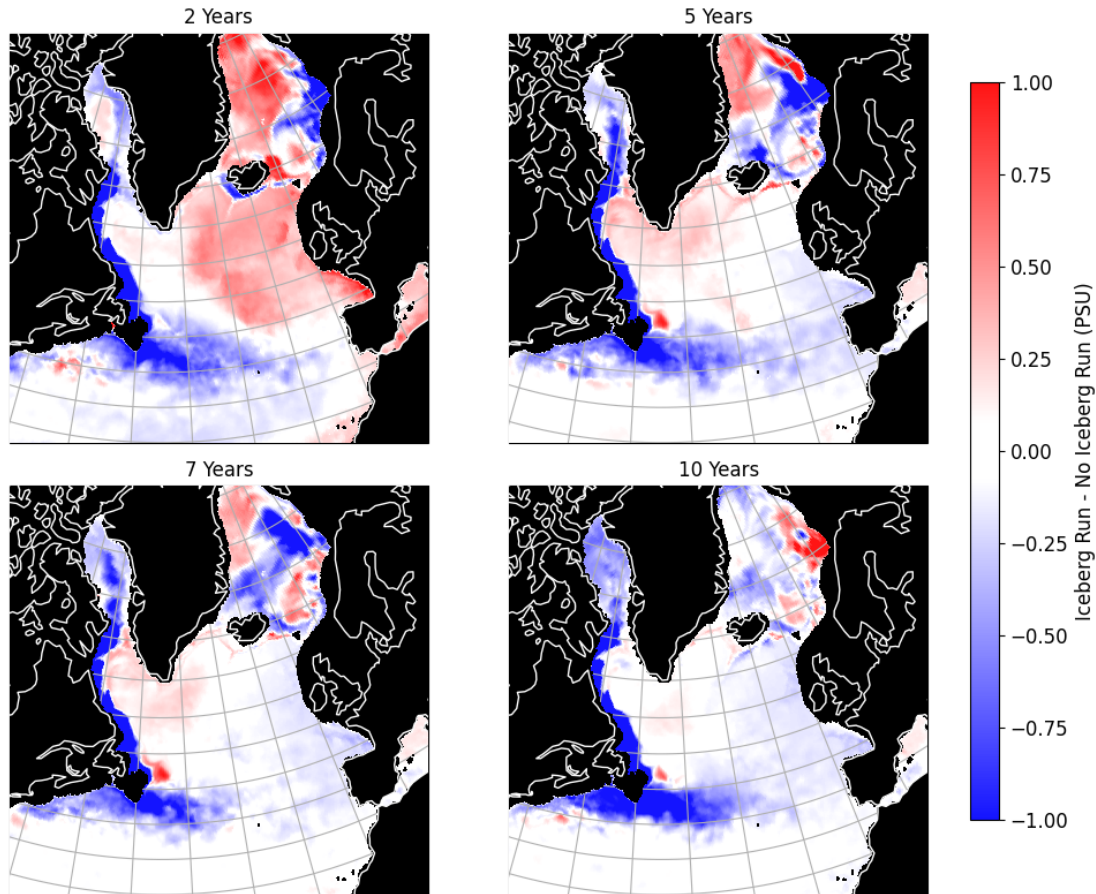


Figure 3-6: Simulated change in North Atlantic sea surface salinity (salinity anomaly) during a Heinrich event simulation of medium-sized icebergs from Hudson Bay after 2, 5, 7, and 10 years. Freshening can be seen in the North Atlantic basin between 40° - 50° N where icebergs are most heavily concentrated, as well as farther afield in the Norwegian Sea. Sea surface salinities anomalies are calculated using the difference between numerical simulations performed with and without icebergs.

3.5 Interpretation and Discussion

It is an intuitive result that icebergs will persist for longer in a colder ocean: if the temperature difference between icebergs and the water that surrounds them is smaller, it will take longer for them to melt due to a reduction in sensible heating. The practical extent of this difference is quantified here, with the result that, for medium sized icebergs, the ocean would likely have needed to be significantly colder than simulated conditions during the LGM to produce the observed extents of Heinrich Layers. This is a reasonable interpretation, as sea surface temperatures are believed to have been colder than LGM during Heinrich Events

(Maslin et al. 1995). With a reasonable assumption about the size distribution of icebergs, these results could conceivably be extrapolated to infer SST from Heinrich Layer extent. Conversely, if SST could be constrained by an independent proxy, the size of icebergs involved in a Heinrich Event could potentially be estimated. Such a strategy would be useful for estimating the volume of ice released during a Heinrich Event, and perhaps the ice sheet dynamics involved in producing the icebergs. It is likely that a number of combinations of SST and iceberg size could produce geologically similar sediment layers. However, this work emphasizes the importance of considering these factors when investigating the climatic significance of Heinrich Layers.

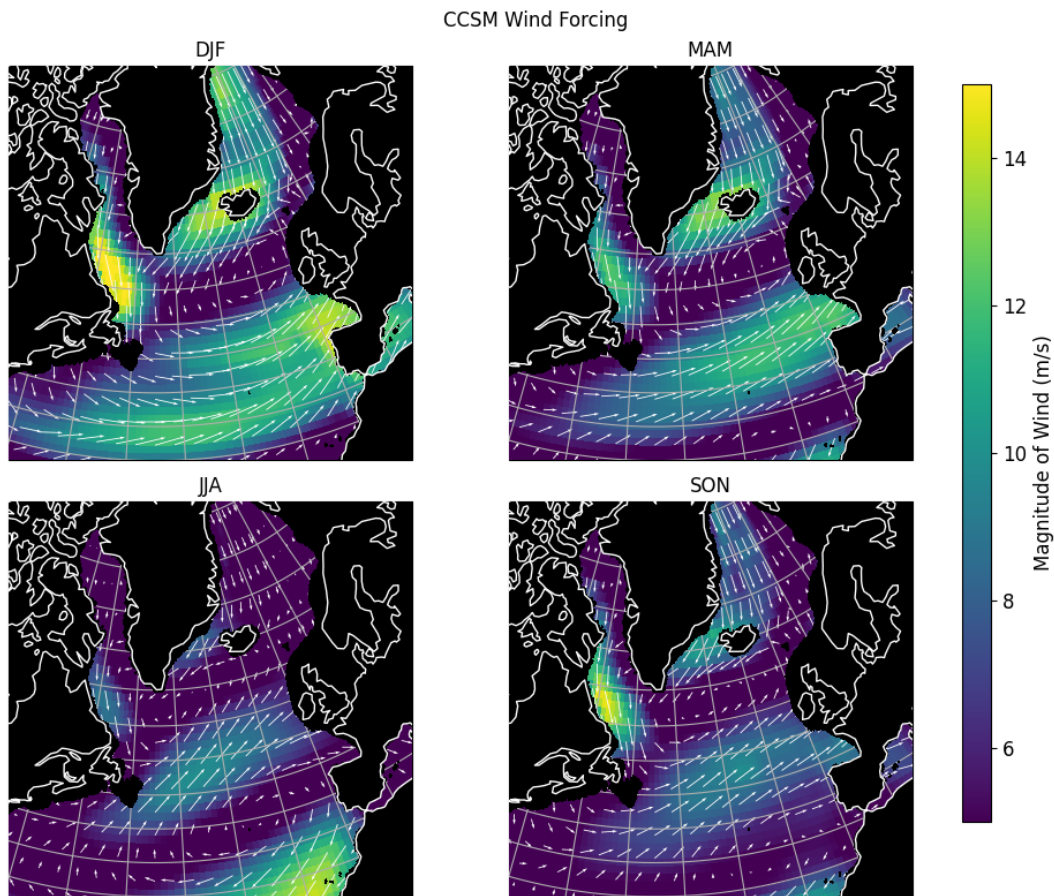


Figure 3-7: Prescribed wind forcing in glacial model (CCSM3) simulations for winter (DJF), spring (MAM), summer (JJA), and fall (SON). The seasonal shifts in the wind match the seasonal shifts in iceberg tracks (Figure 3-4). In particular, the summer forking in iceberg drift aligns with winds shifting to a more meridional patterns and blowing in a northeasterly direction.

Central to considerations of the relative impact of iceberg size and SST is the result

that cooling the ocean has a comparable effect to increasing the size of icebergs. However, this work suggests that while the impacts of these factors are comparable, they may not be indecipherable in the geologic record. Rather, the key to disentangling these two metrics, and to uncovering further information from the geologic record, may involve the forking of iceberg tracks described above. Our results suggest that in a Heinrich Event involving smaller icebergs, more iceberg tracks would be directed to the northeast cutting across the subpolar gyre, whereas larger icebergs will tend to follow the North Atlantic Current approximately due East across the Atlantic. These two scenarios would be recorded differently in the geologic record, with a Heinrich event involving smaller icebergs resulting in a thicker deposit in the center of the gyre. Overall, the fine resolution of our modeling demonstrates that there are subtleties to the sensitivity of iceberg trajectory. The ability to accurately resolve individual iceberg tracks reveals that the spatial extent of Heinrich Layers depends on quantifiable factors in the environment and the icebergs themselves.

An examination of the different atmospheric model forcings and ocean and sea ice fields shows that the only parameter that changed with a magnitude and direction that matched the seasonal shift in iceberg drift trajectories was the wind forcing (Figure 3-7). Seasonal changes in SST, surface currents, and sea ice could be observed, but none of these varied to the degree that could explain the marked seasonal change in iceberg tracks. This result is surprising, given the intuitive expectation that surface currents would have a significant impact on the trajectories of icebergs, and would be influenced by surface winds. However, such a relationship is not observed (Figure A-2). The glacial wind forcing prescribed in our simulations, however, shifts toward the northeast during the summer and fall months, tracking the seasonal shift in iceberg tracks. This suggests that, within the bounds of these simulations, wind is the primary driver of iceberg trajectory. This effect is most marked on our smallest iceberg size class, indicating that smaller icebergs are especially prone to being pushed by wind compared to larger icebergs. We therefore suggest that the different patterns of IRD produced during the six major Heinrich events that occurred over the past 60,000 years could reflect changes in atmospheric circulation patterns. For example, the IRD layer associated with Heinrich Event 3 has a significantly shorter eastern extent, containing a smaller volume of IRD (Hemming 2004). In order to explain this difference, past works have invoked the possibility of a Scandinavian iceberg source with comparably less ice sourced from North America (Grousset et al. 1993, 2000, Gwiazda et al. 1996). This work suggests

that these differences could be explained by the involvement of smaller icebergs in Heinrich Event 3, or perhaps by reduced winds or warmer SSTs. In either case, the same ice volume could be sourced from North America but would result in a less extensive IRD deposit.

3.6 Conclusions and Future Work

This modeling work is the first to use a high resolution, eddy permitting ocean-iceberg model to explicitly study how the size of icebergs and climatic conditions influence iceberg trajectories in the glacial North Atlantic. Our results demonstrate that the longevity and trajectory of icebergs in the North Atlantic depends significantly on the size of icebergs involved. This is true not only in terms of the ability of icebergs to survive long enough to traverse the North Atlantic basin, but also in the sense of the North-East spatial extent: smaller icebergs will more frequently reach the center of the subpolar gyre while diverting in a Northeast direction during the summer months, while large icebergs will tend to maintain a more easterly course. Barring an exceptionally cold ocean, larger icebergs seem also to be required to produce a significant East-West extent. The size distribution of icebergs during Heinrich Events is not well constrained. This study suggests that a substantial population of large icebergs was likely necessary, especially considering where IRD is found abutting Europe. A more in-depth comparison of these modeling results with existing core data could reveal the absence or presence of a significant iceberg track within the subpolar gyre, suggesting the involvement of smaller icebergs.

The impact of iceberg size on iceberg extent is more prominent in the summer and fall months, due to the seasonal shifting of the wind field. These results have significant implications for what can be interpreted from Heinrich Layers. For example, given a reasonable assumption of iceberg size, or iceberg size consistency between Heinrich Events, shifting distributions of IRD between events could suggest shifting wind patterns, or shifting seasonality to the major contribution of icebergs. Seasonality to the release of icebergs could be revealing of the ice sheet dynamics preceding or causing Heinrich Events. Results presented by Hemming (2004) already demonstrate a forking of iceberg tracks in Heinrich Event 1 that is not observed in Events 2, 4, or 5: results that can be interpreted in the context of this study to suggest a shifting of winds, seasonality, or iceberg size during Heinrich Event 1 that did not occur during the other events presented. A preliminary effort to compare our

model outputs to Hemming's 2004 data is presented above, but a more in-depth analyses of these two data sets would be necessary to make a truly significant comparison. These interpretations may likewise require significant assumptions about the ability of icebergs to carry sediment, a question that requires further high-resolution modeling.

In sum, this work presents frameworks for drawing further information from the geologic record of Heinrich Events. It likewise presents the first high resolution spatial distribution of iceberg locations during these events, as well as the associated fresh water signature produced by melting icebergs. These results suggest that Heinrich Layers hold even more information about past climate than previously thought, and that further modeling and exploration will uncover new dynamics to these enigmatic events.

Chapter 4

A Model for the Effect of Partitioning Sediments in Icebergs on Heinrich Layer Extents

4.1 Abstract

In the North Atlantic, relatively coarse grained sediments can be found periodically throughout cores spanning the Last Glacial Period. These sediments were rafted by icebergs purged from the Laurentide Ice Sheet (LIS) in so-called Heinrich Events. “Heinrich Layers” coincide with records of global climate change, suggesting that the impact of these events was propagated beyond the North Atlantic. A possible mechanism for this climate change involves the discharge of cold, fresh water from the LIS in the form of icebergs, slowing the Atlantic Meridional Overturning Circulation and thus disrupting the transport of heat on the planet. In probing the connection between these sedimentary layers and the coincident climate change, it may be illustrative to consider the variation of Heinrich Layer extents and thicknesses, and consider how or if that variation could be related to changes in ice discharge. To tie the discharge of icebergs to the extent and thickness of Heinrich Layers, it is necessary to make assumptions about the nature of icebergs calved from the LIS, and in particular how they carry sediments. In this study we challenge those assumptions by modeling Heinrich Layers as produced with the same volume of sediment and ice distributed differently throughout icebergs. These experiments produce different Heinrich Layers, some

totally distinct from those observed in the North Atlantic, demonstrating that the same volume of ice can result in a profoundly different sediment records.

4.2 Introduction

As described in the previous chapter, sediment cores collected in the North Atlantic basin contain layers of relatively coarse ($>63\mu\text{m}$) sediments, that can be found at periodic intervals of about 7,000 years (Bond et al. 1992, Hemming 2004, McManus et al. 1998). These sediments, in so-called “Heinrich Layers” are believed to have been rafted from the North American continent by icebergs discharged from the Laurentide Ice Sheet. Heinrich Layers extend from where icebergs were calved near Hudson Bay, Canada, almost to the coast of Europe in Portugal (Hemming 2004). Generally, the “belt” of IRD across the Atlantic is described as being largely between $40\text{-}55^\circ\text{N}$, capped on its southern margin by the Gulf Stream. Heinrich Layers are thicker in the western part of the basin and become generally thinner moving East, presumably as icebergs become smaller, fewer, and have dropped more sediment. At their thickest outside of the Labrador Sea, Heinrich Layers are 30-50cm thick, and thin to $<5\text{cm}$ in the northeastern part of the basin (Figure 3-1, Bond et al. 1992, Hemming 2004). Though these descriptions are generally true, there are variations of Heinrich Layer extent and thickness between events. Notably, Heinrich Events 3 ($\sim 31,000$ years ago) and 6 ($\sim 60,000$ years ago) have been considered as atypical events, due to thinner and less extensive Heinrich Layers. Indeed, it has been suggested that these events could involve a Scandinavian source of icebergs and sediment, a different volume of ice discharge, a decrease in the contribution of foraminifera to sediment flux due to low productivity or dissolution of forams, or that these events were in some way significantly different from other Heinrich Events (Gwiazda et al. 1996, Grousset et al. 2000).

Heinrich Events and the associated Heinrich Layers are of particular interest due to their climate significance. These events are coincident with events of global climate change: highstands in lakes in the southwestern United States, weakening of the Asian Monsoon, in addition to other, far-reaching climate impacts (Broecker 1994, Wang et al. 2001, Li et al. 2001, McGee et al. 2018). Thus, though Heinrich Events were immediately local to the North Atlantic, their climate impact was propagated globally. The mechanism often credited with linking Heinrich Events to global climate change is the addition of cold, fresh

water to the Atlantic Meridional Overturning Circulation, or AMOC. This current, driven by differences in salinity and temperature, is one of the main transporters of heat on the planet. As such, the melt associated with numerous icebergs in the North Atlantic could easily be hypothesized to disrupt this current, and consequently global climate. Of particular interest is the volume of ice discharge necessary to perceptibly slow or stop the AMOC, or how a given ice discharge perturbs climate (Boyle & Keigwin 1987, Broecker 1994, McManus et al. 2004). A possible avenue of exploring this question involves investigating the signature of the volume of ice discharged from the LIS in the geologic record.

Comparison of the spatial variation of Heinrich Layer thickness is central to discussions of the climatological and geologic significance of those layers. Layer thickness is necessary to calculate sediment volume, which may be related to ice flux or to the duration of the Event. Despite the importance of this metric, there is not a standard method by which to calculate Heinrich Layer thickness. Heinrich Layers represent a geologically abrupt but practically gradual increase in lithic fragments $>63\mu\text{m}$. It is thus up to the discretion of a researcher to determine where the layer begins and ends, decisions that impact both the reported thickness of the layer and the estimated duration of the associated Heinrich Event. Additionally, multiple methods have been employed to determine where the relatively coarse sediments of Heinrich Layers can be found in cores. One method measures the magnetic susceptibility of the material in the core, which increases with increasingly dense, siliciclastic material (i.e. coarser grains, Grousset et al. 1993, Cortijo et al. 1997). This method is fast and convenient, and as such can be performed at high resolution on-ship soon after a core is collected. Magnetic susceptibility does not permit detailed investigation of the grain distribution of Heinrich Layers, however, which is possible with the labor-intensive method of grain counting. In this method, samples are collected from the core at centimeter-scale intervals and sieved to separate grain sizes. The fraction intervals of grain sizes can then be measured, though at relatively low resolution, and interpolated to provide a smoother record (e.g. McManus et al. 1998). Based on the method employed and decisions made about how to define a Heinrich Layer, there may be significant experimental error in the reported thickness of layers. Indeed, an intercomparison of methods for measuring IRD abundance in cores from the Antarctic margin found that, though methods tend to represent the same trends of IRD, different methods could report IRD counts varying by a factor of two at a given depth in the core (McKay et al. 2022).

A possible avenue for avoiding the issue of sediment thickness involves calculating instantaneous flux of sediment, using the method of ^{230}Th normalization (Bacon 1984, Francois et al. 2004). In this method, the concentration of ^{230}Th is measured in core sediments. ^{230}Th produced at a known rate in seawater, and is removed by particles as they fall to the seafloor. Given a constant sedimentation rate, the concentration of ^{230}Th in core sediments would be constant through time (after accounting for age decay). If there is an increase in sediment flux, the same amount of ^{230}Th is diluted into a larger volume of sediment, and the concentration of ^{230}Th decreases. Samples are thus a measure of the instantaneous flux of sediment when it is buried, and the difficulty of measuring layer thickness is not a concern. This method has been used to estimate the sediment flux during Heinrich Events (McManus et al. 1998, Zhou et al. 2021), though the results of these studies are inconsistent with sediment fluxes calculated from more traditional means (Ruddiman 1977). The likely reason for this discrepancy is the high flux of sediment during Heinrich Events: with a sufficiently high sediment flux, more sediment is deposited than is required to remove ^{230}Th from the water column. Thus, the concentration of ^{230}Th in sediment becomes extremely low, and ^{230}Th normalization may significantly overestimate instantaneous sediment flux (Costa et al. 2020). Though IRD fluxes based on age models (as described above) are not perfectly accurate, the errors involved are more easily estimated than in cases where high sedimentation rates compromise ^{230}Th normalization measurements. For this reason, layer thickness is the preferred metric for the amount of sediment involved in a Heinrich Event in this study.

This study will probe the question of the relationship between the thickness and extent of Heinrich Layers, and the volume of fresh water released from icebergs. Specifically, this work will investigate if the same volume of fresh water could produce significantly different Heinrich Layers by the metrics of extent and thickness, if the sediments are distributed differently within icebergs. In the past, modeling studies have derived an estimate for ice discharge during Heinrich Events by considering icebergs to be uniformly dirty, with sediments evenly distributed throughout the iceberg (e.g. Roberts et al. 2014). This is a mathematically simple scheme that can effectively produce realistic Heinrich Layers, but the results of such studies have the significant caveat of the partitioning of sediment. By contrast, models of sediment incorporation in ice have produce a discrete layer at the base of an iceberg, with effectively clean ice above (Meyer et al. 2019). Observations of Antarctic

icebergs suggest that sediment distribution in ice may in reality be even more complicated, with layers of higher concentrations of sediment distributed throughout the entire thickness of the iceberg at varying angles (Anderson et al. 1980, Dowdeswell & Dowdeswell 1989, Glasser & Hambrey 2001).

Given the lack of research on how icebergs carry sediment in modern times and the further difficulty of applying modern data (i.e. from Greenland, Alaska, Antarctica) to a calving margin that no longer exists, modeling of icebergs is centrally important to investigating sediment transport during Heinrich Events. Though there are a number of studies modeling icebergs and their melt during Heinrich Events (Jongma et al. 2013, Levine & Bigg 2008), there are few that explicitly include the transport of sediment. As mentioned above, the studies that exist employ the simplifying assumption of icebergs with a uniform distribution of sediment (Roberts et al. 2014). In order to effectively study the climate impacts of iceberg melt, Heinrich Event simulations are best performed in a global climate model (GCM). Few GCMs have an adequately fine grid to resolve individual iceberg tracks. Thus, previous works have investigated Heinrich Layers only at a degree-scale resolution. This work introduces an IRD module to the Massachusetts Institute of Technology Global Climate Model (MITgcm, Marshall et al. 1997), a GCM with a high resolution ($1/6^\circ$; 18-km) ocean. Using this particularly high resolution iceberg model, in addition to a new model for sediment partitioning within icebergs, this work endeavors to reveal nuances and insights into the mechanisms of Heinrich Events.

4.3 Methods

4.3.1 Iceberg Model

As in chapter 3 and Fendrock, Condrón & McGee (2022), this study employs a version of MITgcm with an eddy-permitting horizontal global ocean grid resolution of $1/6^\circ$ (~ 18 -km) and 50 vertical levels in the vertical with spacing set from ~ 10 m near the surface to ~ 450 m at a depth of ~ 6000 m (e.g. Condrón & Hill 2021). Our chosen configuration of MITgcm is of particularly high spatial resolution: whereas all of the models included in phase 4 of the Paleoclimate Modeling Intercomparison Project have 1 - 2° spatial resolution, the resolution of our configuration of MITgcm is ~ 5 - 10 times that. This fine resolution allows for tracing the tracks of icebergs at high resolution, and for greater confidence in the location of iceberg

melt. As in chapter 3, the model is configured for LGM boundary conditions per Hill & Condron (2014), with ice sheets at their maximum extents and sea level 120m below modern (Lambeck & Chappell 2001, Dyke et al. 2002). The atmosphere is not coupled: the model is instead forced with averaged monthly outputs from fully coupled Community Climate System Model LGM runs, which is parameterized using PMIP-2 protocols (Otto-Bliesner et al. 2006).

The iceberg module of MITgcm (Condron & Hill 2021, MITberg) can be used to track the paths and fates of icebergs of multiple sizes discharged during Heinrich Events (e.g. Fendrock, Condron & McGee 2022). Individual icebergs are simulated as Lagrangian particles, with their horizontal acceleration calculated from the equation of motion for an iceberg:

$$m \frac{d\vec{v}}{dt} = -mf\hat{z} \times \vec{v} + \vec{F}_a + \vec{F}_w + \vec{F}_s + \vec{F}_p \quad (4.1)$$

where m is the mass of the iceberg, v is iceberg velocity, t is time, and the five terms on the right-hand side represent the various forces exerted on an iceberg: the Coriolis force $-mf\hat{z} \times v$, where f is the Coriolis parameter and \hat{z} is the vertical unit vector; wind drag, F_a ; water drag, F_w ; sea ice drag, F_s ; and the horizontal pressure gradient, F_p . Icebergs have a multi-level keel model where ocean drag on icebergs is the sum of the movement of water at all vertical ocean model levels through which the iceberg penetrates.

Iceberg melt is caused by solar radiation, sensible heating, wave erosion, and buoyant vertical convection. The cold, fresh water produced by iceberg melt is released into the model, and thus it is possible to track the impact of iceberg melt in the ocean. Icebergs melt on both horizontal and vertical axes as required by erosive forces: they change in both thickness and width.

All icebergs are calved from three locations in the the Labrador Sea, shown in Figures 4-2 through 4-5. These locations were chosen as the most likely source of icebergs discharged from dirty outlet glaciers at the margin of the Laurentide Ice Sheet (Hemming 2004). It is possible that an ice shelf existed across the Labrador Sea at the time of Heinrich Events (Marcott et al. 2011), but a continental source is favored in these experiments based on the expectation that ice sourced at these locations would contain more sediment (Alley et al. 2005). All icebergs have the same initial size of 260m thick, 465m wide, and 753m deep. This size is selected as it has been found to best represent the expected spatial extents of icebergs

during Heinrich Events (Fendrock, Condrón & McGee 2022). The ice flux discharged during all simulations is 0.2 Sv. This discharge has been determined to be an appropriate flux by averaging a collection of discharge estimates in previous works (MacAyeal 1993a, Dowdeswell et al. 1995, Hulbe 1997, Marshall & Clarke 1997, Hemming 2004, Roche et al. 2004, Levine & Bigg 2008, Roberts et al. 2014).

4.3.2 IRD Module

For this work, a module was added to MITberg to consider ice rafting of sediments and their deposition. With this module, IRD can be partitioned into icebergs with user-defined concentrations and distributions within the ice. It is thus possible to explicitly simulate the production of Heinrich Layers, and consider how varying the concentration and distribution of sediment can contribute to the spatial extent and thickness of Heinrich Layers.

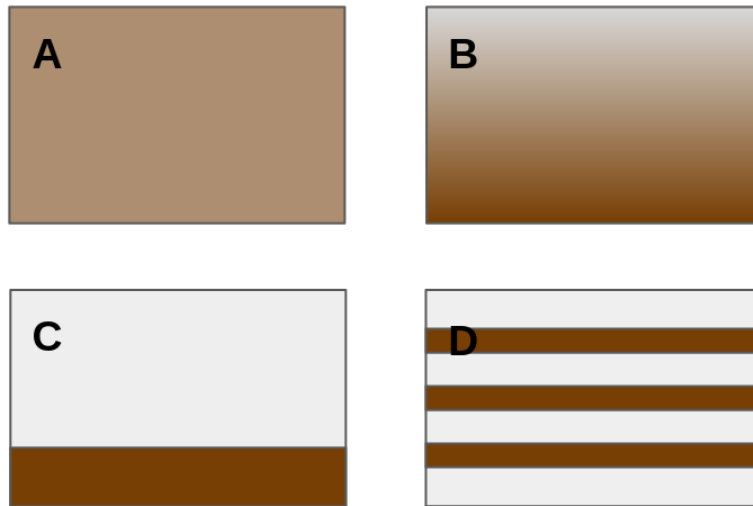


Figure 4-1: Schematic for different sediment partitionings in icebergs: A) the “constant” partitioning, B) the “gradient” partitioning, C) the “basal” partitioning, and D) the “striped” partitioning. Sediment concentrations are distributed that each iceberg is calved with an overall 4% IRD concentration.

In this study, the bulk concentration of sediment in icebergs at time of calving is 4% by volume, using a user-defined sediment density of 2700kg/m^3 (the average density of Earth’s crust, Clarke & Washington 1924). This is consistent with past estimates (Hemming 2004, Roberts et al. 2014), and represents the upper limit of sediment that an iceberg can carry

before sinking. The model permits intervals of the iceberg that have a higher or lower concentration of sediment, but the bulk concentration at the time of calving must be 4%. Within this framework, four experiments are run, each with the same volume of sediment partitioned differently within the iceberg.

First, consistent with previous IRD modeling studies, sediment is evenly distributed throughout in a **constant** concentration (Figure 4-1A). Next, sediment is distributed in a **gradient** from a greater concentration at the base of the iceberg (8% IRD) to clean ice (0% IRD) at the top (Figure 4-1B). A third simulation places all sediments in an extremely IRD-rich (50% IRD), 20m thick **basal** layer, with clean ice in the top 240m of the iceberg (Figure 4-1C). This simulation is meant to replicate the studies where sediments are partitioned completely in the base of the iceberg. Though past studies have considered the basal layer to be 10m thick (Meyer et al. 2019), the possible thickness of such a basal layer is very poorly constrained. This study doubles the thickness used in previous studies as a “best case scenario” for sediment transport in the case of a basal partitioning of sediment. A final simulation distributes the sediment in 5m thick **stripes** of 50% IRD, with clean ice between. This experiment considers icebergs with sediment distributed throughout their volume in concentrated intervals, approximating icebergs observed in modern Antarctica (Anderson et al. 1980).

The concentration of IRD in melt is calculated by scaling the flux of melt from the iceberg (e.g. sediment flux = $0.04 \times$ melt flux). As the iceberg melts, the concentration of sediment in the melt is calculated as a function of the iceberg’s thickness based on the sediment partitioning scenarios described above. Thus, this model only considers sediment melted from the bottom of icebergs, not the sides, a notable limitation. The thickness of the IRD layer is calculated by distributing the IRD in melt evenly over the entire grid cell in which it was melted. This assumes that there is a negligible area of the grid cell into which IRD was not deposited. Thus, these simulations may underestimate IRD thickness at the distal parts of the Heinrich Layer. Given that the size of grains found in Heinrich Layers is normally distributed around $125\mu\text{m}$ (Andrews 2000), the size of individual grains is considered to be negligible. IRD is deposited in the same cell in which it melts: lateral transport of sediment by currents at the scale that would move grains between cells is not considered. The results presented below are scaled from a 10 year run with the simulation at equilibrium with respect to the number of icebergs in the model simulation (Figure A-1),

to represent a 1000 year Heinrich Event. Thus, increasing the length of the Heinrich Event will change the result of the thickness of the deposit, but not its spatial extent.

4.4 Results

As described in the introduction, Heinrich Layers are known to extend from the Labrador Sea almost to Portugal. Though there are inconsistencies in the reporting of layer thickness between methods, a thickness of about 30cm or more would be expected in the heart of the IRD belt, thinning to a few centimeters approaching the most Eastern extent of the layer. Modeling that realistically partitions sediments in icebergs will successfully reproduce both the spatial extents of Heinrich Layers in North-South and East-West, as well as the change in cross-sectional thickness of layers moving East.

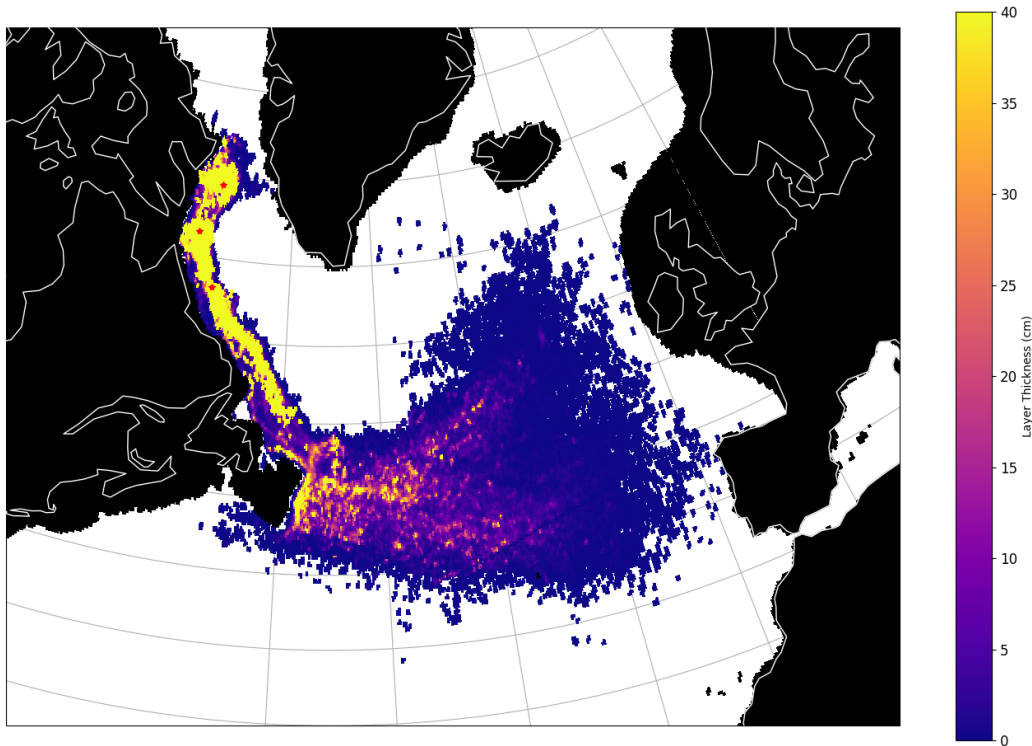


Figure 4-2: Heinrich Layer resulting from constant IRD concentration simulation (4% uniformly throughout). Both the spatial extent and approximate thicknesses compare favorably to observed Heinrich Layer extents, with a thin deposit formed near the coast of Portugal. Icebergs are calved at the red stars in the Labrador Sea.

4.4.1 Lateral Extents of Layers

Both the constant and gradient partitionings of sediment result in spatial extents of IRD comparable to what is observed in the sediment record (Figures 4-2 and 4-3). Since both of these simulations involve icebergs containing sediment throughout their entire volume, it is expected that these simulations would result in very comparable spatial patterns. In both cases, the bulk of sediment is deposited between approximately 55-30°W and 40-60°N, with thinner deposits extending as far as Portugal. It should be noted that, while simulated Heinrich Layers do extend to Portugal, these distal deposits were likely formed by only a few icebergs.

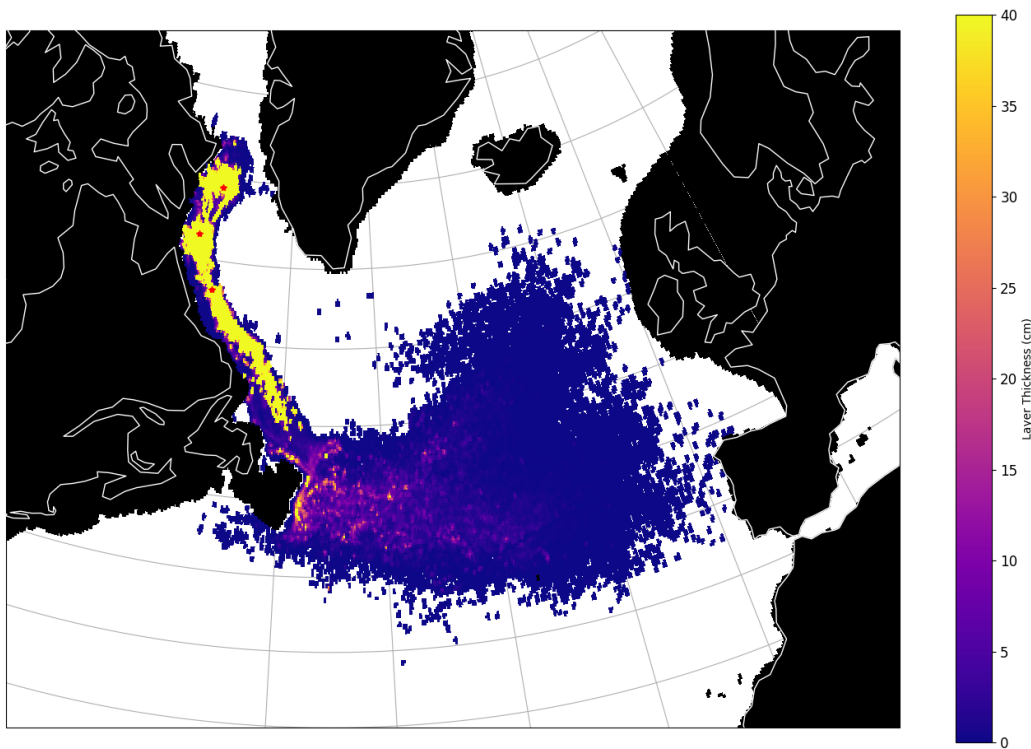


Figure 4-3: Heinrich Layer produced in the IRD gradient partitioning simulation. The extent of this layer is extremely similar to that in the constant concentration simulation (Figure 4-2), as both simulations contained sediment throughout the full volume of the iceberg. This simulation thus also compares favorably to observed Heinrich Layers.

The “striped” simulation presents an interesting result, despite significant model artifacts (Figure 4-4). In this experiment, all icebergs calve with sediment distributed at the same interval. Since icebergs melt at approximately the same rate, sediments are deposited at

comparable intervals moving eastward from their calving locations. Thus, this simulation results in localized, relatively thick “mounds” of sediment where the majority of IRD rich layers melted (e.g. the northern branch of the deposit at approximately 30°N). This simulation results in a sediment-free interval at the mouth of the Labrador Sea, where iceberg melt was primarily clean ice (due in part to the model limitation that IRD is only released from the base of simulated icebergs). Especially given that IRD is only melting from the bottom of icebergs, this is likely not representative of reality: neither would identically sized icebergs be uniformly striped in this manner, nor do Heinrich Layers contain the “mounds” produced by this simulation. However, this experiment does demonstrate that sediments can effectively be rafted further from the source, if concentrated in layers interspersed with clean ice. Thus, while this simulation is not necessarily true to reality, it does demonstrate the efficacy of this partitioning for transporting more sediment, farther East. In situations where a greater concentration of sediment is carried higher in the iceberg, more clean ice can melt earlier in the iceberg’s journey. Partitioning sediments in icebergs in this way therefore can lead to a thicker Heinrich Layer in the Eastern part of the North Atlantic.

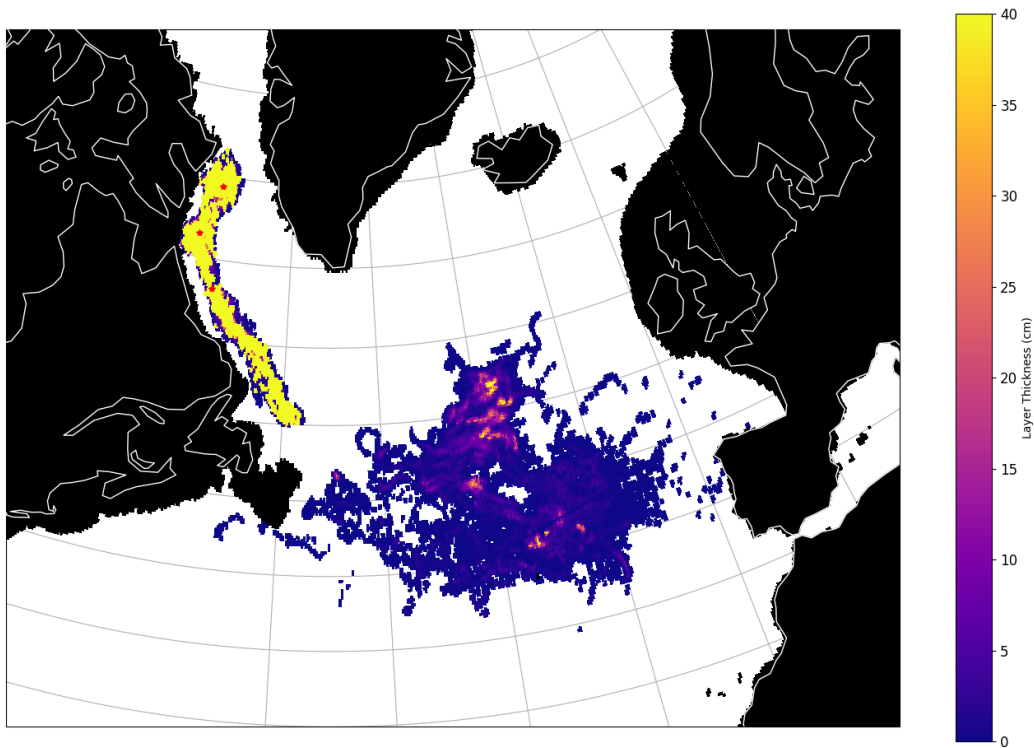


Figure 4-4: The Heinrich Layer produced by partitioning sediment in a banded pattern in the iceberg. Despite dropping relatively more sediment in the Labrador Sea, the simulation using icebergs with the striped partitioning of sediment was able to produce a fairly thick ($\sim 50\text{cm}$) deposit at a longitude of about 30°W , farther East than other simulations.

Despite the basal sediment layer being relatively thick compared to those considered in other studies (20m compared to 10m), this simulation does not produce a Heinrich Layer (Figure 4-5). Instead, the sediments are dropped essentially at the location of calving, creating a localized, enormously thick ($\sim 41\text{km}$) deposit, which is certainly not observed in the sediment record. While there is a possibility that icebergs may melt too quickly in these simulations and thus exaggerate the impact of this sediment partitioning, it is not expected that this effect would be significant enough to compensate for the partitioning of sediment in this simulation. Thus, this sediment partitioning is not considered to have been the primary mode of sediment transport during Heinrich Events.



Figure 4-5: The Heinrich Event simulation using the basal partitioning could not produce a deposit that was either similar to a Heinrich Layer or geologically realistic. Thus, this partitioning is not considered to have significantly contributed to the production of Heinrich Layers.

4.4.2 Thickness of Layers

To first order, both the gradient and constant simulations were of comparable thickness to those reported by Hemming (2004), in approximately comparable locations. These comparisons are somewhat complicated, however, by the considerable spatial variability of both core and simulated data. Thus, the two metrics by which modeled and simulated data were compared were: the thickness of the layer at a given core location or interval of longitude, and the functional form with which the layer thins Eastward across the Atlantic. The basal simulation is not discussed, for the reasons described above.

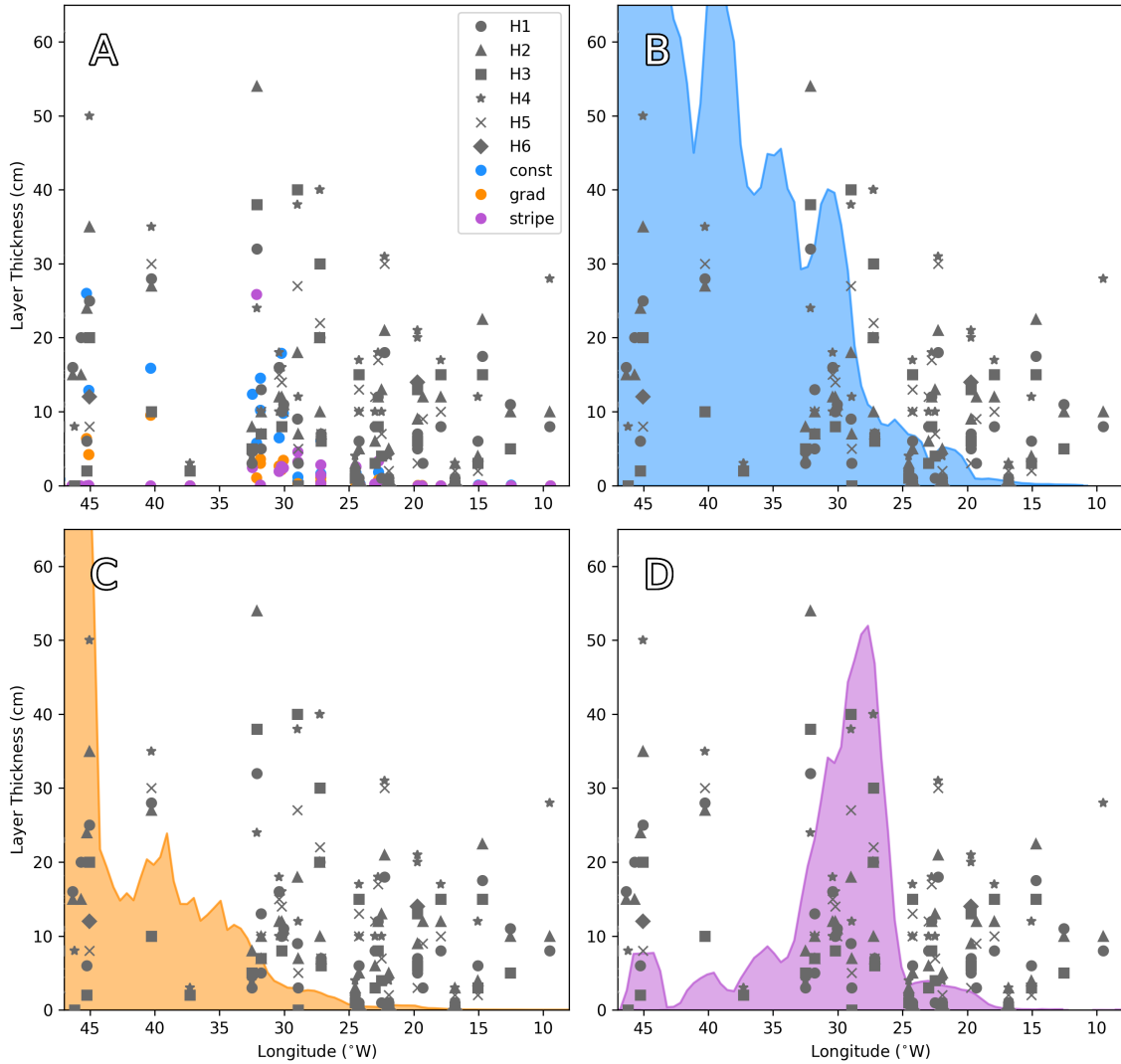


Figure 4-6: Comparisons of modeled Heinrich Layers to core data reported in Hemming (2004). Layer thicknesses in core data are compared to (A): simulated layer thickness in the model cell where the core is located; (B): Maximum modeled layer thickness (blue shading) by longitude for the constant concentration simulation; (C): Maximum modeled layer thickness (orange shading) by longitude for the gradient concentration simulation; and (D): Maximum modeled layer thickness (purple shading) by longitude for the striped simulation. Curves of maxima for simulated core thicknesses are smoothed using a 5 point moving mean.

First, the thickness of a Heinrich Layer in a core reported by Hemming (2004) was compared to the simulated layer thickness in the model cell containing the core location. This comparison is shown in panel A of Figure 4-6: the variability of thickness in a Heinrich Layer at the same longitude, even within the same Heinrich Event, makes a comparison difficult.

However, the trend begins to emerge that the constant and gradient partitionings tend to be within range of the core data, especially West of $\sim 25^{\circ}\text{W}$, and tend to underestimate core thickness East of that boundary.

Cores are intentionally sampled from areas known to have high sedimentation rates (e.g. Bond et al. 1992, , “drift deposits”). While IRD is coarse grained and thus not prone to drifting, the background sediments that may have contributed to a thicker interpretation of a Heinrich Layer are fine grained and easily drifted. Thus, it is a reasonable expectation that layer thicknesses reported in cores may be closer to a maximum thickness for Heinrich Layers. Given this bias, the maximum value of simulated Heinrich Layers at each longitude was then compared to core data. Given the considerable variability of core data even at the same longitude, the constant and gradient simulations compared favorably to core data West of approximately $\sim 25^{\circ}\text{W}$, but were much too thin East of that meridian. West of about $\sim 30^{\circ}\text{W}$, the constant concentration partitioning tended to overestimate the core data, whereas the gradient partitioning compared quite favorably to core data.

In the Western part of the basin, the striped simulation compared unfavorably to core data (Figure 4-6D). Moving Eastward, however, the core data tended to overlap with the “mound” of the striped simulation in the central Atlantic ($\sim 33\text{-}25^{\circ}\text{W}$). As in the case of other simulations, the most Eastern portion of the simulated deposit was too thin. Thus, though the striped simulation generally produced a less realistic Heinrich Layer than the constant or striped simulations, this experiment did perform better than others in reproducing Heinrich Layer thicknesses in the central part of the Atlantic.

In addition to the actual magnitude of modeled and core thickness, it is helpful to consider the “functional form” that the thickness of the deposit takes across the Atlantic: the rate at which it thins, and at what longitude major changes of thickness occur. Within the context of the spread of the data when plotted against longitude, thicknesses reported from sediment cores tended to be of relatively stable thickness across the Atlantic basin, whereas both the constant and gradient simulations had a marked Eastward decline in thickness. This decay is particularly evident in the constant concentration simulation, which thins by about an order of magnitude from $45\text{-}10^{\circ}\text{W}$. Though the constant concentration simulation tended to have more comparable average thicknesses to the core data, the gradient simulation has a preferred functional form because its layer thickness decays more slowly progressing East from $\sim 45^{\circ}\text{W}$. The striped partitioning is thus again not considered comparable, due

to the increase in IRD in the mid-Atlantic which is not observed in core data.

4.5 Discussion

Generally, maps of simulated Heinrich Layers give a positive impression of the comparability of simulated and core data. Particularly for the constant and gradient concentration, the spatial extents are comparable and the thickest parts of the Heinrich Layer are in approximately the correct location (i.e. $\sim 40\text{-}50^\circ\text{N}$ and $45\text{-}30^\circ\text{W}$). In map view, the thicknesses of these layers are compellingly on the correct order of magnitude. In a more detailed examination of the cross sectional thickness of layers, however, comparisons become more challenging. Particularly at the thinner, Eastern extents of the layers, averaged simulated deposits tend to underestimate the thicknesses reported in core data.

Beyond factors external to sediment transport in the model, such as incorrect parameterization of climate conditions, there are a number of possible explanations for the discrepancy between core and simulated layer thickness. First, it is possible that simulated icebergs simply need to be slightly bigger in order to reproduce the distal extents of these deposits. Previous work favored the iceberg size used in this study due to the favorable comparison between iceberg tracks of this size and Heinrich Layers, as well as for the tendency of much bigger icebergs (1000m on a side) to become grounded on the European margin (Fendrock, Condron & McGee 2022). However, previous works have not considered an intermediate iceberg size (e.g. 750m on a side), and did not consider the possibility of clean icebergs outlasting their sediment load. The discrepancy in the distal thickness of Heinrich Layers may thus be reconciled with the involvement of larger icebergs. There are a number of anticipated downsides to simulations of larger icebergs, including the aforementioned possibility of grounding, as well the possible loss of the more favorable comparison between thicker parts of simulated and core deposits. It is likewise possible that there is a geologic reason for this discrepancy, and that adjustments in model parameters are not necessary. As described above, it is known that sediment cores tend to be collected from locations known to have relatively high sediment accumulation rates. Given that the maxima of more Eastern bins of modeled data are within range, or close to within a standard deviation, of core data, it is possible that the maxima of bins are a more reasonable metric for the success of modeling in areas of lower sedimentation rate.

It is also possible that where sedimentation rates are lower, the natural randomness of iceberg drift and sedimentation becomes a more significant factor. Where there are fewer icebergs, it is more likely that not all areas of the seafloor will see IRD, or IRD distribution will be more inconsistent. This may partially explain the discrepancy between model and data where there is less sediment, as well as the spread within the core data themselves. At all parts of the basin, core data of Heinrich Layer thicknesses are spread by up to a factor of ten. This is a feature of the data: Heinrich Layers have been examined in cross section (e.g. Roberts et al. 2014), but these analyses are complicated by the both zonal and meridional thinning of layers. Additionally, even cores sampled relatively close to each other may have discrepancies of tens of centimeters (e.g. Bond et al. 1992, Hemming 2004). This is also true of all model simulations: the constant concentration simulation, for example, results in adjacent grid cells at $\sim 45^\circ\text{W}$ with layer thicknesses $<10\text{cm}$ and $>40\text{cm}$. Heinrich Layers thus are evidently spatially variable by nature, likely due to the fairly inconsistent tracks of icebergs involved. Beyond a possible explanation of the discrepancy between model and data, this reality complicates any attempt to draw a comprehensive narrative of Heinrich Layer extent and thickness, and thus the total volume of sediment involved.

Despite these difficulties, the modeling performed in this study is progress towards the goal of determining what volumes of ice and sediment are necessary to produce a Heinrich Layer. Given the inherent variability of the thickness of Heinrich Layers, the model-data discrepancy of a few centimeters is a considerable success. For the 0.2Sv ice discharge used, both the constant and gradient simulations reasonably simulated a Heinrich Layer. In reality, icebergs will not be of uniform size or sediment distribution as simulated here. However, the success of these two experiments demonstrates the necessity of exceptionally dirty icebergs: not only were simulated icebergs carrying the maximum possible sediment load, that load was distributed throughout the entire iceberg. If the overall flux of ice during the Heinrich Event is increased, clean icebergs of comparable size may also be involved. However, for a 1000 year Heinrich Event with a 0.2Sv flux of ice, all icebergs must have 4% of their volume of sediment distributed throughout the volume of ice.

4.6 Significance

The above simulations each discharge the same volume of ice, containing the same volume of sediment, for the same amount of time. Given the same starting conditions, each experiment would thus cause an identical climate impact. By simply changing how sediment is carried in icebergs, however, these experiments produce drastically different signatures in the geologic record. To first order, this result contributes uncertainty to the interpretation of Heinrich Layers: the link between ice (climate impact) and sediment (geologic record) is complicated at best. Though it is unlikely that Heinrich Events would involve icebergs of uniform size or sediment distribution as simulated in these experiments, it is quite possible that, due to a change in the Laurentide Ice Sheet or the surface it eroded, the amount of sediment in icebergs and how it was distributed could change between Heinrich Events. Model results from this chapter suggest that the same volume of ice could produce a different Heinrich Layer, or a different volume of ice could produce comparable Heinrich Layers. This study thus suggests caution is necessary when attempting to draw climate conclusions from the spatial extent and thickness of Heinrich Layers without the context of additional proxies.

Additionally, this study demonstrates that the nuances between Heinrich Layers produced by different sediment loadings would likely be difficult to glean from sediment cores. The spatial variability of Heinrich Layers (both in cores and as modeled) is such that geographically proximal cores may present Heinrich Layers with thicknesses that differ by up to a factor of ten. The existing spatial frequency/resolution of cores needed to draw a comprehensive narrative of IRD thickness across the Atlantic is likely not possible, but modeling studies such as this may work to bridge the gap between the sparse and variable geologic record, and the processes required to produce it.

To this end, this study takes the significant step of limiting the ice volume discharge associated with sediment during a Heinrich Event. For a flux of 0.2Sv, 1000 year Event, all icebergs must be approximately 4% sediment by volume. The flux of ice may be greater, but involved ice would need to be largely sediment free. For this discharge of ice, this work suggests a Heinrich Event of approximately 1000 years or slightly longer. Regardless of duration of Event or the flux of ice, however, the participation of icebergs containing sediment throughout their volume was central to reproducing Heinrich Layers in this study: these icebergs were responsible for transporting sediment the farthest East in Heinrich Events.

This result could have significant implications for the calving and erosive potential of the Laurentide Ice Sheet, the dynamics of which are not well constrained. Thus, one of the primary findings of this study is that the upstream dynamics of the Laurentide Ice Sheet must allow for the incorporation of large amounts of sediment throughout the volume of icebergs.

4.7 Future Work

The model developed in this work is the first to allow user-defined partitioning of sediment in icebergs. The research presented in this chapter uses this model to clarify the relationship between ice discharge and sediment distribution during Heinrich Events. However, there are a number of possible avenues that could improve these results and leverage their impact. As described above, it may be clarifying and fruitful to repeat the experiments of constant and gradient partitionings, using slightly larger icebergs. This may permit the transport of more sediment to the distal parts of Heinrich Layers, reconciling differences between model and data. This may be at the expense of areas of better model-data agreement (typically where IRD is thicker), and may not be necessary given the qualifiers to layer thicknesses reported in sediment cores. However, performing these experiments would allow for confident discussion of whether the mean size of icebergs should be bigger during Heinrich Events. Additionally, given that icebergs are not expected to have been of uniform size during Heinrich Events, it would be productive to perform the same set of simulations using a distribution of icebergs sizes. Previous works (e.g. Levine & Bigg 2008, Roberts et al. 2014, Condrón & Hill 2021) have used a size distribution based on modern Antarctic icebergs, and using such a distribution would likely produce a more realistic result.

The experiments performed in this study test only one manner of partitioning sediment at a time, and should thus be considered extreme endmembers for Heinrich Layer production. In a more realistic experiment, some fraction of icebergs would carry sediment in the four partitionings described here. Given that the constant and gradient modes of sediment transport best matched Heinrich Layer core data, a higher fraction of icebergs should use these partitionings. Including all modes of sediment transport would likely be more true to reality, and reproduce more of the variability observed in core data. Adjusting the ice discharge involved or the duration of the event, further simulations could test the impact

of a lower concentration of sediment in a higher volume of ice. This study does not assess variations of ice flux, though such variations could significantly impact the interpretation of Heinrich Layers.

This study motivates a number of works that could illuminate the nature of Heinrich Events and the circumstances surrounding them. Particularly, it illustrates a need for further sediment cores of the North Atlantic, and measurements of the thicknesses of the Heinrich Layers therein. Increased spatial resolution in cores would allow for more specific estimates of sediment fluxes during Heinrich Events, which would provide more firm boundary conditions to modeling studies such as this. The combination of more data about Heinrich Events and modeling of those data could effectively bridge the gap between the geologic record of Heinrich Events and the associated climate impacts and forcings. Modeling efforts could likewise be aided by further observations of how modern icebergs carry sediment, data which are severely lacking. Though the Laurentide Ice Sheet could very possibly have produced icebergs unlike those that exist today, observations of modern icebergs, their IRD distributions, and how those sediments become entrained in ice, could build further understanding of the relationship between ice sheet dynamics and IRD. Such observations and further theoretical work could reconcile the the result of this study that icebergs must be extremely dirty with modern observations favoring transport of sediment in the base of icebergs. This understanding would build a more complete view of the fundamental dynamics of the Laurentide Ice Sheet and its role in the production of Heinrich Layers.

Chapter 5

Towards a Sustained Community of Practice Around Pedagogy in EAPS

5.1 Abstract

As the Teaching Development Fellow (TDF) for EAPS in the 2021-2022 academic year, it has been my role to develop resources and host events to encourage discussion and engagement with teaching practice in the department. This has involved conversations with community members at multiple levels of the department in order to determine how best to serve the department's needs. This has resulted in two actions beyond my standard TDF duties: the development of a syllabus and materials for an IAP course on teaching in the Earth Sciences, and a faculty panel to convene a department conversation about ongoing teaching practices. Both of these efforts are directed towards the overarching theme of the department needs assessment: developing a community practice around teaching in EAPS. This chapter describes these efforts and includes resources developed in their support. It also makes recommendations for future actions to encourage the continuity of efforts in this space.

5.2 Introduction

As in most, if not all, academic departments, teaching is central to EAPS. Prominently, both faculty and graduate students may be required to teach at some point during their tenure in the department, as the instructor of a course or a TA. Additionally, both undergraduate and graduate students will participate in courses taught in the department, courses whose

impact depend on good teaching. Teaching is one of the central pillars of academia, and thus it is reasonable that graduate students would hope or expect to gain teaching experience or to learn pedagogical theory in graduate school. Despite this, there are few avenues for pedagogical instruction at MIT, and even fewer that are department specific. MIT's Teaching and Learning Lab (TLL) has worked to fill this gap with the Kaufman Teaching Certificate Program (KTCP) and other workshops directed towards pedagogical theory. One such effort is the development of the Teaching Development Fellow (TDF) Program, where graduate students are tasked with assessing the pedagogical needs of their department, and organizing efforts to meet those needs.

As the EAPS TDF for the 2021-2022 academic year, it was my goal to build a community of practice around pedagogy in EAPS. A community of practice for teaching is a space where teachers can meet to discuss lessons, class time, assignments, or generally their experience of leading and teaching a class. These spaces are meant to foster discussion and encourage feedback: teachers may solicit each others' thoughts and share insights into the strengths and growth areas of each others' teaching practice (Printy 2008). While the skill of teaching well can be learned in classroom as a student, it has been observed that teachers develop their pedagogical skills primarily on the job, in the classroom and, importantly, in communities of practice (Viskovic 2006, Laksov et al. 2008). Additionally, while classroom experience may or may not be available to graduate students in EAPS, an open community of practice would allow a space for graduate students to develop practical experience of teaching. For these reasons, and following the results of my departmental needs assessment, I sought to build a community of practice around teaching in EAPS.

As mentioned above, I began my work as a TDF by assessing the needs of the department in conversations with faculty, students, and pedagogically focused staff. With the confidence from these conversations that a community of practice would suit department needs, I worked towards this goal by organizing a bi-weekly discussion group. To build a greater community momentum, the Fall discussion group was transitioned into a for credit seminar for the IAP term. These efforts are described in detail in this chapter, as are plans to propagate the momentum of this community into future years, with future generations of TDFs.

5.3 Needs Assessment

The needs assessment was performed in conversation with EAPS community members. These discussions, over the course of a few weeks, were with individual faculty members, graduate students, and the EAPS Education Committee. The goal of this needs assessment was to determine which existing programs serve the department well, and what kinds of additional programs could further facilitate discussions of teaching in the department. It was my *a priori* impression that a community of practice around teaching would be helpful in the department, but these discussions codified that impression and helped to determine how to most effectively design this community. Undergraduate students were not involved in these conversations due to the expectation that those students would have less interest, availability, and experience with teaching in the department. This assumption is likely true to an extent, but future efforts of this kind will optimally involve the voices of undergraduates, especially those who TA, are Undergraduate Teaching Fellows (UTF), or have an interest in teaching as a career.

In conversation, individual faculty were in agreement that the department lacks spaces for conversation about teaching theory and practice. Actual desire for such a space ranged from enthusiastic to generally interested, and no faculty expressed an active disinterest or an opinion that there would be no value to conversations around pedagogy. Admittedly, the faculty whose opinions were solicited were chosen for their perceived interest in teaching. Even given this bias, however, there is evidently a sizable number of faculty wishing for greater opportunity to discuss pedagogical practice. The primary barrier to faculty participation cited as a limitation on time: faculty expressed a concern that they did not have the availability to attend regular meetings or to set aside time for discussion of pedagogy. Thus, any effort to involve faculty in discussions of pedagogy would need to consider their limited ability, and thus not require too much of their time.

Individual graduate students were not uniform in their opinion about teaching experiences in EAPS. This is likely due to the inconsistency of teaching opportunities available, as well as the inconsistency of the experience of those who were able to participate in those experiences. Particularly, there are two primary avenues for participation in teaching available to EAPS graduate students: participating in the KTCP, and serving as a Teaching Assistant. The former is external to EAPS, and thus largely beyond the scope of this chap-

ter. Broadly though, many who had participated in the KTCP felt the desire for a more specialized experience of teaching: the program serves all departments at MIT, and thus cannot provide discipline-specific instruction. In contrast, experiences of being a Teaching Assistant may be extremely discipline specific, but were varied in the actual teaching exposure allowed to TAs. That is, some TAs serve in an ad hoc role, providing support to faculty however needed and not always in ways related to pedagogy, while others are given greater opportunity to participate in the teaching of the course. Regardless of the actual role as a TA, students varied in their appreciation of the role: some valued the opportunity to be involved in teaching in any capacity, while others felt that it was a obligation outside of their goals for graduate school. There is thus a variety of opinion regarding the utility or necessity of pedagogically focused spaces in EAPS among graduate students. However, there does exist a significant population among graduate students who wish for more opportunity to spend directed time studying and discussing teaching.

Following the conversations described above, I met with the EAPS Education Committee to solicit their feedback on my impressions of the needs of EAPS and my plans for the semester. In particular, I hoped to hear their thoughts on the idea that any efforts to facilitate discussion of pedagogy must involve the faculty. My primary goal would be to create spaces for both students and faculty to discuss teaching theory and practice, at regular intervals, in the form of a bi-weekly discussion group. These meetings would alternate in their goal: reading-based discussions of pedagogical theory, and discussions of practice based on classroom experiences. The Education Committee was generally supportive of this plan, but emphasized the context that faculty may not be available to attend all meetings. This caveat emphasized that maintaining continuity in attendance may be difficult. The Committee also made two helpful suggestions. First, they noted that a for-credit seminar over IAP would be possible, and may be an effective way to increase attendance among students. They also noted the feedback they had received from students that more practical workshops (e.g. on writing a teaching statement) would be well-attended.

Following these meetings, I proceeded with the following plan: For the fall, I would lead the discussion group as planned, meeting every other week with faculty and students to discuss either readings or classroom practice. During IAP, this format would transition to twice a week in a for-credit seminar. The Education Committee's recommendation for practical, skill-based workshops will be addressed later in this chapter.

5.4 Fall Semester Discussion Group

The discussion group described above met three times over the second half of the Fall semester: an orientation meeting to discuss goals for the group, one practice-based discussion to solicit student feedback, and once to discuss a reading about Backwards Design (Wiggins & McTighe 2005). Due to starting a bit later in the semester, it was impossible to have more than three meetings. The reality of only having three sessions emphasized that meeting every other week would make it difficult to create a sense of continuity. While individual sessions were well attended (~ 3 faculty and ~ 8 students), it was a challenge to maintain the momentum of individual meetings to two weeks later. This is the fundamental challenge to creating a community of practice around teaching in EAPS: it is difficult to maintain the momentum necessary to build a community while balancing the demanding schedules of students and faculty.

5.5 12.s597: Seminar in Teaching in EAPS

Following the encouraging attendance of the Fall discussion group, and to build the community-facilitating momentum described above, the discussion group was transitioned into a for-credit seminar for the January “Independent Activities Period” (IAP), co-taught with David McGee. This course met twice a week (Tuesdays and Thursdays) for one hour from January 4-27 (8 total meetings). Class sessions were divided into two formats, mirroring the Fall term discussion group: Thursdays were discussions based on a reading about a pedagogical concept, theory, or practice; and Tuesdays were an activity called “Bring a Thing”, inviting students to bring a reading, concept, activity, or anything else related to the previous Thursday’s theme, to discuss with classmates.

This section will offer brief summaries of the readings covered in the course, their relevance and significance to the arc of the course. Next, I will describe Bring a Thing in greater detail, providing examples of the conversations that were facilitated by that space. Later in this chapter, I will reflect upon what worked well in this course, what the growth areas are, and how best to run this class in future years.

5.5.1 Topics and Readings

The one topic that was covered in the Fall discussion group was “Backward Design” (Wiggins & McTighe 2005). As not all students in the IAP seminar had attended this session, students were asked to read the assigned book chapter before the beginning of the term. The principle of Backward Design argues that courses are best conceived with intended learning outcomes in mind: that course design must start with a firm grasp of what students ought to learn. This idea contrasts with other methods of course design that may begin from the activities that the instructor wishes to facilitate in class, or the topics they wish to cover, and may not have an a priori sense of the specific learning goals for students. Backward Design posits that learning can be maximized in a course by beginning by determining those learning goals, considering what evidence could demonstrate that the goals were being met, and then finally building lesson plans that facilitate achieving that evidence. This workflow is centered on student learning, rather than on classroom practice, and is thus more able to achieve desired learning outcomes. Backward Design has the added benefit of making it possible to communicate to students what their own learning goals should be: this knowledge can direct their work and focus, and allows them the opportunity to assess for themselves whether or not they are meeting the goals for the course. Backward Design serves as the basis for good course design and effective learning in the classroom. Beginning with this topic provided a firm basis for future discussions, with the understanding that learning starts with learners.

Differences of Prior Knowledge

The first session of 12.s597 was an organizational one, where participants introduced themselves, the goals of the course as defined by students and instructors were discussed, and the syllabus was summarized. The first reading-based discussion was on the subject of differences of prior knowledge. In EAPS, it is common for students in courses to have significantly different backgrounds and statuses: the same class may have students who had completely different undergraduate experiences or who have disparate research topics. Classes may also teach undergraduate students at the same time as graduate students at any point in their first to fifth year. It is thus important to consider the research concerned student differences of these kinds, and how best to manage them. Broadly, research on differences

of prior knowledge recognize that, regardless of prerequisites, students in a course will each have different backgrounds that contribute to different abilities to engage with the material presented in a course. The reading that served as a basis for this discussion (Ambrose & Lovett 2014) names four areas where students can have different backgrounds and abilities: content knowledge, intellectual skills, epistemological beliefs, and metacognition.

Content knowledge is often what comes first to mind when contemplating differences of prior knowledge: some students may already know some of the content covered in the class, because they may have learned it previously. While this form of prior knowledge may give students a leg up in completing assignments, it additionally has been demonstrated to improve students' ability to incorporate new material: prior content knowledge can thus have a multiplicative effect on students' performance in class. In the context of EAPS, content knowledge differences could arise when a class includes students whose primary research area is the subject of the course, when students attended undergraduate institutions with varying specialty in one subject or another, or in any other context where students have differences in past exposure to content.

Rather than actual information, intellectual skills are tools that are central to learning, completing assignments, and otherwise succeeding in the classroom. These may include strategies for studying, reading papers, writing ability, any number of skills that facilitate and demonstrate learning. These skills may be rewarded but overlooked: those students who are better writers will likely receive a better grade in writing assignments, whereas those who have less experience writing are likely to under-perform on assignments with a writing component. If writing skills are not considered one of the learning goals of a course, students may not receive instruction on how to improve their writing. In general, assignments include skills that are beyond the intended learning outcomes of that activity: let it be math, problem solving abilities, writing, coding, reading for comprehension, or any other number of skills that are not actively taught in the course but influence students' ability to effectively complete assignments. This is particularly true in EAPS, where students in the same course may often be undergraduate or graduate students at any stage.

Students may also have varying epistemological beliefs about the nature of knowledge and learning. Beliefs about the nature of knowledge can lead students to value certain activities or exercises more than others. Some students may think that reading papers is the primary way to acquire knowledge; others may believe that the majority of knowledge

is determined from experience in the lab or field. Additionally, students may have varying beliefs about the nature of learning, the speed at which it happens, or their own ability to learn. Students may have an expectation that certain learning exercises are fruitless, and these opinions may vary between students.

Lastly, students' metacognition, or understanding of their own learning, is central to their ability to become independent learners. Some students may have a firm and accurate grasp of their own strengths and growth areas as learners will be more able to navigate a classroom environment successfully. Those who are able to honestly reflect on where their learning is lacking, and what learning strategies work best for them, will be able to more efficiently direct their efforts in compensating for those weaknesses. Students with weaker metacognition may double down on strategies that do not work for them, for example believing they simply failed to spend enough time reviewing material, when rather their efforts would be better spent changing their method of reviewing.

It is not necessarily the instructor's responsibility to compensate completely for all differences of prior knowledge. However, learning outcomes can be improved if these differences are recognized and structures are put in place to allow students opportunity to reflect on the four areas described above. Surveys throughout the semester can allow instructors to recognize these differences and direct students to resources that can support them. For example, intellectual skills and content knowledge can be improved with visits to office hours or time spent with a TA. Metacognition and epistemological beliefs can be encouraged or challenged by building in space for reflection in assignments or class time: simply posing questions about where learning is happening may make a significant difference in students' ability reflect.

Active Learning

Active learning has been demonstrated to be one of the most effective ways to promote learning in a classroom. Wieman (2014), one of the readings for this unit of the course, points out that were a medical drug demonstrated during a trial to be as effective as active learning, that trial would be stopped so that the drug could begin to be used publicly. Using active learning can cut failure rates in courses by more than 10%, and can significantly improve test scores. Active learning is thus an invaluable tool to achieving desired learning outcomes, though there are barriers to its effective use that cannot be overlooked. Since active learning

is a tool primarily for use during class time, this session of 12.s597 allowed students to think more concretely about teaching practice, and the action of leading a classroom. Particularly in EAPS, active learning can be thoughtfully and authentically applied in lab and field settings. Thus, the class discussions and activities surrounding this subject were important for students to begin to consider themselves in the role of leading a classroom, and what strategies exist for effectively doing so.

Active learning includes any activity, particularly classroom activity, that requires students to be actively engaged with content (Felder & Brent 2016). This could include clicker questions, working on practice problems alone or in groups, reflecting through writing or discussion, or any number of other activities. Active learning contrasts with traditional didactic lectures, which allow students to receive information passively, their engagement primarily dependent on their own note-taking. It has been demonstrated that, in such a setting, student attention peaks 10 minutes into lecture and then declines with time (Bunce et al. 2010). Active learning disrupts this pattern by introducing a stimulus that re-engages student attention, allowing students to make more out of class time.

Additionally, active learning requires students to practice recall of information learned: in an optimal active learning activity will synthesize what they have learned by discussing it with classmates, reflecting independently, or applying concepts to practical examples (Brown et al. 2014). Many active learning classroom activities may be similar to what would be done in homework. However, students have the benefit of receiving immediate feedback on their work in class from instructors or other students. This facilitates the process of integrating new information, applying that learning, reframing the information in response to feedback, and proceeding with learning.

The primary drawback of active learning is that it may involve more work by the instructor to design multiple activities, rather than simply lecturing from slides from previous semesters. However, once the activities are designed, they can likewise be recycled in following years. Additionally, instructors may find class time to be less onerous if students are independently engaged with activities during time that would otherwise require lecturing. A further barrier to the effective use of active learning is that it may be more taxing on students. Rather than being able to “zone out” during lecture, students are required to repeatedly, actively engage with the class, which may feel demanding. It may thus be helpful to explicitly explain to students what active learning is, and that the work they are

doing in class will likely mean they need to spend less time outside of class synthesizing information. Such transparency may help otherwise resistant students accept the benefits of active learning.

Since we all live on Earth, it can feel natural to incorporate active learning in EAPS classrooms: field trips and labs are a common and often fundamental part of how classes are structured. EAPS thus lends itself to many authentic active learning exercises, and most classes include some such element. The challenge is more often that active learning can be relegated to the lab or field, while class time itself remains didactic. While keeping these valuable field and lab experiences, it would likely improve learning to include smaller, related activities in class meetings throughout the semester. These activities could scaffold, or build skills, towards a longer, more focused field or lab experience while also keeping students engaged with classroom material.

Effective Assessments and Feedback

The final readings of the IAP term were concerned with assessing learning and giving effective feedback. This subject was meant to prompt 12.s597 participants to reflect upon ways of assessing the impact of their teaching and incorporate the feedback of those assessments as a course progresses. In EAPS, assessments may come in many forms in a variety of subjects. Thus, this topic also allowed for some creativity about the role of field courses, labs, writing, coding, and traditional tests in an Earth Science classroom. The intention of these readings and the associated class times was for students to discover that effective feedback can come in many forms, and that Earth Science in particular lends itself to developing engaging, rewarding assessments.

Effective assessments give both students and instructors feedback on how well students are learning information. Instructors can use this information to adjust the pace of the class, emphasize or revisit areas where students are tending to struggle. For students, being assessed and receiving effective feedback can be one of the most important tools for learning effectively and growing skills (Ambrose et al. 2010). To give an extreme example, if a student was simply given a letter grade at the end of the semester with no other context, they would not know which material they understood correctly or where they had gaps of skill or information. It is thus important to give adequate feedback, throughout the course of the class to give students time to iterate on their learning and make adjustments. It

is likewise important that assessments both be well written in the sense of interrogating students on the information and skills they are meant to be learning in the course, and that those learning goals be communicated transparently to students (Andrade 2001).

An important aspect of effective feedback is striking an appropriate frequency. While it is generally good to receive more feedback, it is possible to overwhelm students with too much. Ideally, feedback is given frequently, in small amounts (Hattie & Timperley 2007, Martin et al. 2005). This can come in the form of low stakes in-class exercises where both students and instructors can check for understanding, and students have the opportunity to ask clarifying questions in the moment. For larger, higher stakes assignments such as tests and written reports, feedback may be best given infrequently, perhaps once on a draft and once on a final grade. Essentially, the quantity of feedback must be balanced against the significance of the activity: it is neither productive nor practical to give detailed feedback on smaller exercises, and that effort is better spent on assignments of greater weight.

Effective feedback must also be well timed in order to give students the ability to incorporate it into their learning in a way that is both effective and fair (Ambrose et al. 2010). Optimally, the majority of feedback will be given in a low stakes environment, where students have the freedom to be wrong and check for understanding. Feedback given after an assignment has been submitted (i.e. in association with a final grade) may provide some opportunity to check for understanding, but does not necessarily give opportunity to incorporate that feedback. If the same feedback could be given earlier in the class, perhaps on a draft of the assignment, students are allowed the opportunity to actually employ the feedback on their final submission. Within the bounds of time, each iteration will lead to an improved product and greater learning. Thus, planning feedback to allow for iteration, particularly in advance of higher stakes assignments, will lead to improved learning outcomes.

Importantly, aspects of feedback may occur in advance of students completing an assignment. If instructors are transparent about the goals of an assignment, students may more effectively meet those goals (Rothkopf & Billington 1979). This does not necessarily require being prescriptive in one an assignment should look like or providing a rubric for students to check boxes (though both may be effective in the right context). Rather, it is important that instructors communicate to students what they would like students to learn or get out of an assessment, or what particular areas they are attempting to assess. This is particularly true

in diverse groups including underserved students: students of a more privileged background are more likely to be privy to instructor intention or know how to look for cues of learning in assignments. Thus, simply being explicit and explaining outright what an instructors goals are can lead to a more equitable learning environment (Winkelman et al. 2016).

Giving effective feedback can seem time consuming or onerous, so it is important to consider strategies that can render the process less taxing. Namely, peer feedback can be invaluable for equalizing learning outcomes in class. In assessing each others' understanding, more advanced students can communicate their learning to their peers who may be struggling. This has a benefit to both students: the struggling student improves their understanding, and the advanced student can deepen their own understanding through the process of teaching. This requires minimal effort from the instructor, who must simply facilitate a peer feedback activity. Generally, feedback is central to student learning, and thus ought to be considered a priority in teaching. An appropriate frequency and timing can allow students to iterate on their understanding to much improved learning outcomes. To facilitate equitable learning, these learning outcomes are best communicated openly to the class when an assessment is assigned. This can be an intensive process, but peer feedback and other strategies can lessen the burden on instructors.

5.5.2 “Bring a Thing”

Following reading-based discussions on Thursdays, Tuesday class time was spent on an activity called “Bring a Thing”. For this, students were asked to bring some sort of artifact or idea related to that week’s reading (i.e. differences of prior knowledge, active learning, or effective assessments and feedback). The “Thing” they brought could be an additional paper on the subject, a classroom practice they had either used or experienced as a student, a syllabus, simply an idea, or anything really: intentionally, the only limit that was placed on the “Thing” was that it ought to be related to the subject of the week. Prior to class, students were asked to write a short reflection about their Thing and what they would like to discuss during class time. Then, the entire class period was spent broken into smaller groups of 3-4. Each student was given 10 minutes to use as they wished: they could speak for the full 10 minutes about the significance of what they brought, describe it briefly and use the remainder of their time to facilitate a discussion or solicit feedback, or anything in-between. After all students in the group had presented, any time that remaining in the

class period could be used to share lingering thoughts or discuss the Things in the context of the collective presentations.

The general consensus in the class was that Bring a Thing was an effective activity and a positive experience. Both students registered for the class and listeners actively engaged in this exercise, and while some students failed to write their reflection, no student ever failed to Bring a Thing. There was a broad diversity of items brought, though students tended away from things that they had created themselves. Nonetheless, in what they brought, students demonstrated thoughtfulness and insight into the challenges of teaching effectively, especially in the Earth Sciences. For example, one student brought the question of giving effective feedback in a the context of a mineral identification quiz. The student pointed out that the possible feedback to give can feel limited (i.e. is it the correct mineral or not?), and that examples can likewise be limited to the number of hand samples available in the department. At the same time, the task of learning mineral identification is largely one of memorization and seeing many examples, so teaching strategies that involve active learning may or may not be possible. This led to an interesting, practical discussion of effectively teaching mineral identification and material like it. Solutions included rubrics that allowed partial credit for explaining the reasoning: mis-remembering the crystal of a mineral may lead to wrong identification, even if the rest of a student's reasoning is correct. It was likewise suggested that it may be helpful to limit grading of tasks of this kind and instead providing many opportunities to mutually work through identifications.

For a different session of Bring a Thing, a student brought an in-class activity that had been used in a class he took at his undergraduate institution. The activity (a worksheet) asked students quick, low-stakes content questions, then asked them to rate their confidence in their answer. The worksheets would be handed in for feedback but not graded. For students, these worksheets provided in-class opportunities to practice recall, and encouraged metacognition as they reflected on their own understanding. For the course instructor, the worksheets served as a barometer to gauge student understanding, and adjust the pace of the class accordingly. The discussion of this Bring a Thing was largely about these worksheets as a successful strategy for achieving learning goals. Thus, while the discussion of mineralogy was largely a thought partnership to solve a challenging pedagogical problem, the discussion of the worksheets was an opportunity to reflect on the positive aspects of a teaching strategy, and how it might be incorporated into any particular class. Bring a Thing was varied in its

expression, but effectively created a space for students to apply pedagogical concepts.

This activity served multiple purposes. First, it worked toward the pedagogical goal of allowing students to practice recall. In presenting and giving feedback on other presentations, students had the opportunity to explore the subjects of the readings in greater detail, particularly the aspects that most interest them. In this setting, students received immediate, low-stakes feedback, primarily from their peers, allowing them to make adjustments in their understanding quickly, as needed. Bring a Thing also served the purpose of allowing students to lead a subset of the class, and in that sense practice teaching. This activity gave students a microcosm of preparing a lesson plan, and deciding how best to spend the class time allotted to them. This was of course not a fully authentic experience: 10 minutes is not a full class period, and the intention of Bring a Thing was more to learn collectively than to teach. However, it did provide the opportunity to experience facilitating a discussion or lecturing on a topic of one's choice. Finally, Bring a Thing served the important purpose of building community. While Tuesday class sessions intentionally provided ample space for discussion in and out of smaller groups, the discussion spaces of Bring a Thing were intentionally facilitated by the students themselves. Because of this, the momentum of the class was driven by student involvement, building a collective responsibility for the trajectory of class. This sense of mutual responsibility served both the classroom environment and my own EAPS-level goal of building a community around teaching in the department. Segueing this goal beyond the space of 12.s597 in January of 2022 remains an open question, and ideas for this are discussed in detail later in this chapter.

Super Bring a Thing

For our final class, it was our goal to promote a conversation that included applications in all areas of all three reading areas. To do this, each instructor brought a Thing, and students were divided into two groups to give feedback on these things. Both Things were assignments: a writing assignment for a paleoclimate course taught by co-instructor David McGee, and a project assignment written to be intentionally difficult and obtuse for a fictional climate modeling course. In their two groups, students were asked “What would need to happen to make this a successful assessment, both in class and in the assessment description itself?”, and to edit or annotate the provided document to make it a more effective assessment.

In doing this exercise, students were asked to assimilate all of the information they had

learned, and apply it to a product that could be used in a real classroom setting. Whereas previous iterations of Bring a Thing allowed some flexibility in terms of goals and ownership of the product, Super Bring a Thing required a firm, written or communicated stance of how the Thing should be changed, and what the basis was for that change. In that sense, this final activity was higher stakes: each group was required to present a justified edit to both their classmates and instructors. As was the case for the rest of the term, this activity was not graded. However, there was an attempt to raise the stakes by removing students' advanced knowledge of content (they were not the ones Bringing the Thing), and requiring them to commit their thoughts to writing (editing the document). This was not a perfect final exercise, and certainly could be improved upon. However, it made a solid effort towards the goals of raising the stakes for a final exercise, and adding a more public report-out.

5.5.3 Strengths and Growth Areas of this Course

This course was effective towards one of my primary goals as a TDF: creating a community of practice towards pedagogy in EAPS. Twice a week for the month of January, a group of about 11 EAPS members (including instructors: 9 graduate students, 1 postdoc, and one faculty member) met to discuss pedagogical theory and practice in the context of Earth Science. The frequency of these meetings effectively created a sense of continuity and community, at least from my own perspective as an instructor. While graduate students have access to TLL programming and faculty are able to teach courses, for the one postdoc this provided perhaps a sole on-campus outlet for an interest in teaching. Additionally, while TLL programming is available to graduate students, those resources span departments and thus do not allow a space for very specific content. Though participants in this seminar spanned subdisciplines (PAOC, Geology, the Joint Program, etc.), all had at least some background in Earth Science. This allowed for discussion and feedback on much more specific examples, situations, and applications.

Despite these successes, a number of growth areas remain for 12.s597. As an IAP course, the seminar was necessarily limited in the number of topics it could cover. With an introductory session and a final reflective session, only three readings and related Bring a Thing sessions were possible. This is a very limited scope of possible teaching topics, and while the topics were chosen to be appropriately introductory, a greater diversity of subjects and more specificity would be helpful. The short duration of the course was also limiting in regards to

providing opportunity for practical applications. With more time, students would have the opportunity to learn material, time to discuss and synthesize the material, and then space to apply what they learned by producing their own deliverables. The time frame of IAP simply does not allow for all of these steps to happen. Lastly, while the twice weekly frequency allowed for momentum to be built towards community among participants, it also limits participation by faculty. It seems, then, that different strategies are necessary to involve faculty in a pedagogical community of practice.

5.6 Faculty Panel

This term, I will organize a panel of faculty to discuss teaching in EAPS. This panel will be a group of about four faculty who have demonstrated a particular interest in teaching. Ideally, the panel will involve faculty with expertise in teaching for the field, lab courses, writing intensive courses, and coding intensive courses, spanning many of the teaching challenges in EAPS. Faculty will be able to speak to the specific difficulties they face in their courses and, since most courses involve some subset of these categories, other panelists will be able to engage in discussing what works or does not in different types of classes.

This panel will serve two purposes. First, it will offer attendees the insights shared by the faculty panelists from their diverse perspectives. Other faculty attendees will have the opportunity to hear their colleagues' insights and incorporate new strategies into their own courses. Students who attend the panel will hear practical discussions from faculty who have taught for years, a resource that is not formally available in other EAPS-specific settings. The second purpose of this panel will be to facilitate a conversation among the faculty about teaching in EAPS, and hopefully include them in the community of practice that we have been working to build in the department. This panel will likely only require an hour of time from both panelists and attendees, and thus will be accommodating of faculty's busy schedules. If a panel such as this were hosted every semester, it would significantly contribute towards the goal of having regular discussions and spaces dedicated towards pedagogy in the department.

5.7 Reflections and Looking Forward

As I finish my time as EAPS Teaching Development Fellow, it has become clear that there is plenty of work left for future TDFs. The challenge of facilitating events frequently enough to create momentum towards a community of practice, while not so frequently as to over-exert faculty, is nontrivial. It is my belief that a combination of the projects described above could strike this balance: offering 12.s597 each IAP would build momentum and enthusiasm for EAPS-specific pedagogy among students, and a faculty panel in each of the Fall and Spring terms would propagate this momentum and facilitate faculty involvement. Were I the TDF next year, those events and activities are where I would place my effort each year. In service of this, a roadmap for a 3-year rotation of topics for 12.s597 is laid out below. However, it is my hope that future Teaching Development Fellows in the department will see the flaws and shortcomings of my vision, and improve upon it with their own insight and creativity.

5.7.1 Future Iterations Of 12.s597

Myself, my co-instructor, and a number of participants in 12.s597 expressed interest in finding ways to make it possible for the course to be taught every year, and to be taken more than once without repeating the same material. Having a rotation of three years of course materials would allow students to take the course three times, and would also address the shortcoming that only three topics are possible with the IAP format. Optimally, the course that was taught this year would be a “Teaching Theory” version of the course. Next year, a hyper-specific iteration of the course could mirror the faculty panel to focus on the specific challenges faced in teaching in an EAPS classroom, and a third year in the rotation would be a more practical, application-heavy iteration themed “Classroom Practice”. Each year would have three topics distinct from previous years. The rotation could thus be:

- Year 1: Teaching Theory
 - Differences of Prior Knowledge
 - Active Learning
 - Feedback and Effective Assessments

- Year 2: Teaching Challenges in EAPS

- Managing Coding-Heavy Courses
 - Leading Effective Field Trips
 - Teaching in the Lab
- Year 3: Classroom Practice
 - Syllabus Writing
 - Scaffolding a Lesson
 - Designing Authentic Assessments

Year 2 and especially Year 3 would likely leverage Bring a Thing to require students to produce their own products: an outline of a syllabus, an in-class exercise, a brief lesson plan. This trajectory would allow students who took all three years of the course a firm basis in the theory of teaching well, how that theory can be applied specifically to Earth Science classrooms, and the practice of actually writing the class materials. Students would likely not be able to take these courses in order, so care would need to be taken to bolster students who had not taken previous iterations of 12.s597, while encouraging other students to leverage their prior knowledge for maximum outcome.

5.7.2 Future Teaching Development Fellows

I believe that the goals I had this year as the EAPS TDF were worthy, and that the actions I have taken have been effective in progress towards those goals. However, I have also found that one of the great strengths of the Teaching Development Fellow program is that it is collaborative. In my biweekly meetings with TDFs from other departments, I have received feedback and insights that I could never have reached on my own. In that sense, the work that I did this year in EAPS is the product of many invaluable thought partnerships. But it also demonstrates the importance of acknowledging the limitations of any one perspective. So, while I hope future TDFs in EAPS will frame their efforts with my past work in mind, I have a much greater wish that they will build their efforts around their own passions and insights, and with the growth mindset that is so common in TDF cohort meetings. While I am proud of what I have done, there is very much still to do and I have great faith in future EAPS Teaching Development Fellows to do it.

Appendix A

Supplementary Figures

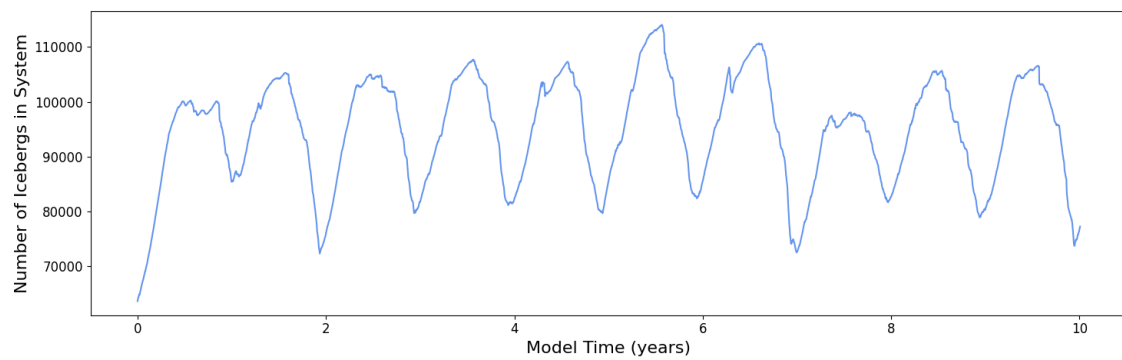


Figure A-1: Time series of icebergs in the model system from the beginning to end of a 10-year Heinrich Event. The number of icebergs varies by calving season but is stable on the time scale of the experiment.

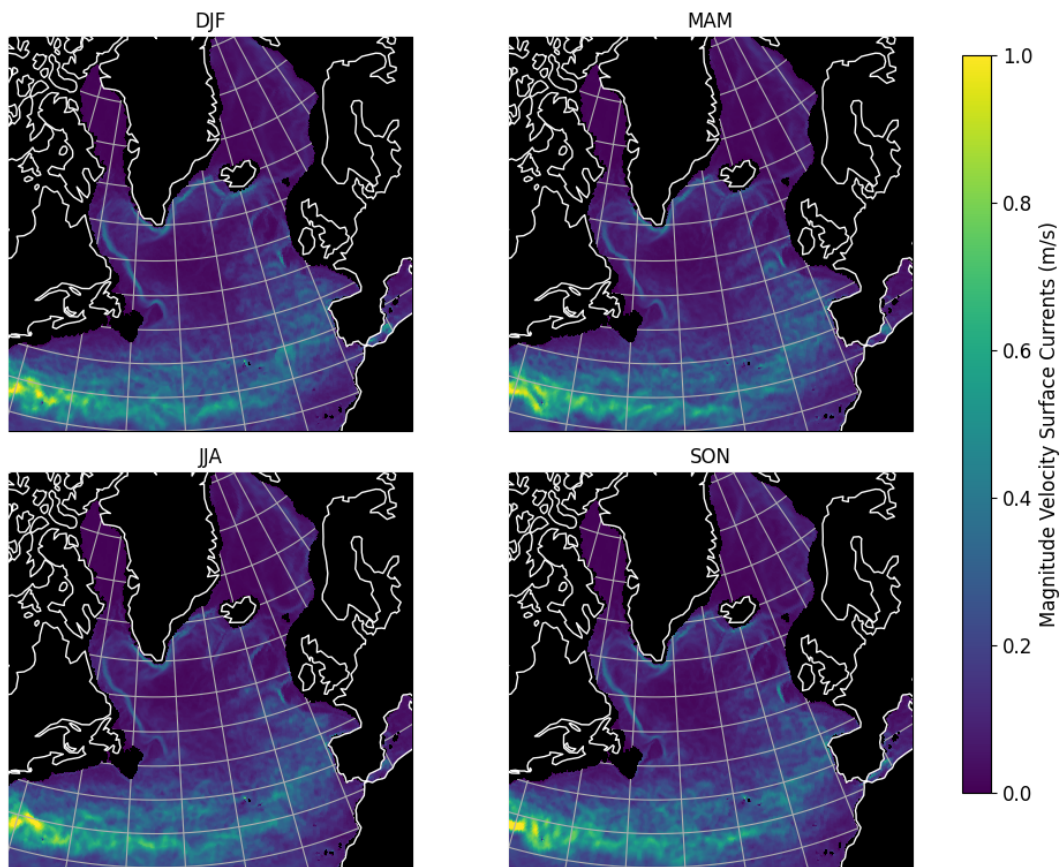


Figure A-2: Average seasonal magnitude of surface currents during Heinrich Events. These currents do not change with the magnitude or direction necessary to explain the change in iceberg trajectories.

Bibliography

- Abdelmoula, W. M., Balluff, B., Englert, S., Dijkstra, J., Reinders, M. J., Walch, A., McDonnell, L. A. & Lelieveldt, B. P. (2016), ‘Data-driven identification of prognostic tumor subpopulations using spatially mapped t-SNE of mass spectrometry imaging data’, *Proceedings of the National Academy of Sciences* **113**(43), 12244–12249.
- Ahn, J. & Brook, E. J. (2008), ‘Atmospheric CO₂ and climate on millennial time scales during the last glacial period’, *Science* **322**(5898), 83–85.
- Alfeld, M., Pedetti, S., Martinez, P. & Walter, P. (2018), ‘Joint data treatment for Vis–NIR reflectance imaging spectroscopy and XRF imaging acquired in the Theban Necropolis in Egypt by data fusion and t-SNE’, *Comptes Rendus Physique* **19**(7), 625–635.
- Alley, R. B., Andrews, J. T., Barber, D. & Clark, P. U. (2005), ‘Comment on “Catastrophic ice shelf breakup as the source of Heinrich event icebergs” by CL Hulbe et al.’.
- Alley, R. & MacAyeal, D. (1994), ‘Ice-rafted debris associated with binge/purge oscillations of the Laurentide Ice Sheet’, *Paleoceanography* **9**(4), 503–511.
- Alvarez-Solas, J., Robinson, A., Montoya, M. & Ritz, C. (2013), ‘Iceberg discharges of the last glacial period driven by oceanic circulation changes’, *Proceedings of the National Academy of Sciences* **110**(41), 16350–16354.
- Ambrose, S. A., Bridges, M. W., DiPietro, M., Lovett, M. C. & Norman, M. K. (2010), *How learning works: Seven research-based principles for smart teaching*, John Wiley & Sons, chapter 5.
- Ambrose, S. A. & Lovett, M. C. (2014), Prior knowledge is more important than content: Skills and beliefs also impact learning, *in* ‘Applying science of learning in education: Infusing psychological science into the curriculum’, Society for the Teaching of Psychology.
- Anderson, J. B., Domack, E. W. & Kurtz, D. D. (1980), ‘Observations of sediment-laden icebergs in Antarctic waters: implications to glacial erosion and transport’, *Journal of Glaciology* **25**(93), 387–396.
- Andrade, H. G. (2001), ‘The effects of instructional rubrics on learning to write’, *Current issues in education* **4**.
- Andrews, J. T. (2000), ‘Icebergs and iceberg rafted detritus (IRD) in the North Atlantic: facts and assumptions’, *Oceanography* pp. 100–108.
- Awramik, S. M. & Buchheim, H. P. (2015), ‘Giant stromatolites of the Eocene Green River Formation (Colorado, USA)’, *Geology* **43**(8), 691–694.

- Bacon, M. P. (1984), ‘Glacial to interglacial changes in carbonate and clay sedimentation in the Atlantic Ocean estimated from ^{230}Th measurements’, *Chemical geology* **46**(2), 97–111.
- Barker, S., Diz, P., Vautravers, M. J., Pike, J., Knorr, G., Hall, I. R. & Broecker, W. S. (2009), ‘Interhemispheric Atlantic seesaw response during the last deglaciation’, *Nature* **457**(7233), 1097–1102.
- Becht, E., Dutertre, C.-A., Kwok, I. W., Ng, L. G., Ginhoux, F. & Newell, E. W. (n.d.), ‘Evaluation of UMAP as an alternative to t-SNE for single-cell data’.
- Benson, L. (1994), ‘Carbonate deposition, Pyramid Lake subbasin, Nevada: 1. Sequence of formation and elevational distribution of carbonate deposits (tufas)’, *Palaeogeography, Palaeoclimatology, Palaeoecology* **109**(1), 55–87.
- Benson, L. V., Currey, D. R., Dorn, R. I., Lajoie, K. R., Oviatt, C. G., Robinson, S. W., Smith, G. I. & Stine, S. (1990), ‘Chronology of expansion and contraction of four Great Basin lake systems during the past 35,000 years’, *Palaeogeography, Palaeoclimatology, Palaeoecology* **78**(3-4), 241–286.
- Bischoff, J. L., Stine, S., Rosenbauer, R. J., Fitzpatrick, J. A. & Stafford Jr, T. W. (1993), ‘Ikaite precipitation by mixing of shoreline springs and lake water, Mono Lake, California, USA’, *Geochimica et cosmochimica acta* **57**(16), 3855–3865.
- Blunier, T. & Brook, E. J. (2001), ‘Timing of millennial-scale climate change in Antarctica and Greenland during the last glacial period’, *science* **291**(5501), 109–112.
- Bond, G., Heinrich, H., Broecker, W., Labeyrie, L., McManus, J., Andrews, J., Huon, S., Jantschik, R., Clasen, S., Simet, C. et al. (1992), ‘Evidence for massive discharges of icebergs into the North Atlantic ocean during the last glacial period’, *Nature* **360**(6401), 245–249.
- Boyle, E. A. & Keigwin, L. (1987), ‘North Atlantic thermohaline circulation during the past 20,000 years linked to high-latitude surface temperature’, *Nature* **330**(6143), 35–40.
- Brasier, A., Wacey, D., Rogerson, M., Guagliardo, P., Saunders, M., Kellner, S., Mercedes-Martin, R., Prior, T., Taylor, C., Matthews, A. et al. (2018), ‘A microbial role in the construction of Mono Lake carbonate chimneys?’, *Geobiology* **16**(5), 540–555.
- Broecker, W. S. (1994), ‘Massive iceberg discharges as triggers for global climate change’, *Nature* **372**(6505), 421–424.
- Broecker, W. S. & Orr, P. C. (1958), ‘Radiocarbon chronology of Lake Lahontan and Lake Bonneville’, *Geological Society of America Bulletin* **69**(8), 1009–1032.
- Brown, P., Roediger, H., McDaniel, M. & Stick, M. I. (2014), ‘The Science of Successful Learning’.
- Bunce, D. M., Flens, E. A. & Neiles, K. Y. (2010), ‘How long can students pay attention in class? A study of student attention decline using clickers’, *Journal of Chemical Education* **87**(12), 1438–1443.
- Candy, I. & Schreve, D. (2007), ‘Land–sea correlation of Middle Pleistocene temperate sub-stages using high-precision uranium-series dating of tufa deposits from southern England’, *Quaternary Science Reviews* **26**(9-10), 1223–1235.

- Celik, T. (2009), ‘Unsupervised change detection in satellite images using principal component analysis and *k*-means clustering’, *IEEE Geoscience and Remote Sensing Letters* **6**(4), 772–776.
- Clarke, F. W. & Washington, H. S. (1924), *The composition of the earth’s crust*, Vol. 127, US Government Printing Office.
- Collins, M., Booth, B. B., Bhaskaran, B., Harris, G. R., Murphy, J. M., Sexton, D. M. & Webb, M. J. (2011), ‘Climate model errors, feedbacks and forcings: a comparison of perturbed physics and multi-model ensembles’, *Climate Dynamics* **36**(9), 1737–1766.
- Condrón, A. & Hill, J. C. (2021), ‘Timing of iceberg scours and massive ice-rafting events in the subtropical North Atlantic’, *Nature Communications* **12**(1), 1–14.
- Cook, B. I., Mankin, J. S. & Anchukaitis, K. J. (2018), ‘Climate change and drought: From past to future’, *Current Climate Change Reports* **4**(2), 164–179.
- Cortijo, E., Labeyrie, L., Vidal, L., Vautravers, M., Chapman, M., Duplessy, J.-C., Elliot, M., Arnold, M., Turon, J.-L. & Auffret, G. (1997), ‘Changes in sea surface hydrology associated with Heinrich event 4 in the North Atlantic Ocean between 40 and 60 n’, *Earth and Planetary Science Letters* **146**(1-2), 29–45.
- Costa, K. M., Hayes, C. T., Anderson, R. F., Pavia, F. J., Bausch, A., Deng, F., Dutay, J.-C., Geibert, W., Heinze, C., Henderson, G. et al. (2020), ‘230Th normalization: New insights on an essential tool for quantifying sedimentary fluxes in the modern and Quaternary ocean’, *Paleoceanography and Paleoclimatology* **35**(2), e2019PA003820.
- Council, T. C. & Bennett, P. C. (1993), ‘Geochemistry of ikaite formation at Mono Lake, California: implications for the origin of tufa mounds’, *Geology* **21**(11), 971–974.
- DeConto, R. M., Pollard, D., Alley, R. B., Velicogna, I., Gasson, E., Gomez, N., Sadai, S., Condrón, A., Gilford, D. M., Ashe, E. L. et al. (2021), ‘The Paris Climate Agreement and future sea-level rise from Antarctica’, *Nature* **593**(7857), 83–89.
- Dee, S., Parsons, L., Loope, G., Overpeck, J., Ault, T. & Emile-Geay, J. (2017), ‘Improved spectral comparisons of paleoclimate models and observations via proxy system modeling: Implications for multi-decadal variability’, *Earth and Planetary Science Letters* **476**, 34–46.
- DeMott, L. M., Napieralski, S. A., Junium, C. K., Teece, M. & Scholz, C. A. (2020), ‘Microbially influenced lacustrine carbonates: A comparison of Late Quaternary Lahontan tufa and modern thrombolite from Fayetteville Green Lake, NY’, *Geobiology* **18**(1), 93–112.
- Dowdeswell, J. A. & Dowdeswell, E. K. (1989), ‘Debris in icebergs and rates of glaci-marine sedimentation: observations from Spitsbergen and a simple model’, *The Journal of Geology* **97**(2), 221–231.
- Dowdeswell, J. A., Whittington, R. J. & Hodgkins, R. (1992), ‘The sizes, frequencies, and freeboards of east greenland icebergs observed using ship radar and sextant’, *Journal of Geophysical Research: Oceans* **97**(C3), 3515–3528.

- Dowdeswell, J., Maslin, M., Andrews, J. & McCave, I. (1995), 'Iceberg production, debris rafting, and the extent and thickness of Heinrich layers (h-1, h-2) in North Atlantic sediments', *Geology* **23**(4), 301–304.
- Dunn, J. R. (1953), 'The origin of the deposits of tufa in Mono Lake [California]', *Journal of Sedimentary Research* **23**(1), 18–23.
- Dyke, A., Andrews, J., Clark, P., England, J., Miller, G., Shaw, J. & Veillette, J. (2002), 'The Laurentide and Innuitian ice sheets during the last glacial maximum', *Quaternary Science Reviews* **21**(1-3), 9–31.
- Dyke, A. & Prest, V. (1987), 'Late Wisconsinan and holocene history of the Laurentide ice sheet', *Géographie physique et Quaternaire* **41**(2), 237–263.
- Evans, M. N., Tolwinski-Ward, S. E., Thompson, D. M. & Anchukaitis, K. J. (2013), 'Applications of proxy system modeling in high resolution paleoclimatology', *Quaternary science reviews* **76**, 16–28.
- Fang, M. & Li, X. (2019), 'An artificial neural networks-based tree ring width proxy system model for paleoclimate data assimilation', *Journal of Advances in Modeling Earth Systems* **11**(4), 892–904.
- Felder, R. M. & Brent, R. (2016), *Teaching and learning STEM: A practical guide*, John Wiley & Sons, chapter 6.
- Fendrock, M., Chen, C. Y., Olson, K. J., Lowenstein, T. K. & McGee, D. (2022), 'A Computer Vision Algorithm for Interpreting Lacustrine Carbonate Textures at Searles Valley, USA', *Computers and Geosciences . (In Revisions)*.
- Fendrock, M., Condrón, A. & McGee, D. (2022), 'Modeling Iceberg Longevity and Distribution During Heinrich Events', *Paleoceanography and Paleoclimatology . (In Revisions)*.
- Ford, T. & Pedley, H. (1996), 'A review of tufa and travertine deposits of the world', *Earth-Science Reviews* **41**(3-4), 117–175.
- Francois, R., Frank, M., Rutgers van der Loeff, M. M. & Bacon, M. P. (2004), '230Th normalization: An essential tool for interpreting sedimentary fluxes during the late Quaternary', *Paleoceanography* **19**(1).
- Glasser, N. F. & Hambrey, M. J. (2001), 'Styles of sedimentation beneath Svalbard valley glaciers under changing dynamic and thermal regimes', *Journal of the Geological Society* **158**(4), 697–707.
- Grousset, F. E., Pujol, C., Labeyrie, L., Auffret, G. & Boelaert, A. (2000), 'Were the North Atlantic Heinrich events triggered by the behavior of the European ice sheets?', *Geology* **28**(2), 123–126.
- Grousset, F., Labeyrie, L., Sinko, J., Cremer, M., Bond, G., Duprat, J., Cortijo, E. & Huon, S. (1993), 'Patterns of ice-rafted detritus in the glacial North Atlantic (40–55° N)', *Paleoceanography* **8**(2), 175–192.
- Guo, X. & Chafetz, H. S. (2012), 'Large tufa mounds, Searles Lake, California', *Sedimentology* **59**(5), 1509–1535.

- Guo, X. & Chafetz, H. S. (2014), ‘Trends in $\delta^{18}\text{O}$ and $\delta^{13}\text{C}$ values in lacustrine tufa mounds: palaeohydrology of Searles Lake, California’, *Sedimentology* **61**(1), 221–237.
- Gwiazda, R., Hemming, S. & Broecker, W. (1996), ‘Provenance of icebergs during Heinrich event 3 and the contrast to their sources during other Heinrich episodes’, *Paleoceanography* **11**(4), 371–378.
- Hargreaves, J. C., Annan, J. D., Ohgaito, R., Paul, A. & Abe-Ouchi, A. (2013), ‘Skill and reliability of climate model ensembles at the Last Glacial Maximum and mid-Holocene’, *Climate of the Past* **9**(2), 811–823.
- Hattie, J. & Timperley, H. (2007), ‘The power of feedback’, *Review of educational research* **77**(1), 81–112.
- He, C., Liu, Z., Zhu, J., Zhang, J., Gu, S., Otto-Bliesner, B. L., Brady, E., Zhu, C., Jin, Y. & Sun, J. (2020), ‘North Atlantic subsurface temperature response controlled by effective freshwater input in “Heinrich” events’, *Earth and Planetary Science Letters* **539**, 116247.
- Hemming, S. R. (2004), ‘Heinrich events: Massive late Pleistocene detritus layers of the North Atlantic and their global climate imprint’, *Reviews of Geophysics* **42**(1).
- Hill, J. C. & Condron, A. (2014), ‘Subtropical iceberg scours and meltwater routing in the deglacial western North Atlantic’, *Nature Geoscience* **7**(11), 806–810.
- Hostetler, S. W. & Bartlein, P. J. (1990), ‘Simulation of lake evaporation with application to modeling lake level variations of Harney-Malheur Lake, Oregon’, *Water Resources Research* **26**(10), 2603–2612.
- Hsiao, S.-C., Chiang, W.-S., Jang, J.-H., Wu, H.-L., Lu, W.-S., Chen, W.-B. & Wu, Y.-T. (2021), ‘Flood risk influenced by the compound effect of storm surge and rainfall under climate change for low-lying coastal areas’, *Science of the total environment* **764**, 144439.
- Hulbe, C. L. (1997), ‘An ice shelf mechanism for Heinrich layer production’, *Paleoceanography* **12**(5), 711–717.
- Huntingford, C., Jeffers, E. S., Bonsall, M. B., Christensen, H. M., Lees, T. & Yang, H. (2019), ‘Machine learning and artificial intelligence to aid climate change research and preparedness’, *Environmental Research Letters* **14**(12), 124007.
- Jagniecki, E. A., Lowenstein, T. K., Demicco, R. V., Baddouh, M., Carroll, A. R., Beard, B. L. & Johnson, C. M. (2021), ‘Spring origin of Eocene carbonate mounds in the Green River Formation, Northern Bridger Basin, Wyoming, USA’, *Sedimentology* .
- Jayko, A. S., Forester, R. M., Kaufman, D. S., Phillips, F. M., Yount, J., McGeehin, J., Mahan, S. A., Reheis, M., Hershler, R. & Miller, D. (2008), ‘Late Pleistocene lakes and wetlands, Panamint Valley, Inyo County, California’, *SPECIAL PAPERS-GEOLOGICAL SOCIETY OF AMERICA* **439**, 151.
- Jongma, J., Renssen, H. & Roche, D. M. (2013), ‘Simulating Heinrich event 1 with interactive icebergs’, *Climate Dynamics* **40**(5), 1373–1385.
- Kanungo, T., Mount, D. M., Netanyahu, N. S., Piatko, C. D., Silverman, R. & Wu, A. Y. (2002), ‘An efficient k-means clustering algorithm: Analysis and implementation’, *IEEE transactions on pattern analysis and machine intelligence* **24**(7), 881–892.

- Kaufman, A. & Broecker, W. (1965), ‘Comparison of Th230 and C14 ages for carbonate materials from Lakes Lahontan and Bonneville’, *Journal of geophysical Research* **70**(16), 4039–4054.
- Keigwin, L. D. & Lehman, S. J. (1994), ‘Deep circulation change linked to heinrich event 1 and Younger Dryas in a middepth North Atlantic core’, *Paleoceanography* **9**(2), 185–194.
- Keigwin, L., Sachs, J., Rosenthal, Y. & Boyle, E. (2005), ‘The 8200 year BP event in the slope water system, western subpolar North Atlantic’, *Paleoceanography* **20**(2).
- Klimczak, L. J., von Eschenbach, C. E., Thompson, P. M., Buters, J. T. & Mueller, G. A. (2020), ‘Mixture analyses of air-sampled pollen extracts can accurately differentiate pollen taxa’, *Atmospheric Environment* **243**, 117746.
- Knutson, T., Camargo, S. J., Chan, J. C., Emanuel, K., Ho, C.-H., Kossin, J., Mohapatra, M., Satoh, M., Sugi, M., Walsh, K. et al. (2020), ‘Tropical cyclones and climate change assessment: Part II: Projected response to anthropogenic warming’, *Bulletin of the American Meteorological Society* **101**(3), E303–E322.
- Kobak, D. & Berens, P. (2019), ‘The art of using t-SNE for single-cell transcriptomics’, *Nature communications* **10**(1), 1–14.
- Kobak, D. & Linderman, G. C. (2019), ‘UMAP does not preserve global structure any better than t-SNE when using the same initialization’, *bioRxiv* .
- Ku, T.-L., Luo, S., Lowenstein, T. K., Li, J. & Spencer, R. J. (1998), ‘U-series chronology of lacustrine deposits in Death Valley, California’, *Quaternary Research* **50**(3), 261–275.
- Laksov, K. B., Mann, S. & Dahlgren, L. O. (2008), ‘Developing a community of practice around teaching: A case study’, *Higher Education Research & Development* **27**(2), 121–132.
- Lambeck, K. & Chappell, J. (2001), ‘Sea level change through the last glacial cycle’, *Science* **292**(5517), 679–686.
- Levine, R. C. & Bigg, G. R. (2008), ‘Sensitivity of the glacial ocean to Heinrich events from different iceberg sources, as modeled by a coupled atmosphere-iceberg-ocean model’, *Paleoceanography* **23**(4).
- Li, J., Lowenstein, T. K., Brown, C. B., Ku, T.-L. & Luo, S. (1996), ‘A 100 ka record of water tables and paleoclimates from salt cores, Death Valley, California’, *Palaeogeography, Palaeoclimatology, Palaeoecology* **123**(1-4), 179–203.
- Li, T., Liu, Z., Hall, M. A., Berne, S., Saito, Y., Cang, S. & Cheng, Z. (2001), ‘Heinrich event imprints in the Okinawa trough: evidence from oxygen isotope and planktonic foraminifera’, *Palaeogeography, Palaeoclimatology, Palaeoecology* **176**(1-4), 133–146.
- Li, W., Cerise, J. E., Yang, Y. & Han, H. (2017), ‘Application of t-SNE to human genetic data’, *Journal of bioinformatics and computational biology* **15**(04), 1750017.
- Linderman, G. C. & Steinerberger, S. (2019), ‘Clustering with t-SNE, provably’, *SIAM Journal on Mathematics of Data Science* **1**(2), 313–332.

- Liu, Z., Zhu, J., Rosenthal, Y., Zhang, X., Otto-Bliesner, B. L., Timmermann, A., Smith, R. S., Lohmann, G., Zheng, W. & Timm, O. E. (2014), ‘The Holocene temperature conundrum’, *Proceedings of the National Academy of Sciences* **111**(34), E3501–E3505.
- Losch, M., Menemenlis, D., Campin, J.-M., Heimbach, P. & Hill, C. (2010), ‘On the formulation of sea-ice models. Part 1: Effects of different solver implementations and parameterizations’, *Ocean Modelling* **33**(1-2), 129–144.
- MacAyeal, D. (1993a), ‘Binge/purge oscillations of the Laurentide ice sheet as a cause of the North Atlantic’s Heinrich events’, *Paleoceanography* **8**(6), 775–784.
- MacAyeal, D. (1993b), ‘A low-order model of the Heinrich event cycle’, *Paleoceanography* **8**(6), 767–773.
- Marcott, S. A., Clark, P. U., Padman, L., Klinkhammer, G. P., Springer, S. R., Liu, Z., Otto-Bliesner, B. L., Carlson, A. E., Ungerer, A., Padman, J. et al. (2011), ‘Ice-shelf collapse from subsurface warming as a trigger for Heinrich events’, *Proceedings of the National Academy of Sciences* **108**(33), 13415–13419.
- Margold, M., Stokes, C. R. & Clark, C. D. (2018), ‘Reconciling records of ice streaming and ice margin retreat to produce a palaeogeographic reconstruction of the deglaciation of the Laurentide Ice Sheet’, *Quaternary science reviews* **189**, 1–30.
- Marshall, J., Adcroft, A., Hill, C., Perelman, L. & Heisey, C. (1997), ‘A finite-volume, incompressible Navier Stokes model for studies of the ocean on parallel computers’, *Journal of Geophysical Research: Oceans* **102**(C3), 5753–5766.
- Marshall, S. J. & Clarke, G. K. (1997), ‘A continuum mixture model of ice stream thermo-mechanics in the Laurentide Ice Sheet 2. Application to the Hudson Strait Ice Stream’, *Journal of Geophysical Research: Solid Earth* **102**(B9), 20615–20637.
- Martin, B., Koedinger, K. R., Mitrovic, A. & Mathan, S. (2005), On Using Learning Curves to Evaluate ITS., in ‘AIED’, pp. 419–426.
- Maslin, M. A., Shackleton, N. J. & Pflaumann, U. (1995), ‘Surface water temperature, salinity, and density changes in the northeast Atlantic during the last 45,000 years: Heinrich events, deep water formation, and climatic rebounds’, *Paleoceanography* **10**(3), 527–544.
- McGee, D., Moreno-Chamarro, E., Marshall, J. & Galbraith, E. (2018), ‘Western US lake expansions during Heinrich stadials linked to Pacific Hadley circulation’, *Science advances* **4**(11), eaav0118.
- McKay, R., Albot, O., Dunbar, G. B., Lee, J. I., Lee, M. K., Yoo, K.-C., Kim, S., Turton, N., Kulhanek, D., Patterson, M. et al. (2022), ‘A comparison of methods for identifying and quantifying Ice Rafted Debris on the Antarctic margin’, *Paleoceanography and Paleoclimatology* p. e2021PA004404.
- McManus, J. F., Anderson, R. F., Broecker, W. S., Fleisher, M. Q. & Higgins, S. M. (1998), ‘Radiometrically determined sedimentary fluxes in the sub-polar North Atlantic during the last 140,000 years’, *Earth and Planetary Science Letters* **155**(1-2), 29–43.

- McManus, J. F., Francois, R., Gherardi, J.-M., Keigwin, L. D. & Brown-Leger, S. (2004), ‘Collapse and rapid resumption of Atlantic meridional circulation linked to deglacial climate changes’, *nature* **428**(6985), 834–837.
- Meinshausen, M., Smith, S. J., Calvin, K., Daniel, J. S., Kainuma, M. L., Lamarque, J.-F., Matsumoto, K., Montzka, S. A., Raper, S. C., Riahi, K. et al. (2011), ‘The RCP greenhouse gas concentrations and their extensions from 1765 to 2300’, *Climatic change* **109**(1), 213–241.
- Meyer, C. R., Robel, A. A. & Rempel, A. W. (2019), ‘Frozen fringe explains sediment freeze-on during Heinrich events’, *Earth and Planetary Science Letters* **524**, 115725.
- Mugford, R. & Dowdeswell, J. (2010), ‘Modeling iceberg-rafted sedimentation in high-latitude fjord environments’, *Journal of Geophysical Research: Earth Surface* **115**(F3).
- Munroe, J. S. & Laabs, B. J. (2013), ‘Temporal correspondence between pluvial lake high-stands in the southwestern US and Heinrich Event 1’, *Journal of Quaternary Science* **28**(1), 49–58.
- Neukom, R., Schurer, A. P., Steiger, N., Hegerl, G. C. et al. (2018), ‘Possible causes of data model discrepancy in the temperature history of the last Millennium’, *Scientific Reports* **8**(1), 1–15.
- Njock, P. G. A., Shen, S.-L., Zhou, A. & Lyu, H.-M. (2020), ‘Evaluation of soil liquefaction using AI technology incorporating a coupled ENN/t-SNE model’, *Soil Dynamics and Earthquake Engineering* **130**, 105988.
- Oppo, D. W., Curry, W. B. & McManus, J. F. (2015), ‘What do benthic $\delta^{13}\text{C}$ and $\delta^{18}\text{O}$ data tell us about Atlantic circulation during Heinrich Stadial 1?’, *Paleoceanography* **30**(4), 353–368.
- Osman, M. B., Tierney, J. E., Zhu, J., Tardif, R., Hakim, G. J., King, J. & Poulsen, C. J. (2021), ‘Globally resolved surface temperatures since the Last Glacial Maximum’, *Nature* **599**(7884), 239–244.
- Otto-Bliesner, B. L., Brady, E. C., Clauzet, G., Tomas, R., Levis, S. & Kothavala, Z. (2006), ‘Last glacial maximum and Holocene climate in CCSM3’, *Journal of Climate* **19**(11), 2526–2544.
- Otto-Bliesner, B. L., Brady, E. C., Zhao, A., Brierley, C. M., Axford, Y., Capron, E., Govin, A., Hoffman, J. S., Isaacs, E., Kageyama, M. et al. (2021), ‘Large-scale features of Last Interglacial climate: results from evaluating the lig127k simulations for the Coupled Model Intercomparison Project (CMIP6)–Paleoclimate Modeling Intercomparison Project (PMIP4)’, *Climate of the Past* **17**(1), 63–94.
- Palacio-Niño, J.-O. & Berzal, F. (2019), ‘Evaluation metrics for unsupervised learning algorithms’, *arXiv preprint arXiv:1905.05667*.
- Pedregosa, F., Varoquaux, G., Gramfort, A., Michel, V., Thirion, B., Grisel, O., Blondel, M., Prettenhofer, P., Weiss, R., Dubourg, V. et al. (2011), ‘Scikit-learn: Machine learning in Python’, *the Journal of machine Learning research* **12**, 2825–2830.

- Peng, T.-H., Goddard, J. & Broecker, W. (1978), 'A Direct Comparison of ^{14}C and ^{230}Th Ages at Searles Lake, California', *Quaternary Research* **9**(3), 319–329.
- Pérez-Ortiz, M., Durán-Rosal, A. M., Gutiérrez, P. A., Sánchez-Monedero, J., Nikolaou, A., Fernández-Navarro, F. & Hervás-Martínez, C. (n.d.), 'On the use of evolutionary time series analysis for segmenting paleoclimate data'.
- Petryshyn, V. A., Rivera, M. J., Agić, H., Frantz, C. M., Corsetti, F. A. & Tripathi, A. E. (2016), 'Stromatolites in Walker Lake (Nevada, Great Basin, USA) record climate and lake level changes ~ 35,000 years ago', *Palaeogeography, palaeoclimatology, palaeoecology* **451**, 140–151.
- Pouyet, E., Rohani, N., Katsaggelos, A. K., Cossairt, O. & Walton, M. (2018), 'Innovative data reduction and visualization strategy for hyperspectral imaging datasets using t-SNE approach', *Pure and Applied Chemistry* **90**(3), 493–506.
- Printy, S. M. (2008), 'Leadership for teacher learning: A community of practice perspective', *Educational administration quarterly* **44**(2), 187–226.
- Reheis, M. C., Adams, K. D., Oviatt, C. G. & Bacon, S. N. (2014), 'Pluvial lakes in the Great Basin of the western United States—A view from the outcrop', *Quaternary Science Reviews* **97**, 33–57.
- Roberts, W. H., Valdes, P. J. & Payne, A. J. (2014), 'A new constraint on the size of Heinrich Events from an iceberg/sediment model', *Earth and Planetary Science Letters* **386**, 1–9.
- Roche, D. M., Paillard, D., Caley, T. & Waelbroeck, C. (2014), 'LGM hosing approach to Heinrich Event 1: results and perspectives from data–model integration using water isotopes', *Quaternary Science Reviews* **106**, 247–261.
- Roche, D., Paillard, D. & Cortijo, E. (2004), 'Constraints on the duration and freshwater release of Heinrich event 4 through isotope modelling', *Nature* **432**(7015), 379–382.
- Rothkopf, E. Z. & Billington, M. J. (1979), 'Goal-guided learning from text: inferring a descriptive processing model from inspection times and eye movements.', *Journal of educational psychology* **71**(3), 310.
- Ruddiman, W. F. (1977), 'Late Quaternary deposition of ice-rafted sand in the subpolar North Atlantic (lat 40 to 65 n)', *Geological Society of America Bulletin* **88**(12), 1813–1827.
- Scholl, D. W. (1960), 'Pleistocene algal pinnacles at Searles Lake, California', *Journal of Sedimentary Research* **30**(3), 414–431.
- Scholl, D. W. & Taft, W. H. (1964), 'Algae, contributors to the formation of calcareous tufa, Mono Lake, California', *Journal of Sedimentary Research* **34**(2), 309–319.
- Screen, J. A., Deser, C., Smith, D. M., Zhang, X., Blackport, R., Kushner, P. J., Oudar, T., McCusker, K. E. & Sun, L. (2018), 'Consistency and discrepancy in the atmospheric response to Arctic sea-ice loss across climate models', *Nature Geoscience* **11**(3), 155–163.
- Shearman, D., McGugan, A., Stein, C. & Smith, A. (1989), 'Ikaite, $\text{CaCO}_3 \cdot 6\text{H}_2\text{O}$, precursor of the thinolites in the Quaternary tufas and tufa mounds of the Lahontan and Mono Lake Basins, western United States', *Geological Society of America Bulletin* **101**(7), 913–917.

- Smith, G. I. (2009), *Late Cenozoic geology and lacustrine history of Searles Valley, Inyo and San Bernardino Counties, California*, US Geological Survey.
- Stine, S. (1990), 'Late holocene fluctuations of Mono Lake, eastern California', *Palaeogeography, Palaeoclimatology, Palaeoecology* **78**(3-4), 333–381.
- Van der Maaten, L. & Hinton, G. (2008), 'Visualizing data using t-SNE.', *Journal of machine learning research* **9**(11).
- Viskovic, A. (2006), 'Becoming a tertiary teacher: learning in communities of practice', *Higher Education Research & Development* **25**(4), 323–339.
- Vorster, P. (1985), A water balance forecast model for Mono Lake, California, Master's thesis, Calif. State University, Hayward.
- Wang, Y.-J., Cheng, H., Edwards, R. L., An, Z., Wu, J., Shen, C.-C. & Dorale, J. A. (2001), 'A high-resolution absolute-dated late Pleistocene monsoon record from Hulu Cave, China', *Science* **294**(5550), 2345–2348.
- Wattenberg, M., Viégas, F. & Johnson, I. (2016), 'How to use t-SNE effectively', *Distill* **1**(10), e2.
- Wieman, C. E. (2014), 'Large-scale comparison of science teaching methods sends clear message', *Proceedings of the National Academy of Sciences* **111**(23), 8319–8320.
- Wiggins, G. P. & McTighe, J. (2005), *Understanding by design*, Ascd, chapter 1.
- Winkelmes, M.-A., Bernacki, M., Butler, J., Zochowski, M., Golanics, J. & Weavil, K. H. (2016), 'A teaching intervention that increases underserved college students' success', *Peer Review* **18**(1/2), 31–36.
- Zhou, Y., McManus, J. F., Jacobel, A. W., Costa, K. M., Wang, S. & Caraveo, B. A. (2021), 'Enhanced iceberg discharge in the western North Atlantic during all Heinrich events of the last glaciation', *Earth and Planetary Science Letters* **564**, 116910.